

# FIT4NANO Workshop

## 11-13 July 2022



### Scientific Committee:

- Gregor Hlawacek Helmholtz  
Zentrum Dresden-Rossendorf e.V., Germany
- Gerhard Hobler  
Technische Universität Wien, Austria
- Katja Höflich  
Ferdinand Braun Institute, Germany
- Tom Wirtz  
Luxembourg Institute of Science and Technology, Luxembourg
- Marta Marszałek  
Institute of Nuclear Physics Polish Academy of Sciences, Poland

### Local organisation:

- Marta Marszałek  
Institute of Nuclear Physics Polish Academy of Sciences, Poland
- Marzena Mitura-Nowak  
Institute of Nuclear Physics Polish Academy of Sciences, Poland



Seeing beyond

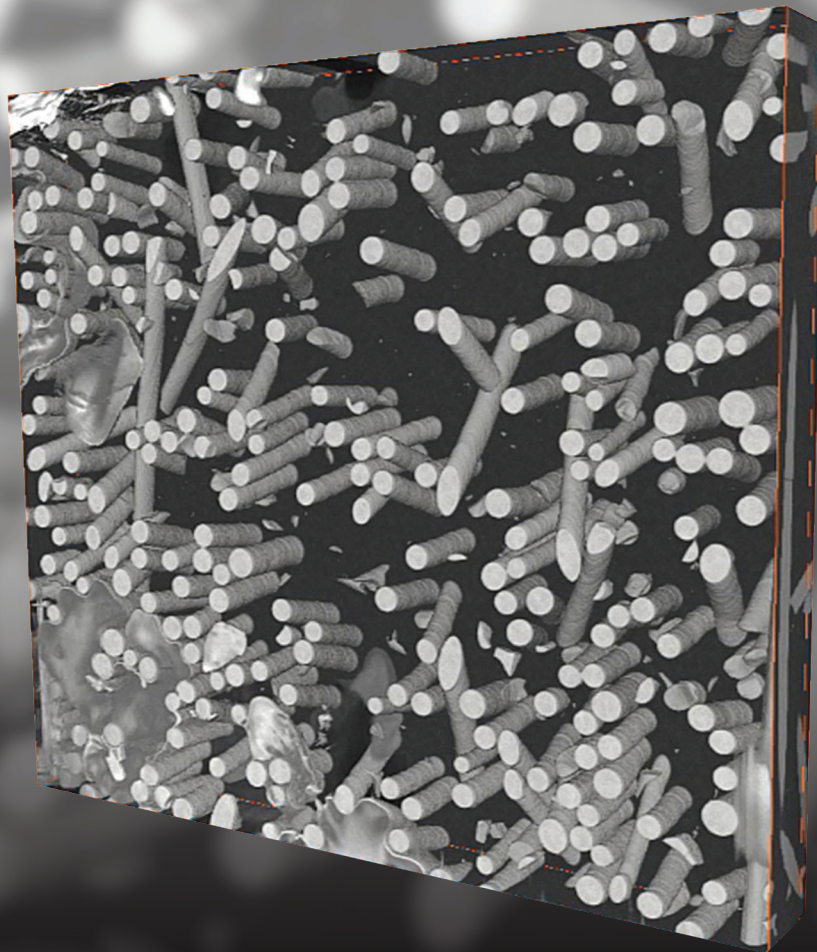
<b>Monday, 11 July</b>		
9:00-10:00	G. Hlawacek	FIT4NANO Core group meeting (on invitation only)
10:00-12:00	G. Hlawacek	FIT4NANO MC meeting (on invitation only)
12:00-13:00		Registration/Coffee
13:00-13:30	Arkady V. Krasheninnikov	Engineering the structure and properties of 2D materials by defect creation and intercalation
13:30-13:50	D. Tsoukalas	Demonstration of enhanced switching variability and conductance quantization properties in a SiO <sub>2</sub> conducting bridge resistive memory with embedded 2D MoS <sub>2</sub> material
13:50-14:10	D. Kölle	Nb and NbN constriction Josephson junctions and nanoSQUIDs patterned by He and Ne fo-cused ion beams
14:10-14:30	S. Lohmann	Influence of crystal structure on helium-induced tendril formation in an FeCoCrNiV high-entropy alloy
14:30-14:50	Andrej Kuznetsov	Polymorphic transformations induced by ion beams
14:50-15:20		Coffee break
15:20-15:50	E. Bielejec	Overview of Sandia's Focused Ion Beam Capabilities and the Development of Novel Sources for Implantation and Irradiation
15:50-16:10	David C Cox	The Challenges of Deterministic Single Ion Implantation
16:10-16:30	QD-Microscopy: H. Frerichs	Two Microscopes are better than One – In-situ Correlative Analysis by combination of AFM, SEM, and FIB
16:30-16:50	Zeiss: F. Zhou	Fabrication of micropillar array using Laser FIB for micromechanical testing
16:50-17:10		Coffee break
17:10-17:30	M. Perzanowski	A perspective for application of ion beams to modulate magnetic properties of thin films
17:30-17:50	M. Krupinski	Large scale arrays of nanomagnets and magnetically modulated patterns generated by ion irradiation
17:50-18:10	V. Deinhart	Keeping skyrmions on the track by tailoring the magnetic anisotropy landscape with focused He-ion irradiation
18:10-20:00		Poster session/Snacks
<b>Tuesday, 12 July</b>		
9:00-9:30	T. Löber	Benefits of a Cs FIB with a low temperature ion source compared to a standard Ga FIB
9:30-9:50	T. Wirtz	Advanced multimodal analytical capabilities on FIB instruments using SIMS: Do we need to care about primary ions?
9:50-10:10	Raith: T. Richter	Explore unlimited process pathways for FIB nanopatterning and ion imaging using VELION
10:10-10:30	Thermofisher: Min Wu	Advanced microstructure analysis using cutting edge multiple ion species plasma FIB
10:30-11:00		Coffee break
11:00-11:30	Stéphane Guillous	PELIICAEN setup status: Performances and new developments for elaboration and characterization of materials at nanoscale
11:30-11:50	E. Salançon	Insulator on conductor ion source: first results and measurements
11:50-12:10	O. De Castro	Laser-cooled Cs <sup>+</sup> source meets magnetic sector SIMS: a unique platform for highest sensitivity nano-analytics
12:10-12:30	K. Wiczerzak	Ion yields enhancement in FIB-TOF-SIMS by fluorine gas coinjection - A comprehensive study of 41 pure elements and multicomponent samples



12:30-13:30		Midday break
13:30-14:00	Gregor L. Weiss	Combining cryo-FIB milling with cryo-electron tomography enables macromolecular insights into biological samples
14:00-14:20	Alba Salvador-Porroche	High-throughput direct writing of metallic micro- and nanostructures by focused Ga <sup>+</sup> beam irradiation of palladium acetate films
14:20-14:40	I. B. Szymańska	Selection of coordination compounds for the study of interactions with a focused ion beam
14:40-15:00	B.R. Jany	New Cu Precursors for Ion Beam Induced Deposition under Gallium FIB
15:00-15:30		Coffee break
15:30-18:00	T.Wirtz G.Hobler K.Höflich G. Hlawacek	WG1/2/3/4 meeting (open to all, parallel sessions)
18:00	Magic Cracow : walking tour through downtown of Kraków	
20:00	Workshop dinner	
<b>Wednesday, 13 July</b>		
9:00 - 9:30	R. Córdoba	Additive nano-manufacturing of advanced superconductors, and devices using focused ion beam technology
9:30 - 9:50	Zeiss: Stephen T. Kelly	The importance of data representivity in the analysis of modern battery materials: Why FIB tomography voxel size is critical?
9:50 - 10:10	L. McElwee-White	Comparison of Electron- and Ion-Induced Chemistry in FEBID/FIBID Precursors
10:10 - 10:30	P. Nag	Ion Induced Decomposition of Iron Pentacarbonyl
10:30 - 11:00		Coffee
11:00 - 11:30	M. Toth	Nanofabrication and Knock-on Doping Using an Inert Plasma FIB and Solid/Gaseous Precursors
11:30 - 11:50	Thermofisher: Wu	Femtosecond laser integrated multiple species ion plasma FIB and its interaction with soft and hard materials
11:50 - 12:10	P. Le Gal	Comparative study of copper contents obtained by focused electron & ion beam induced deposition (Ga <sup>+</sup> , Xe <sup>+</sup> ) with Cu(II)(hfac) <sub>2</sub> ·xH <sub>2</sub> O
12:10 - 12:30	M. Huth	Locally selective magnon excitation in FEBID/FIBID nanostructures
12:30 - 14:00		Midday break
14:00-14:30	J. M. De Teresa	Recent advances in superconducting FIBID nanostructures and Cryo-FIBID
14:30 - 15:00	H. Fairbrother	Electrons/Ions Stimulated Surface Reactions of Organometallic Precursors
15:00		Excursion to Cyclotron Center Bronowice

## POSTER CONTRIBUTIONS

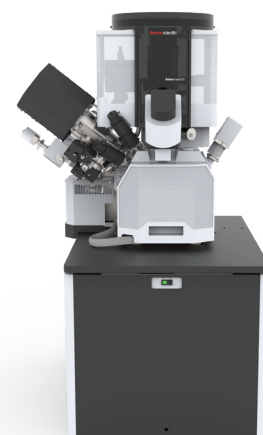
<u>D. Bedrane</u>	Coaxial ion source: characterization of field ionization under gas flow
<u>K. Berent</u>	Application of FIB/SEM tomography for the advanced microstructural characterization of solid oxide fuel cells
<u>A. Butrymowicz</u>	New gold(I) and gold(II) complexes with amidinates as potential precursors for vapor deposition methods
<u>Khairi F. Elyas</u>	Fabrication of nanostructured van der Waals heterostructures using He ion beam patterning
A.T. Escalante-Quiceno	Transfer of knowledge of new techniques based on Focused Electron/Ion Beam Induced Deposition (FEBID/FIBID)
<u>E. Gacka</u>	Electron and ion beam deposited nanowires as probes for atomic force microscopy
A.-T. Iacob	Development and biological assessment in terms of cytotoxicity and hemolytic effect of hyaluronic acid (HA) based electrospun nanofibers
Oana M. Ionescu	Polyethylene oxide-hyaluronic acid-based electrospun nanofibers: in vitro and in vivo studies
P.-H. Lu	Focused ion beam-fabricated thin film phase masks for electron lens aberration correction and structured illumination electron ptychography
K. Madajska	Binuclear rhenium(III) complexes with amidinate and amidate. Volatility and electron interaction studies
B. Naidych	Structure and morphology of the surface of cadmium sulfide thin films
W. Pilz	Cobalt and Dysprosium Liquid Alloy Ion Sources for Magnetic Nanostructures
C. P. Reis	Innovative and Minimally Invasive Therapy for Melanoma using a Hybrid Nanosyste Combined with NIR Laser Irradiation
S. Schintke	Plasma treatment and electrowetting on polymer thin films and nanofiber membranes
A. Tsarapkin	Direct Writing of Chiral and Nonlinear Plasmonic Devices
<u>I. Utke</u>	Innovative and Minimally Invasive Therapy for Melanoma using a Hybrid Nanosyste Combined with NIR Laser Irradiation
E. J. D. Vredenburgt	Study of Focused Rb <sup>+</sup> Ion Beam Applications



3D reconstruction of an automotive oil filter casing (polymer/glass fiber composite) acquired with a Helios Hydra CX DualBeam using  $O^+$  focused ion beam and AS&V4 Software for automated serial sectioning (HFW is 350  $\mu\text{m}$ ).

## Helios Hydra DualBeam

The new Thermo Scientific™ Helios™ Hydra™ DualBeam delivers four different ion species as the primary beam, allowing you to choose the ions that provide the best results for your samples and use cases, such as S/TEM sample preparation and 3D materials characterization. Switching between argon, nitrogen, oxygen and xenon is easy and can be done in under ten minutes without sacrificing performance. This unprecedented flexibility significantly expands the potential application space of FIB and enables research of ion-sample interactions to optimize the existing use cases.



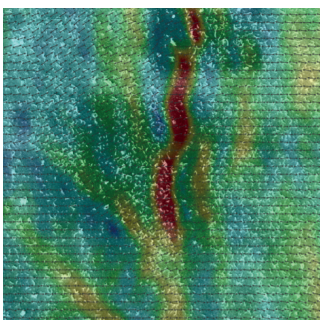
Find out more at [thermofisher.com/helioshydra](https://thermofisher.com/helioshydra)

**ThermoFisher**  
SCIENTIFIC

# Linking materials performance to microstructure



## In Situ Lab for ZEISS FE-SEM



Implement unattended automated in situ workflows with the in situ lab for your ZEISS FE-SEM. Combine a tensile or compression stage, a heating unit, and high-temperature detectors with EDS or EBSD. Control all components from a single PC. Collect highly reproducible, precise, and reliable data at high throughput. Create statistically representative results. Process your data using digital image correlation.

[zeiss.com/fesem-insitu](https://zeiss.com/fesem-insitu)



Seeing beyond



stable.

reliable.

flexible.

Fingerspitzengefühl



 **kleindiek**  
■ nanotechnik

Give Your Microscope A Hand!

gas injection • (cryo-)TEM sample preparation solutions • mechanical characterization  
in situ electrical probing • in situ AFM • linear stages • anti-curtaining solutions  
nanomanipulation using light microscopy, SEM, FIB, or beam line (UHV)

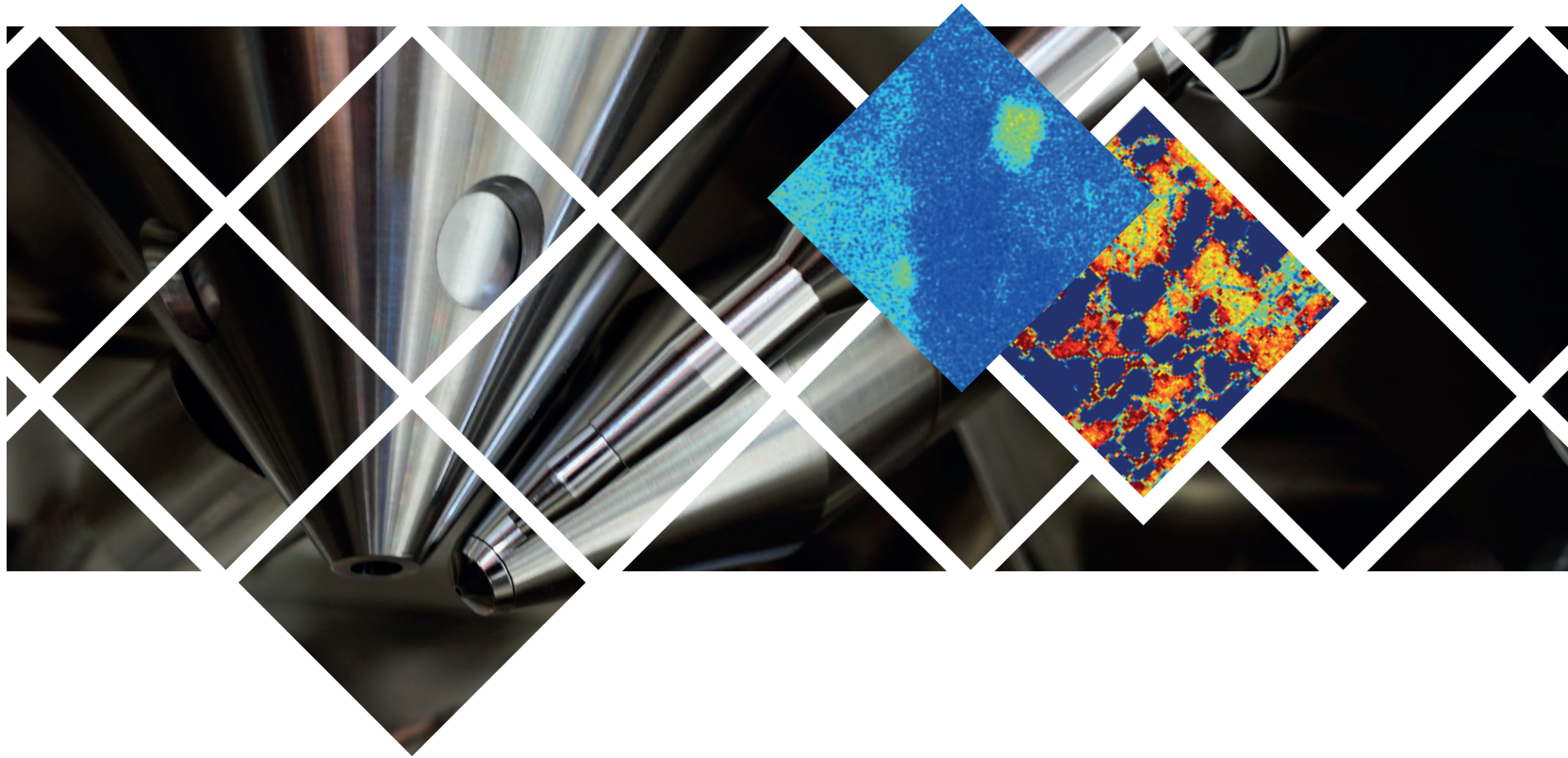
[www.kleindiek.com](http://www.kleindiek.com)



fib TOF

## Sensitive 3D chemical imaging

Bring FIB-SIMS capabilities to commercial FIB-SEM microscopes



### Features

- 3D chemical imaging of all elements
- Spatial lateral resolution <50 nm and depth profiling resolution <10 nm
- Isotopic imaging to study transport, diffusion, or reaction mechanisms
- Unambiguous elemental identification with high mass resolving power
- Compatible with major commercial FIB-SEM microscopes

### Applications

- Low-mass element detection
- Thin film depth profiling
- Nanoparticle detection
- Clean energy, Li- batteries

**TOFWERK**

[www.tofwerk.com](http://www.tofwerk.com)

[fib.info@tofwerk.com](mailto:fib.info@tofwerk.com)

**JEOL Ltd**  
*JEOL: Japan Electron Optic Laboratory*

Established in 1949, JEOL is a leading global supplier of scientific instruments used for research and development in the fields of nanotechnology, life sciences, optical communication, forensics, and biotechnology. Utilizing its unique technologies, products, services, and knowledge, JEOL helps its customers make significant breakthroughs in product development and scientific research. JEOL products include scientific instrumentation and industrial equipment, based on five major product groups.

JEOL products include scientific instrumentation and industrial equipment, based on six major product groups.

- ◆ **Electron Microscopes :**
  - Transmission Electron Microscope (TEM)
  - Scanning Electron Microscope (SEM)
  - Force Atomic Microscope
  
- ◆ **Surface Analysis :**
  - Electron Probe Microanalyser (EPMA)
  - Auger Microprobe
  - Scanning Probe Microscope
  
- ◆ **Analytical Instruments**
  - Mass Spectrometer
  - Nuclear Magnetic Resonance Spectrometer
  - Electron Spin Resonance Spectrometer
  
- ◆ **Semiconductor Equipment :**
  - Electron Beam Lithography
  - Wafers Inspection system
  - Fine Process Inspection
  
- ◆ **Medical Equipment :**
  - Amino Acid Analyser
  - BioMajesty series
  - Equipement Diagnostic (Thermographie Médicale, etc.)
  
- ◆ **Industrial Equipment :**
  - High power Electron Beam source
  - Capacitor
  - 3D Printer

JEOL Ltd. is present in more than eighty countries, is certified ISO 9001, 14001 and CE-MARK thanks to the seriousness of its manufacturing.

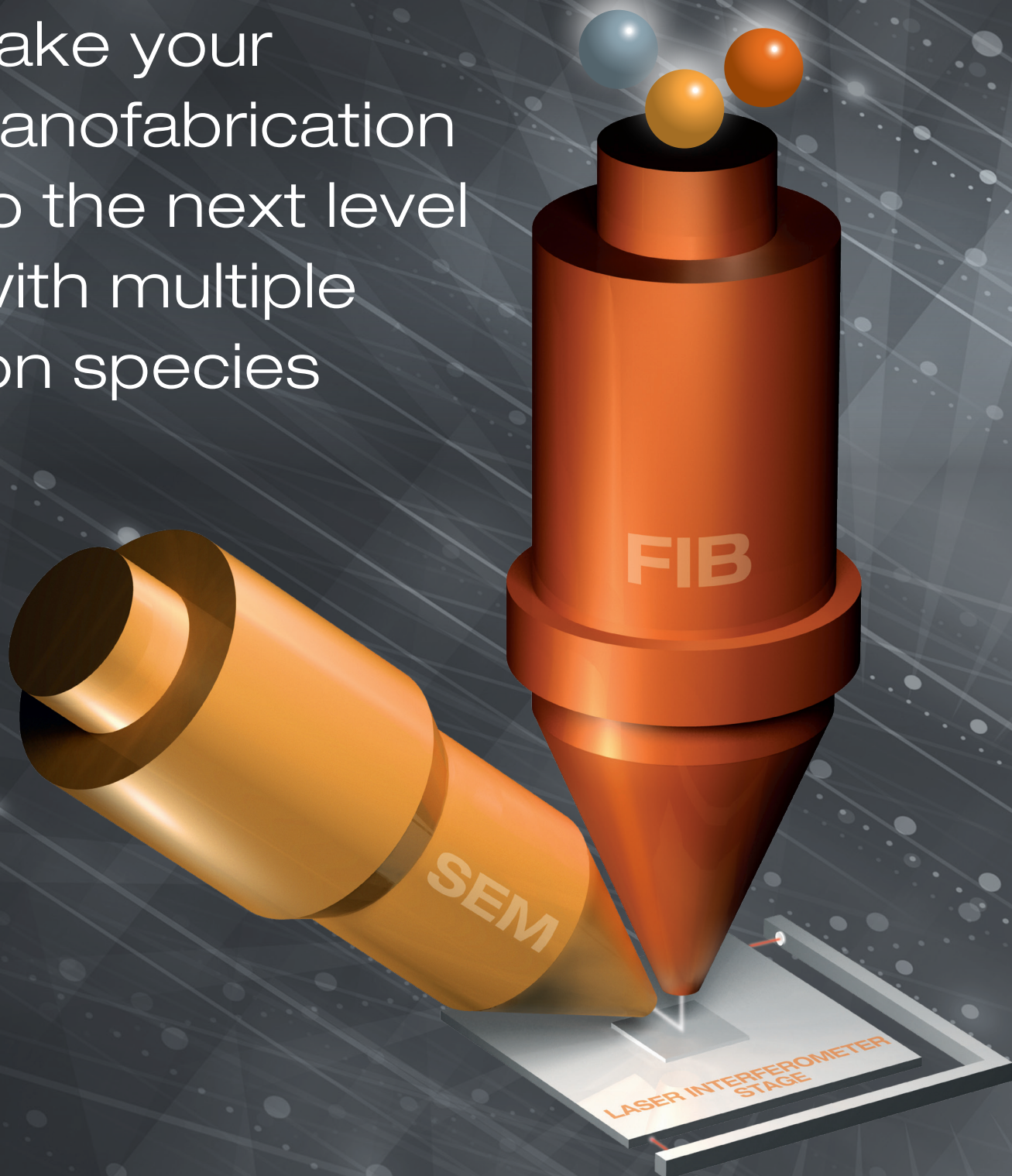
For more , Visit our website : [www.jeol.com](http://www.jeol.com)





# VELION

Take your  
nanofabrication  
to the next level  
with multiple  
ion species



[www.raith.com/velion](http://www.raith.com/velion)

**RAITH**  
NANOFABRICATION





# **ORAL CONTRIBUTIONS**



# **Engineering the structure and properties of 2D materials by defect creation and intercalation**

Arkady V. Krasheninnikov<sup>1,2</sup>

<sup>1</sup> Institute of Ion Beam Physics and Materials Research, Helmholtz-Zentrum Dresden-Rossendorf, 01328  
Dresden, Germany

<sup>2</sup> Department of Applied Physics, Aalto University, PO Box 11100, 00076 Aalto, Finland

Following isolation of graphene, many other 2D systems, e.g., single sheets of transition metal dichalcogenides (TMDs) have been manufactured. All these materials contain defects and impurities, which may govern their electronic and optical properties. Moreover, defects can intentionally be introduced using beams of energetic particles – ions and electrons. Formation of defects may also give rise to phase transformations in these materials and/or tune their properties. All of these calls upon the studies on defects and mechanisms of their formation under irradiation. In my talk, I will present the results of our recent theoretical studies [1] of point and line defects (such as mirror twin boundaries) in 2D TMDs obtained in close collaboration with several experimental groups. I will also dwell upon the effects of ion irradiation on 2D materials. I will further discuss how new 2D phases of materials can be created upon atom intercalation between graphene sheets and address the role of defects in this process.

[1] The list of publications can be found at <https://users.aalto.fi/~ark/publist.html>.

# Demonstration of enhanced switching variability and conductance quantization properties in a SiO<sub>2</sub> conducting bridge resistive memory with embedded 2D MoS<sub>2</sub> material

D. Tsoukalas<sup>1</sup>, S. Kitsios<sup>1</sup>, M. Kainourgiaki<sup>1</sup>, M. Tsigkourakos<sup>1</sup>, P. Bousoulas<sup>1</sup>

<sup>1</sup>Department of Physics, National Technical University of Athens, 15373, Athens, Greece

E-Mail: dtsouk@central.ntua.gr

Molybdenum disulfide (MoS<sub>2</sub>) is a layered compound of the transition metal dichalcogenide class that presents many interesting electrical, optical and mechanical properties. MoS<sub>2</sub> is a semiconductor and in its 2D form, which is single or few layers, it is a great candidate material for microelectronic and sensing applications. Single-layer MoS<sub>2</sub> flakes were grown via CVD on a Si/SiO<sub>2</sub> (300nm) substrate using pure sulfur powder and an aqueous solution of sodium molybdate (Na<sub>2</sub>MoO<sub>4</sub>) as the S and Mo precursors respectively [1].

Neuromorphic engineering is advancing information technologies by developing electronic devices that emulate biological synapses for the implementation of neural networks at the hardware level. Conductive Bridge resistive switching memory (CBRAM) based on SiO<sub>2</sub> operates through the formation and disruption of conductive filaments (CF) formed in the oxide and exhibits interesting neuromorphic properties. Along these lines, we propose the incorporation of layers of MoS<sub>2</sub> within a SiO<sub>2</sub>-based CBRAM and explore the properties of the new device. The proposed layered structure of the MoS<sub>2</sub> will practically act as an atomic sieve, controlling the growth mechanism of the CF within the oxide and tuning the degree of volatility or non-volatility of the respective memory device (Fig. 1, 2). Despite the significant progress shown in the realization of QC in memristive devices, it is still hard to accomplish a notable control and development on the atomic-point-contact (APC) in order to propagate a desirable QC. For this reason, 2D materials have gained wide attention as a constituent of memory devices due to their unique properties. Previous studies of various 2D materials as non-volatile memory elements such as graphene, hexagonal boron nitride (hBN) and black phosphorus have been reported.

It is well established that the CF formation in CBRAM devices emerges from the migration of Ag ions within the oxide layer as a result of electrochemical reactions during the application of DC voltage sweeps or pulses. In this work, we demonstrate that by encapsulating thin layers of MoS<sub>2</sub> in the oxide of a CBRAM, enhanced APC can be achieved (Fig. 3, 4). MoS<sub>2</sub> exhibits a layered structure, in which two atomic planes of sulphur atoms enclose an atomic plane of molybdenum atoms with an intrinsic lattice constant of 0.31nm, while a single monolayer possesses a thickness of just 0.7 nm. Considering that the diameter of Ag ion is 0.26 nm, we can argue that MoS<sub>2</sub> is a perfect atomic sieve for ion diffusion. In this study, two different device configurations were compared, namely, a reference device Ag/SiO<sub>2</sub>/SiO<sub>2</sub>/TiN and a device with MoS<sub>2</sub> embedded, Ag/SiO<sub>2</sub>/MoS<sub>2</sub>/SiO<sub>2</sub>/TiN, in order to investigate how it is affected by the incorporated 2D material in terms of memory properties (endurance, retention, variability). On top of that, enhanced synaptic properties were recorded, regarding the linearity of the potentiation and depression procedures, which render also our structure attractive in emulating neuromorphic functionalities [2]. To further advance research involving 2D materials embedded within other matrices, FIB will be increasingly needed for TEM sample preparation because of the non-uniform nature of 2D materials deposition over the substrate area.

[1] M. Tsigkourakos et al., Thin Solid Films 733 (2021) 138808

[2] S. Kitsios et al., ACS Applied Electronic Materials (2022) (<https://doi.org/10.1021/acsaelm.2c00362>)

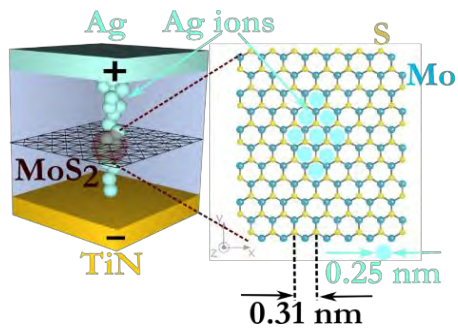


Figure 1. Schematic illustration of the proposed CBRAM device with MoS<sub>2</sub> embedded into a sputtered SiO<sub>2</sub> layer.

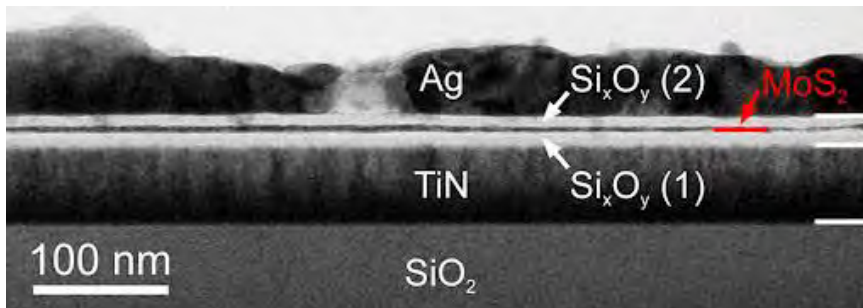


Figure 2. Transmission Electron Microscopy cross section of the Metal-Insulator-Metal structure [2]

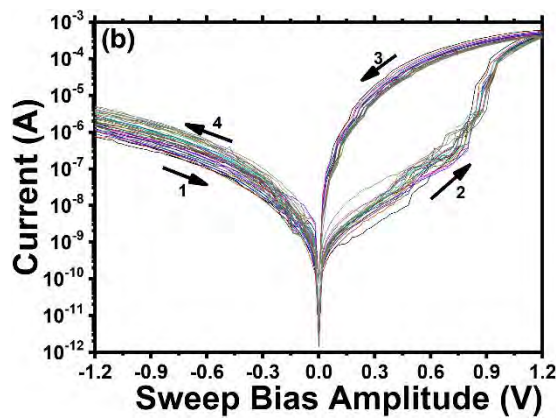


Figure 3. a) I-V cycles for the MoS<sub>2</sub> embedded sample.

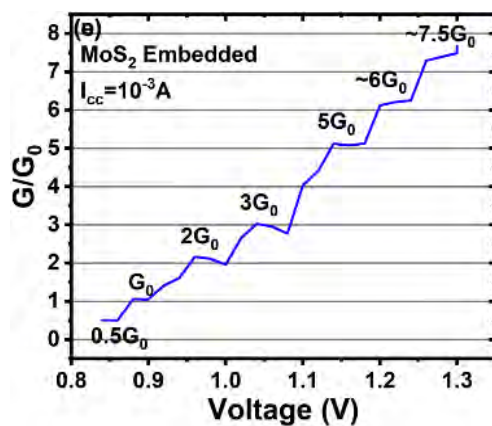


Figure 4. Quantized conductance under DC measurements

## **Nb and NbN constriction Josephson junctions and nanoSQUIDs patterned by He and Ne focused ion beams**

T. Griener<sup>1</sup>, S. Pfander<sup>1</sup>, J. Linek<sup>1</sup>, J. A. Potter<sup>2</sup>, O. W. Kennedy<sup>2</sup>, U. Drechsler<sup>3</sup>, T. Weimann<sup>4</sup>, R. Kleiner<sup>1</sup>, P. A. Warburton<sup>2</sup>, A. Knoll<sup>3</sup>, O. Kieler<sup>4</sup>, D. Koelle<sup>1</sup>

<sup>1</sup>Physikalisches Institut, Center for Quantum Science (CQ) and LISA<sup>+</sup>, Univ. Tübingen, Germany

<sup>2</sup>London Centre for Nanotechnology, University College London, United Kingdom

<sup>3</sup>IBM Research Center Europe – Zürich, Rüschlikon, Switzerland

<sup>4</sup>Department Quantum Electronics, Physikalisch-Technische Bundesanstalt (PTB) Braunschweig, Germany

E-Mail: koelle@uni-tuebingen.de

Nanopatterning of superconducting thin film structures with focused He or Ne ion beams (He/Ne-FIB) offers a flexible tool for creating constriction-type Josephson junctions (cJJs) and strongly miniaturized superconducting quantum interference devices (nanoSQUIDs) based on cJJs for applications in magnetic sensing on the nanoscale. We present our attempts to use He/Ne-FIB for fabricating Nb and NbN cJJs and nanoSQUIDs which shall provide ultra-low noise and high spatial resolution for their application in scanning SQUID microscopy (SSM). The nanoSQUIDs are designed as sensors for magnetic flux and dissipation. They shall be integrated on custom-made Si cantilevers, which will provide the possibility of simultaneous conventional topographic imaging by atomic force microscopy (AFM). We will discuss the status of this project and challenges that have to be met on the way to combine SSM and AFM on the nanoscale.

We acknowledge the European Commission under H2020 FET Open grant ‘FIBsuperProbes’ (number 892427)

# Influence of crystal structure on helium-induced tendrils formation in an FeCoCrNiV high-entropy alloy

S. Lohmann<sup>1</sup>, R. Goodall<sup>2</sup>, G. Hlawacek<sup>1</sup>, R. Hübner<sup>1</sup>, L. Ma<sup>2</sup>, and A. S. Gandy<sup>2</sup>

<sup>1</sup>Institute of Ion Beam Physics and Materials Research, Helmholtz-Zentrum Dresden-Rossendorf, 01328, Dresden, Germany

<sup>2</sup>Department of Materials Science and Engineering, University of Sheffield, S10 2TN, Sheffield, United Kingdom

E-Mail: s.lohmann@hzdr.de

High-entropy alloys (HEAs) are a relatively new class of metal alloys composed of several principal elements, usually at (near) equiatomic ratios. It has previously been reported that some HEAs display superior radiation damage resistance, with composition and microstructure being cited as contributing factors, though the precise mechanism is still unknown. To study the influence of the crystal structure on the response to radiation, we have chosen FeCoCrNiV as a model system. While FeCoCrNi has a face-centred cubic (fcc) structure, adding V leads to a structural transformation towards a body-centred tetragonal (bct) structure with both phases present at near-stoichiometric composition [1].

The as-cast sample was characterised by energy-dispersive X-ray spectroscopy (EDXS) and electron backscatter diffraction (EBSD) in a scanning electron microscope (SEM) confirming the presence of both phases. Irradiations were performed with a focussed He beam provided by a helium ion microscope (HIM) at temperatures between room temperature and 500°C. The irradiation fluence was varied between  $6 \times 10^{17}$  ions/cm<sup>2</sup> and  $1 \times 10^{20}$  ions/cm<sup>2</sup>. High-resolution images of the irradiated areas were taken with the same HIM, and an example is shown in Fig. 1a. Selected irradiated areas were additionally studied by transmission electron microscopy (TEM) in combination with EDXS.

Under irradiation, pores start to be generated in the material with pore sizes differing significantly between the two phases. At higher fluences and above a critical temperature, a tendrils structure as exemplary shown for the bct phase in Fig. 1a forms in both phases. We have found that the critical temperature depends on the phase and is lower for fcc. TEM images reveal that the tendrils span the whole depth of the irradiated area and are accompanied by bubbles of various sizes as shown in Fig. 1b for the bct phase. Scanning TEM-based EDXS of these structures indicates a He-induced change in composition.

A.G. acknowledges support by the Royal Academy of Engineering and the Leverhulme Trust.

[1] Z. Leong et al., *Scientific Reports*, 7 (2017) 39803

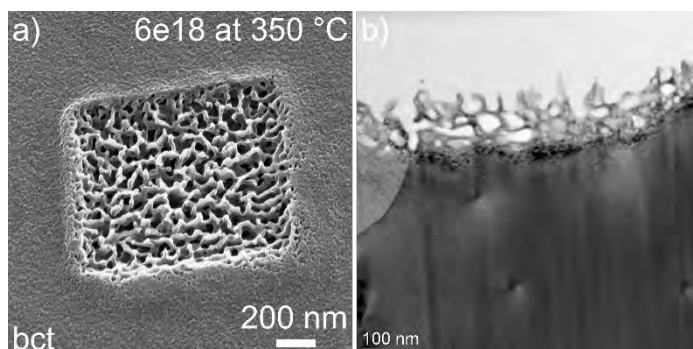


Figure 1: bct phase of FeCoCrNiV sample after irradiation by a focussed He beam. The He energy was 5 keV and the irradiation fluence  $6 \cdot 10^{18}$  ions/cm<sup>2</sup> under normal incidence. The sample was kept at 350°C during irradiation. a) HIM image b) TEM cross section.

# Polymorphic transformations induced by ion beams

Alexander Azarov<sup>1</sup>, Vishnukanthan Venkatachalapathy<sup>1,2</sup> and Andrej Kuznetsov<sup>1</sup>

<sup>1</sup>University of Oslo, Centre for Materials Science and Nanotechnology, N-0316 Oslo, Norway

<sup>2</sup>National Research Nuclear University, "MEPhI", 115409 Moscow, Russian Federation

E-Mail: Andrej.kuznetsov@fys.uio.no

Polymorphs are common in nature and can be stabilized by applying external pressure in materials. We have discovered a new method to fabricate regular polymorph films with ion beams and this presentation aims to review these data.

The core concept of our new method for the polymorph fabrication by ion beam is in the idea that the pressure/strain can be induced by the gradually accumulated radiation disorder. Meanwhile, it is known that in semiconductors, the radiation disorder accumulation typically results in the amorphization instead of engaging polymorphism. By studying these phenomena in gallium oxide ( $\text{Ga}_2\text{O}_3$ ) we found that the amorphization may be prominently suppressed by the monoclinic to orthorhombic phase transition. Utilizing this discovery, a highly oriented single-phase orthorhombic film on the top of the monoclinic  $\text{Ga}_2\text{O}_3$  substrate was fabricated [1]. Exploring this system, a novel mode of the lateral polymorphic regrowth not previously observed in solids was detected [1].

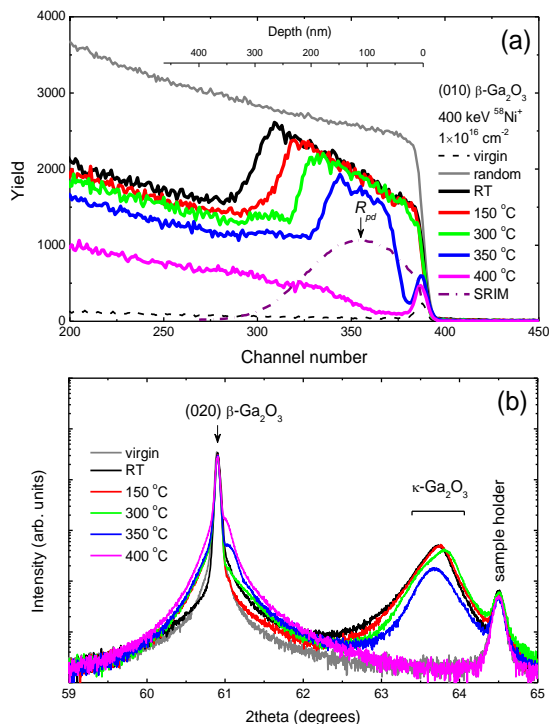


Fig.1. Data for 400 keV  $\text{Ni}^+$  ion implants into beta- $\text{Ga}_2\text{O}_3$  with  $1 \times 10^{16}$  ions/ $\text{cm}^2$ ; (a) Rutherford backscattering spectroscopy in channeling mode (RBS/C) spectra and (b) the corresponding x-ray diffraction (XRD) 2theta scans. Depending on the implantation temperature there are three kappa-polymorph fabrication conditions revealed by Fig.1: continuous surface film at RT-300°C, buried layer at 350°C, and no polymorph transformation at 400°C. Importantly, the buried kappa-layer obtained at 350°C implants, can be readily used in the transistors design, conceptually similar to that while using ternary alloys to vary the bandgaps of the binary materials.

In this presentation we review the data from Ref.[1] and specifically emphasize on our new data devoted to the formation of a kappa-polymorph layer sandwiched inside beta-polymorph substrate. Such interesting structure was fabricated by applying variations of the radiation temperature, see Fig.1.

Indeed, Fig.1 shows the data for 400 keV  $\text{Ni}^+$  ion implants into beta- $\text{Ga}_2\text{O}_3$  with  $1 \times 10^{16}$  ions/ $\text{cm}^2$ ; (a) Rutherford backscattering spectroscopy in channeling mode (RBS/C) spectra and (b) the corresponding x-ray diffraction (XRD) 2theta scans. Depending on the implantation temperature there are three kappa-polymorph fabrication conditions revealed by Fig.1: continuous surface film at RT-300°C, buried layer at 350°C, and no polymorph transformation at 400°C. Importantly, the buried kappa-layer obtained at 350°C implants, can be readily used in the transistors design, conceptually similar to that while using ternary alloys to vary the bandgaps of the binary materials.

Indeed, Fig.1 shows the data for 400 keV  $\text{Ni}^+$  ion implants into beta- $\text{Ga}_2\text{O}_3$  with  $1 \times 10^{16}$  ions/ $\text{cm}^2$ ; (a) Rutherford backscattering spectroscopy in channeling mode (RBS/C) spectra and (b) the corresponding x-ray diffraction (XRD) 2theta scans. Depending on the implantation temperature there are three kappa-polymorph fabrication conditions revealed by Fig.1: continuous surface film at RT-300°C, buried layer at 350°C, and no polymorph transformation at 400°C. Importantly, the buried kappa-layer obtained at 350°C implants, can be readily used in the transistors design, conceptually similar to that while using ternary alloys to vary the bandgaps of the binary materials.

[1] A. Azarov, C. Bazioti, V. Venkatachalapathy, P. Vajeeston, E. Monakhov and A. Kuznetsov, "Disorder-induced ordering in gallium oxide polymorphs." Physical Review Letters, 128, 15704 (2022).





# Overview of Sandia's Focused Ion Beam Capabilities and the Development of Novel Sources for Implantation and Irradiation

E. Bielejec<sup>1</sup>

<sup>1</sup>Sandia National Laboratories, 87109, Albuquerque, NM, United States

E-Mail: esbiele@sandia.gov

We present an overview of Sandia's Ion Beam Laboratory (IBL) capabilities with an emphasis on focused ion beams (FIB) for implantation and irradiation. This includes the development of novel liquid metal alloy ion sources (LMAIS).

The IBL currently operates seven FIB systems that range in ion energy from less than 1 keV to greater than 70 MeV, including a wide range of ion species from protons (H) to lead (Pb) over a range of spot sizes from nm to  $\mu\text{m}$ . These systems are used to produce localized implantation and irradiation studies in a wide range of materials and devices. Examples range from, the fabrication of high precision arrays of defect centers in wide bandgap materials such as diamond, SiC, GaN, etc.... allowing for the creation of highly controlled single photon sources using in-situ single ion implantation and detection and in-situ photoluminescence, to localized irradiation of state-of-the-art gate-all-around CMOS devices studying the effects of single ion irradiation. In particular, we will concentrate on the usage of our two mass filtered FIB systems, the A&D nanoImplanter and the Raith Velion, both of which include high spatial resolution with CAD based patterning to enable the formation of arbitrary patterned implantation in combination with LMAIS.

For novel ion source development, we present an overview of the available LMAIS for the mass filtered systems, as well as fabrication details and results using both novel Pb and N sources. The Pb source is based on a SnPb alloy using a custom Kovar wire tip in place of the standard tungsten tip usually used for FIB applications. This source has demonstrated a long lifetime comparable to our other alloy-based sources of greater than 2000  $\mu\text{A}\cdot\text{hr}$  and less than 50 nm resolution without optimization of the tip design. The atomic N source is based on an AuSn alloy implanted with nitrogen up to the saturation limit and verified using elastic recoil detection (ERD). This N source has demonstrated a relatively short lifetime of less than 100-200  $\mu\text{A}\cdot\text{hr}$  and is limited to a total N ion production rate of approximately 2,000 to 10,000 ions/s corresponding to up to approximately 1 fA of current of singly charged nitrogen ions.

The demonstration of these novel sources continues the development of high-resolution localized implantation and irradiation capabilities enabling the fabrication of custom implanted samples for cutting edge physics and quantum optics experiments at Sandia's IBL.

Sandia National Laboratories is a multimission laboratory managed and operated by National Technology & Engineering Solutions of Sandia, LLC, a wholly owned subsidiary of Honeywell International Inc., for the U.S. Department of Energy's National Nuclear Security Administration under contract DE-NA0003525.

## The Challenges of Deterministic Single Ion Implantation

David C Cox and Kristian Stockbridge

National Ion Beam Centre, University of Surrey, U.K.

E-Mail: d.cox@surrey.ac.uk

Techniques for deterministic implantation of single ions are currently of high interest for quantum technology applications. Here we present single ion implant detection results from the first commercially produced single ion implanter designed specifically for rapid and precise positioning of deterministically single ions. This system uses a pulsed, low current beam of ions from a liquid metal or duoplasmatron source; Wein filter mass/charge filtering; and secondary electron detection to determine when an implantation event has occurred. The waveform captured by the channel electron multiplier detectors show transient response(s) that each likely correspond to an ion impact. The distribution of integrated CEM signal for a large number of implant sites shows clustering corresponding to integer numbers of ions in a pulse. This additional information will help quantify the success probability of implant jobs improving quality control.



One of the two Ionoptika single ion implanters in the NIBC.

# Two Microscopes are better than One – In-situ Correlative Analysis by combination of AFM, SEM, and FIB

H. Frerichs<sup>1\*</sup>, S. Seibert<sup>1</sup>, L. Stühn<sup>1</sup>, M. Wolff<sup>1</sup>, C.H. Schwalb<sup>1</sup>

<sup>1</sup>Quantum Design Microscopy GmbH, 64293 Darmstadt, Germany

E-Mail: frerichs@qd-microscopy.com

Combining different analytical methods into one instrument is of great importance for the simultaneous acquisition of complementary information. Especially the *in-situ* combination of scanning electron microscopy (SEM) and atomic force microscopy (AFM) enables completely new insights into the micro and nano-world. In this work, we present the unique *in-situ* combination of scanning electron / ion microscopy (SEM/FIB) with atomic force microscopy (AFM) for nanoscale characterization [1-2].

A particularly important aspect for advanced AFM measurements are the cantilevers themselves. Especially the cantilever-tips need to have special properties in order to measure not only topography but also electrical and magnetic material characteristics. In this context, the focused electron beam induced deposition (FEBID) is a promising approach to design and fabricate sophisticated tips. We will present a variety of case studies to highlight the advantages of interactive correlative *in-situ* nanoscale characterization for different materials and nanostructures, using FEBID-constructed tips. We show results for the *in-situ* electrical characterization using conductive AFM for 2D materials as well as electrostatic force microscopy (EFM) for piezoceramic films, that enables the precise analysis of grain boundary potential barriers in semiconducting BaTiO<sub>3</sub>-based ceramics [3]. The grain boundaries were located by BSE-SEM and subsequently measured via the *in-situ* EFM method. The barriers were shown to be significantly thinner and more pronounced as the amount of SiO<sub>2</sub> increased from 0 to 5 mol% (see Figure 1). These results can be directly correlated with electron backscatter diffraction (EBSD) measurements in order to link the AFM and SEM data to the crystallographic microstructure.

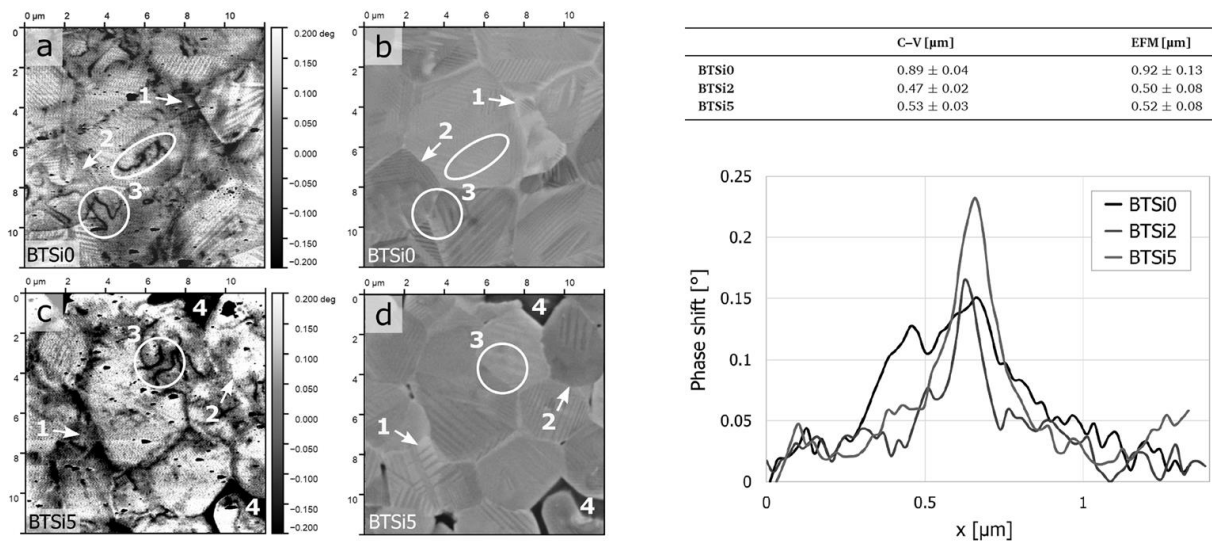


Figure 1: (Left) EFM signal of (a) BTSi0 and (c) BTSi5 and corresponding BSE-SEM images (b) and (d) of the exact same sample area. The EFM images were recorded with an external voltage of -3 V. (Right) Grain boundary potential barriers of BaTiO<sub>3</sub> based ceramics with varying SiO<sub>2</sub> content. Images extracted from [3].

\*Corresponding author: email: frerichs@qd-microscopy.com

In addition, we will present results for the *in-situ* characterization of magnetic nanostructures by the combination of SEM and high-vacuum magnetic force microscopy (MFM). For the *in-situ* MFM measurements we use specialized magnetic cantilever probes that are fabricated using electron beam induced deposition (FEED) for high-aspect ratio magnetic tips that surpass standard magnetic cantilever tips in lateral and magnetic resolution. The SEM enables to identify the grain boundaries on multilayer thin-film samples or stainless steel in order to measure the magnetic properties directly via MFM with nanometer resolution (see Figure 2).

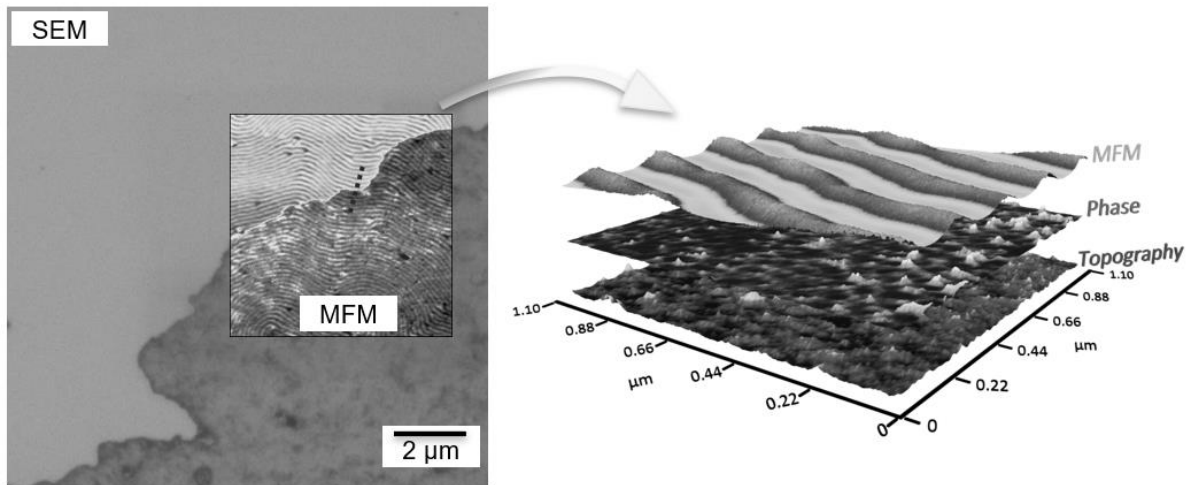


Figure 2: (Left) SEM image of multilayer magnetic sample with correlative MFM image at a grain boundary. (Right) AFM data overlay of topography, phase, and MFM signals.

- [1] D. Yablon, et al., *Microscopy and Analysis*, **31** (2), 14-18 (2017)
- [2] S.H. Andany, et al., *Beilstein J. Nanotechnol.*, **11**, 1272-1279 (2020)
- [3] J.M. Prohinig, J. Hütner, K. Reichmann, S. Bigl, *Scripta Materialia*, **214**, 114646 (2022)

## Fabrication of micropillar array using LaserFIB for micromechanical testing

F. Zhou<sup>1</sup>, T. Schubert<sup>2</sup>, R. Pero<sup>3</sup>, N. X. Randall<sup>3</sup>, T. Bernthaler<sup>2</sup>

<sup>1</sup>Carl Zeiss Microscopy GmbH, Carl-Zeiss-Strasse 22, 73447 Oberkochen, Germany

<sup>2</sup>Materials Research Institute Aalen, Aalen University, Beethovenstrasse 1, 73430 Aalen, Germany

<sup>3</sup>Alemnis AG, Business Park Gwatt, Schorenstrasse 39, 3645 Gwatt (Thun), Switzerland

E-Mail: fang.zhou@zeiss.com

Micropillars are conventionally machined using Focused Ion Beam (FIB) which is an extremely time-consuming process especially for larger pillars. Thus, fabrication of good quality micropillar arrays with great control over the size and location on a large test volume is so far hardly possible. In this work, an all-in-one LaserFIB solution is applied to speed up the fabrication of micropillar array. A femtosecond laser is used to fabricate micropillar array over an area of hundreds of microns up to centimeters within minutes. A 5x5 array of pillars of 1.4301 stainless steel with 50 microns in diameter and 100 microns in height are fabricated by means of combining superfast fs-laser milling and FIB polishing (cf. Fig.1). In micromechanical compression test, the reproducibility of test results and possibility to test using various compression modes are important. Therefore, micropillar array or many pillars with identical or different sizes need to be fabricated for a meaningful data collection.

The machined micropillars of 1.4301 stainless steel are compressed *in-situ* in a SEM using a diamond flat punch to extract stress-strain curves while simultaneously recording the SEM video. Compression behavior of the alloy as a function of the temperature, in the range from 27 °C down to -150 °C, is investigated using a low-temperature micromechanical compression assembly. Several micropillars with the same geometry and clean top loading surfaces are required for the multiple temperature tests using various compression modes.

Fig.2 shows the effects of temperature at a constant displacement rate on the load-displacement behavior of the 1.4301 stainless steel pillars. With the decrease of temperature, there is a transition from parabolic to sigmoidal behavior. The observed variation in the curve shape with temperature is consistent with that observed by previous studies using labor tensile testing, and the inflections in the low temperature curves identify the formation of strain-induced martensite [1,2].

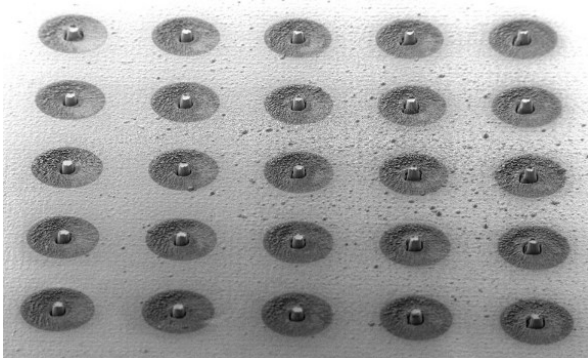


Fig. 1 5x5 array of pillars with 50 microns in diameter and 100 microns in height are fabricated using LaserFIB combination.

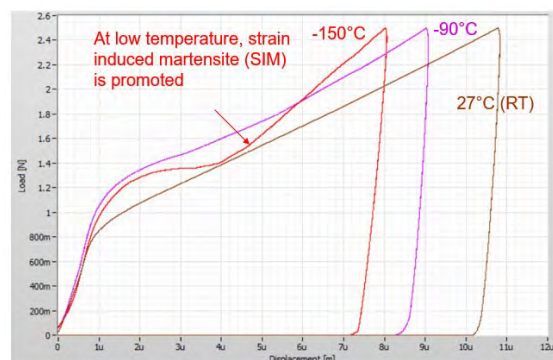


Fig. 2 The effects of temperature at a constant displacement rate on the load-displacement behavior of the 1.4301 stainless steel

[1] Cios, G., et al., (2017) Metallurgical and Materials Transactions A, 48(10), 4999-5008

[2] Zimmermann, M., et al., (2010) Journal of Physics: Vol. 240, No. 1, p. 012040

## **A perspective for application of ion beams complemented by nanosphere lithography to tailoring of thin films and nanostructures**

M. Perzanowski, M. Krupinski and M. Marszalek

Department of Magnetic Materials and Nanostructures, Institute of Nuclear Physics Polish Academy of Sciences, 31-342, Krakow, Poland

E-Mail: Marcin.Perzanowski@ifj.edu.pl

Nanosphere lithography technique is a method of thin films patterning which utilizes self-assembled nanoparticles with diameter from 20 nm up to 1 micron, and allows to produce well-arranged and homogeneous arrays of nanostructures over large areas of 100 cm<sup>2</sup> and more [1-3]. Hexagonally-arranged assemblies of particles were mostly applied as masks for deposition of materials and used for fabrication of arrays of antidots [1,3,4], nanocaps [5,6], or islands [7,8]. In this talk, we want to discuss the application of nanoparticles as masks for ion beam irradiation as an alternative and supplement for focused ion beam patterning.

Here, we present a concept for fabrication spatially modulated magnetic media by combination of nanosphere lithography and ion beam irradiation. In particular, this approach can be applied for exchange-biased films, synthetic antiferromagnets, and 3d-4d metal alloys. The geometry of the irradiation masks can be adjusted by the radio-frequency (RF) plasma etching and the result is dependent on the time of the process. Ion irradiation is a method in which structural damages are deliberately induced into material and their amount is dependent on ion type, beam energy, and irradiation dose. Combination of these two experimental methods allow to fabricate materials with locally engineered magnetic properties.

After the deposition of a magnetic film, its surface is covered by the nanospheres. Then, the system is irradiated with an ion beam. This results in alteration of the material's microstructure in places between the particles. Afterwards, the nanospheres are treated by RF plasma etching to decrease their size and the system is irradiated for the second time. The regions which were irradiated in the first step receive a second dose but some parts of the samples, previously shadowed by the nanospheres, are ion bombarded for the first time. This process of RF treatment and ion irradiation can be repeated several times to create onion-like structures where each "onion ring" will have distinct magnetic and structural properties. At the end, the nanospheres can be removed for further studies i.e. imaging of magnetic domains using magnetic force microscopy or Lorentz microscopy. Such procedure is highly flexible and allows to fabricate various magnetic structures in one physical system by changing size of the nanoparticles, ion type, beam energy, and irradiation dose. Contrary to the focused ion beam method, this procedure allows faster fabrication of macroscopic arrays of magnetic structures, and constitutes valuable background for local structural modifications done by ion beams.

[1] M. Perzanowski et al. *ACS Appl. Mater. Interfaces* 9 (2017), 33250-33256.

[2] A. Kosiorok et al. *Nano Lett.* 4 (2004), 1359.

[3] M. Krupinski et al. *Nanotechnology* 28 (2017), 085302.

[4] P. Tiberto et al. *J. Appl. Phys.* 107 (2010), 09B502.

[5] J. K. née Moser et al. *J. Appl. Phys.* 107 (2010), 09C506.

[6] P. B. Aravind et al. *Nanotechnology* 30 (2019), 405705.

[7] N. Martin et al. *Adv. Funct. Mater.* 21 (2011), 891-896.

[8] H. Zhong et al. *Nanotechnology* 19 (2008), 095703.

## Large scale arrays of nanomagnets and magnetically modulated patterns generated by ion irradiation

M. Krupinski<sup>1</sup>, R. Bali<sup>2</sup>, A. Zarzycki<sup>1</sup>, K. Potzger<sup>2</sup>, M. Albrecht<sup>3</sup>, and M. Marszałek<sup>1</sup>

<sup>1</sup>The H. Niewodniczanski Institute of Nuclear Physics, Polish Academy of Sciences, 31-342 Krakow, Poland

<sup>2</sup>Helmholtz-Zentrum Dresden-Rossendorf, 01328 Dresden, Germany

<sup>3</sup>Institute of Physics, University of Augsburg, 86159 Augsburg, Germany

E-Mail: [michal.krupinski@ifj.edu.pl](mailto:michal.krupinski@ifj.edu.pl)

Large-scale periodic arrays of trigonal ferromagnetic islands embedded in a paramagnetic matrix have been fabricated by deposition of 202, 508, and 784 nm size polystyrene nanospheres on 40 nm thick B2-Fe<sub>60</sub>Al<sub>40</sub> thin films. Subsequently, the system was irradiated by 20 keV Ne<sup>+</sup> ions at  $6 \times 10^{14}$  cm<sup>-2</sup> fluence, which induced chemical disorder and thus a ferromagnetic phase in the uncovered Fe<sub>60</sub>Al<sub>40</sub>. Using SQUID and Kerr magnetometry, changes in coercive field, saturation magnetization, loop squareness, and magnetic anisotropy constant have been determined in a temperature range of 5 K – 350 K and correlated with the radiation damage obtained from simulations of the ion stopping and range (SRIM [1]). The domain shapes and sizes together with the switching behaviour were studied by scanning magnetoresistive microscopy (SMRM) measurements in variable external field [2].

SMRM images showed that the periodicity in the domain structure could be noticed even in zero field. The evolution of the magnetic domain structure with magnetic field for one selected area located between three adjacent paramagnetic islands in an array with a period of 508 nm is shown in figure below. The magnetic configuration in this area is similar to the “three-leaf clover”, which is an indicator of a vortex-like state. The possible arrangement of magnetic moments, explaining the contrast, is shown by white arrows inside the triangle of the first scan. As the external magnetic field increases, the vortex-like structure disappears.

The results demonstrated that the proposed approach with broad ion beam complemented by un-conventional lithography method can be effectively used to produce large-area magnetic arrays embedded within a topographically flat surface with magnetic properties tuneable by temperature and patterning period. It has been shown that the proposed approach can be used to create non-collinear magnetic structures and marks the great potential of using focused ion beams for further local modification of magnetic nanopatterns.

[1] J.F. Ziegler, J.P. Biersack, [www.srim.org](http://www.srim.org)

[2] D. Mitin, M. Grobis, M. Albrecht, *Rev. Sci. Instrum.* 87, 023703 (2016).

[3] M. Krupinski, R. Bali, D. Mitin, P. Sobieszczyk, J. Gregor-Pawlowski, A. Zarzycki, R. Bottger, M. Albrecht, K. Potzger, M. Marszałek, *Nanoscale* 11, 8930-8939 (2019).



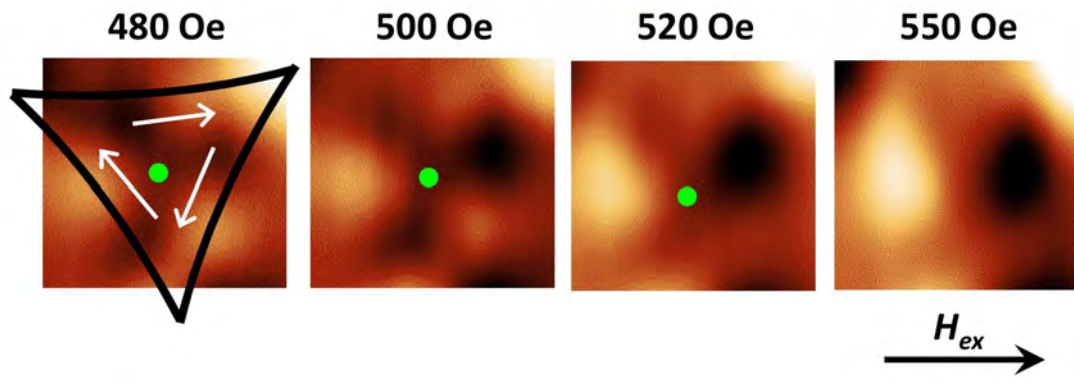


**Figure 1.** SMRM images (200 nm x 200 nm) of the sample with a period of 508 nm showing the evolution of domain formation with increasing external field. The area marked with a triangle is the irradiated region revealing a vortex state at 480 Oe. The green dot marks the vortex core. [3]

# Keeping skyrmions on the track by tailoring the magnetic anisotropy landscape with focused He-ion irradiation

L.-M. Kern<sup>1</sup>, B. Pfau<sup>1</sup>, V. Deinhart<sup>1,2,3</sup>, M. Schneider<sup>1</sup>, C. Klose<sup>1</sup>,  
K. Gerlinger<sup>1</sup>, S. Wittrock<sup>1</sup>, D. Engel<sup>1</sup>, I. Will<sup>1</sup>, C. M. Günther<sup>4</sup>, R. Liefferink<sup>5</sup>,  
J. H. Mentink<sup>5</sup>, S. Wintz<sup>3</sup>, M. Weigand<sup>3</sup>, M.-J. Huang<sup>6</sup>, R. Battistelli<sup>3</sup>,  
D. Metternich<sup>3</sup>, F. Büttner<sup>3</sup>, K. Höflich<sup>2,3</sup> and S. Eisebitt<sup>1,4</sup>

<sup>1</sup> Max Born Institute for Nonlinear Optics and Short Pulse Spectroscopy, 12489 Berlin, Germany

<sup>2</sup> Ferdinand-Braun-Institut gGmbH, Leibniz-Institut für Höchstfrequenztechnik, 12489 Berlin, Germany

<sup>3</sup> Helmholtz-Zentrum für Materialien und Energie GmbH, 14109 Berlin, Germany

<sup>4</sup> Technische Universität Berlin, 10623 Berlin, Germany

<sup>5</sup> Radboud University, 6525 AJ Nijmegen, Netherlands

<sup>6</sup> Deutsches Elektronen-Synchrotron (DESY), 22607 Hamburg, Germany

E-Mail: victor.deinhardt@fbh-berlin.de

Magnetic skyrmions are vortex-like topological structures which can be stabilized in materials with perpendicular magnetic anisotropy (PMA) and high Dzyaloshinskii–Moriya interaction [1]. Here, we study skyrmions in a Pt/CoFeB/MgO-based multilayer system. Within this system, skyrmions can be nucleated, annihilated and shifted by spin-polarized currents generating spin-orbit torque (SOT) [2]. Skyrmions can also be nucleated by ultrashort laser pulses, which is a faster and, potentially, more energy efficient generation method [3]. Still, several challenges have to be met to make use of their properties. For example, skyrmions generated with either method appear stochastically distributed in the magnetic material, limiting the ability to exploit their properties for, e.g., computational applications. In addition, skyrmions are affected by a transverse deflection (skyrmion Hall effect) when moved by an electric current inside a magnetic strip line making it challenging to move skyrmions over long distances.

To obtain full control of the skyrmion position on the nanometer scale, we employ focused 30 kV He-ion irradiation to modify the magnetic anisotropy landscape of the material system without altering its topography [4]. Irradiation of areas with sizes on the order of the skyrmion dimension creates well-defined nucleation sites for SOT and laser-induced nucleation [5]. Thereby, we transform the stochastic nucleation process into a deterministic one. Furthermore, the skyrmions nucleated can be detached from their nucleation sites and moved by applying current pulses. By irradiating additional channels with He-ions, we combine controlled nucleation with the guided motion of a skyrmion over micrometer distances, suppressing unwanted deflections from the skyrmion Hall effect.

Hence, tailoring the magnetic anisotropy landscape by He-ion irradiation opens up new possibilities for skyrmion based computing devices and creates a platform for controlled experiments on the fundamental properties of skyrmions and other topological magnetic structures.

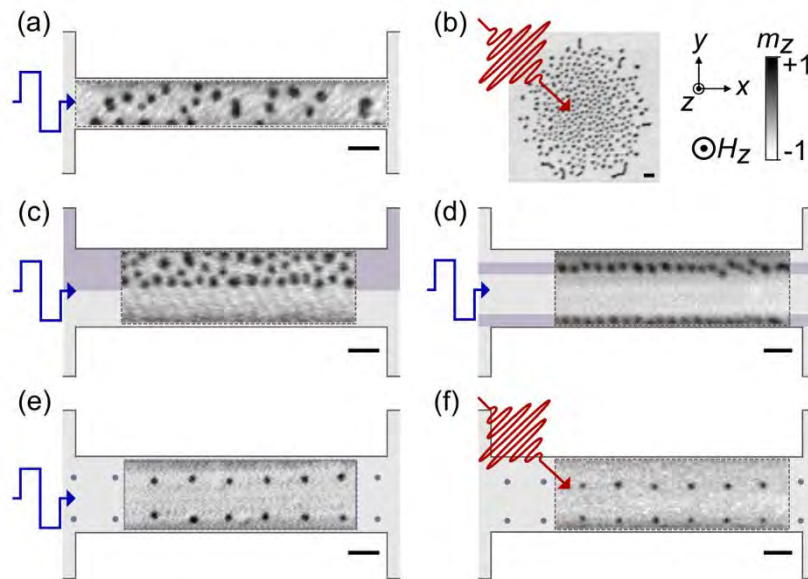


Figure 1. Localized current-induced and optical skyrmion nucleation. Panel (a) and (b) show stochastically distributed nucleated skyrmions in the pristine material by a single current and laser pulse, respectively. In panels (c) to (f), different areas are irradiated with He-ions (rectangular in (c), tracks in (d) and dots in (e) and (f)) resulting in nucleated skyrmions only in the pre-determined areas indicated by the dark shaded areas. All inset images are taken with a scanning x-ray microscope using polarized x-rays resulting in a contrast indicating the out-of-plane magnetization. All scalebars correspond to 500 nm.

- [1] Fert et al., *Nature Nanotech* 8, 152–156 (2013).
- [2] Büttner et al., *Nature Nanotech* 12, 1040-1044 (2017).
- [3] Büttner et al., *Nat. Mater.* 20, 30–37 (2021).
- [4] Fassbender et al., *J. Phys. D: Appl. Phys.* 37, R179 (2004).
- [5] Kern et al., *Nano Lett.* 22, 10, 4028–4035 (2022)

## Benefits of a Cs FIB with a low temperature ion source compared to a standard Ga FIB

Dr. Thomas Loeber, Dr. Bert Laegel, Prof. Dr. Georg von Freymann  
Nano Structuring Center (NSC), Physics Department, University of Kaiserslautern

Focused ion beam (FIB) systems are long established as a standard tool in micro and nano structuring. The most common ion beam source uses Gallium ions, because they are relatively easy to generate and handle. The beam current can vary from pA up to nA, so a wide range of applications can be covered with this kind of FIB. One of the limitations of a Ga FIB is its utilization for milling very fine structures, i.e. in the lower nm range. There are other FIBs commercially available, for example, the helium ion microscope, which has a gas field ion source. Therewith, it is possible to take high resolution images and mill very fine (small) structures. The disadvantage here is that Helium and Neon (as second possible gas source) have a very low sputter rate and large patterns take a long time to mill.

This April, the very first of a new kind of FIB, made by company ZeroK Nanotech, (Gaithersburg, MD, U.S.) was installed at the Nano Structuring Center of the TU Kaiserslautern, Germany. It employs a low temperature ion source that uses Cesium ions which are laser cooled down to almost  $T = 0K$  [1,2]. The source has a Cs oven which emits Cs atoms at a constant flux. The atom beam is cooled down and also shaped by magneto optical traps in several stages. Finally, the atoms are ionized by two overlapping focused lasers (see Fig. 1). The intensity and the diameter of the laser can be changed such that the Cs ion beam current can be varied continuously from a few pA up to several nA. Due to the low energy spread of the ions (0.45 eV; compared to 5 eV for Ga) the source can be operated at significant lower acceleration voltages from 16 down to 2 kV. A minimum spot size of about 2 nm is achieved. The Cs source has also a remarkably higher brightness than a typical Ga source (Cs:  $2.4 \times 10^7 \text{ A m}^{-2} \text{ sr}^{-1} \text{ eV}^{-1}$ ; Ga:  $10^6 \text{ A m}^{-2} \text{ sr}^{-1} \text{ eV}^{-1}$ ) [3]. In our setup the source is mounted on a standard FEI Helios 600 chamber and can be controlled with the FEI xT software just like a standard FEI Ga FIB.

The Cs FIB is used for structuring and analysis of different kind of samples. Milling is demonstrated in e.g. in silicon and other III/V semiconductors as well as different kind of metals. For ion beam characterization purposes benchmark tests are performed to measure e.g., the depth of focus of the Cs source (see Fig. 2). Also, the resolution and contrast of ion images of different samples is measured. Since we also have a standard FEI 650 NanoLab Ga FIB available at our lab, the results can be compared directly compared to this new Cs FIB.

- [1] "Cold atomic beam ion source for focused ion beam applications"  
Journal of Applied Physics 114, 044303 (2013); B. Knuffman, A. V. Steele, and J. J. McClelland
- [2] "Bright focused ion beam sources based on laser-cooled atoms"  
Applied Physics Reviews 3, 011302 (2016); J. J. McClelland, A. V. Steele, B. Knuffman, K. A. Twedt, A. Schwarzkopf, and T. M. Wilson
- [3] "High-brightness Cs focused ion beam from a cold-atomic-beam ion source"  
Nano Futures 1, 015005 (2017); A. V. Steele, A. Schwarzkopf, J. J. McClelland and B. Knuffman

# LOW Temperature Ion Souerce LOTIS

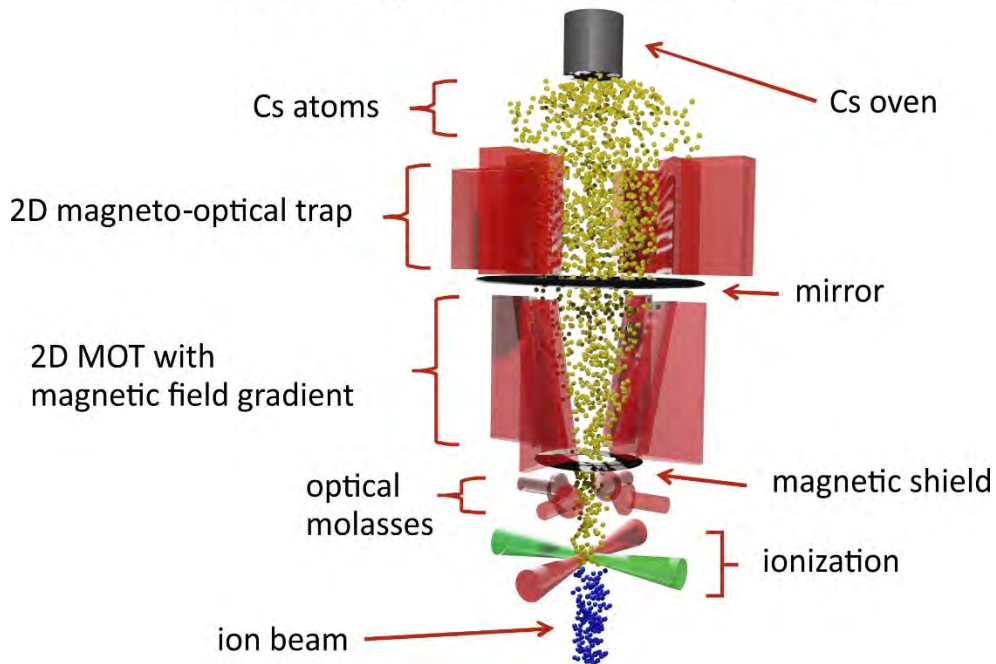


Figure 1: 3D model of the Cs ion source with the Cs oven, the different stages of cooling and the ionization of the atoms

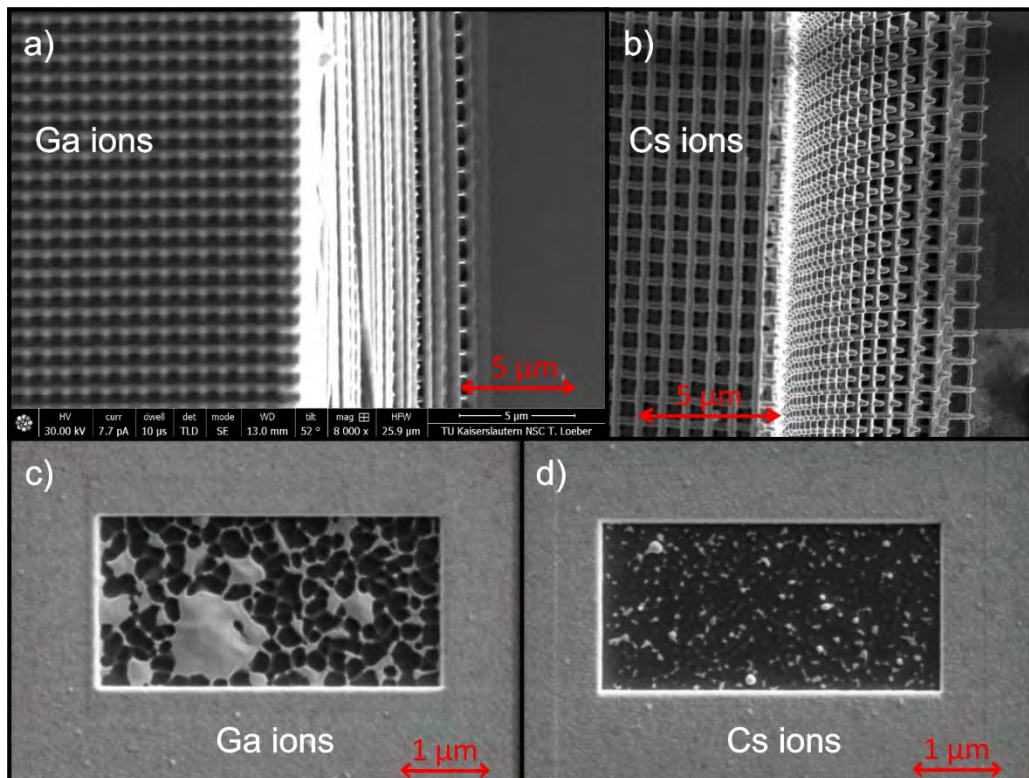


Figure 2: Images a) and b) show the comparison of the depth of focus of the Ga and Cs ion source. Both ion beams were focused at the bottom of a 120 μm high polymer structure. In the case of the Ga beam the top of the structure is out of focus, while the Cs beam is well in focus over the complete height. In images c) and d) rectangles are milled almost through a 120 nm thick polycrystalline gold film. The left structure milled with the Ga beam shows the typical inhomogeneous sputter rate artefacts due to the channeling effect. With the Cs beam this effect is much less present and an almost homogenous sputter rate is achieved

## Advanced multimodal analytical capabilities on FIB instruments using SIMS:

### Do we need to care about primary ions?

T. Wirtz, P. Philipp, O. De Castro, H.Q. Hoang, A. Ost, C. Stoffels, A. Biesemeier, J.-N. Audinot

Advanced Instrumentation for Nano-Analytics (AINA), MRT Department, Luxembourg Institute of Science and Technology (LIST), 4422 Belvaux, Luxembourg

E-Mail: tom.wirtz@list.lu

Secondary Ion Mass Spectrometry (SIMS) is an extremely powerful technique for analyzing surfaces, owing to its ability to detect all elements from H to U and to differentiate between isotopes, its excellent sensitivity and its high dynamic range. SIMS analyses can be performed in different modes: acquisition of mass spectra, depth profiling, 2D and 3D chemical imaging. Adding SIMS capability to focused ion beam (FIB) instruments offers a number of interesting possibilities, including highly sensitive analytics, highest resolution SIMS imaging (~10 nm), in-situ process control during patterning and milling, and direct correlation of SIMS data with data obtained by other analytical or imaging techniques on the same instrument, such as high-resolution secondary electron (SE) images, back-scattered electron (BSE) images or Energy-Dispersive X-Ray Spectroscopy (EDX) spectra.

In this context, we developed a double focusing magnetic sector SIMS system equipped with a novel continuous focal plane detector. This SIMS system allows for the detection of all masses in parallel for each single pixel, resulting in acquisition times as low as 1 s to obtain a full mass spectrum or 2 min to obtain a 512 x 512 pixel SIMS image with highest signal-to-noise ratio and excellent dynamic range.

This SIMS system is now operating on several multi-modal FIB platforms, including Thermo Fisher Dual-Beam systems [1], ZEISS ORION NanoFab Helium Ion Microscopes [2,3] and the zeroK SIMS:ZERO platform [4]. The FIB columns of these instruments cover a diverse range of ion species: He, Ne, Ar, Ga, Xe, Cs. Due to their differences in size, mass and chemical reactivity, they lead to differences in sputter yields, fragmentation, dimensions of the collision cascades triggered in the sample and ionization probabilities of the sputtered atoms and molecules.

Here, we will first briefly present the different instruments with a focus on new developments. We will then discuss the specificities related to the different primary ions that are used and present several examples from various fields of applications (nanoparticles, battery materials, photovoltaics, micro-electronics, tissue and sub-cellular imaging in biology, geology, ...).

[1] Magnetic sector secondary ion mass spectrometry on FIB-SEM instruments for nanoscale chemical imaging, O. De Castro, J.-N. Audinot, Q. H. Hoang, C. Coulbary, O. Bouton, R. Barrahma, A. Ost, C. Stoffels, C. Jiao, M. Dutka, M. Geryk, T. Wirtz, *Anal. Chem* (2022)

[2] Imaging and analytics on the Helium Ion Microscope, T. Wirtz, O. De Castro, J.-N. Audinot, P. Philipp, *Annual Review of Analytical Chemistry* 12 (2019) 523-543

[3] Highest resolution chemical imaging based on Secondary Ion Mass Spectrometry performed on the Helium Ion Microscope, J.-N. Audinot, P. Philipp, O. De Castro, A. Biesemeier, Q. H. Hoang, T. Wirtz, *Rep. Prog. Phys.* 84 (2021) 105901

[4] High-brightness Cs focused ion beam from a cold-atomic-beam ion source, A. V. Steele, A. Schwarzkopf, J. McClelland, B. Knuffman, *Nano Futures* 1 (2017) 015005



## Explore unlimited process pathways for FIB nanopatterning and ion imaging using VELION

T. Richter, A. Nadzeyka, L. Bruchhaus, P. Mazarov

Raith GmbH, Konrad-Adenauer-Allee 8, 44263 Dortmund, Germany

torsten.richter@raith.de

Focused Ion Beam (FIB) nano patterning has become established as a versatile and precise fabrication method of manifold features at the nanoscale. Applications in nanoscale science require high resolution fabrication techniques at high fidelity, accuracy and reproducibility over multiple write fields in an automated manner.

VELION's configurable multi-ion species FIB technology enables tailoring of various nanostructures according to application related challenges. Various ion species can be selected from universal ion sources providing fast or slow and light or heavy ions from a single source [1]. This approach paves the way for unlimited process pathways based on a FIB system merged with a true lithography platform. Unmatched large-area FIB patterning and unlimited perfect write field stitching or patterning overlay facilitates various patterning strategies according to specific applications. As VELION utilizes comprehensive automation for unattended, uninterrupted reliable nanofabrication over several days, the instrument is the ideal companion for machine driven nanofabrication.

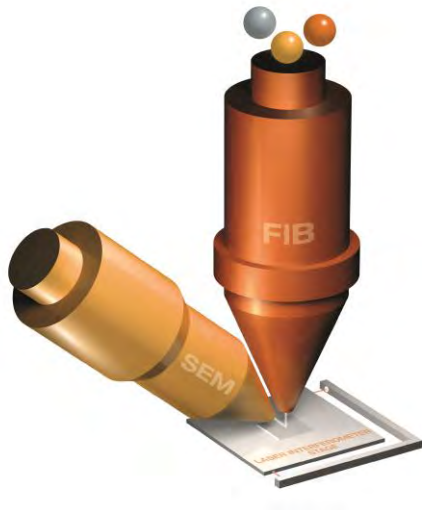
In this contribution we present the instrument concept, an overview of various nanofabrication approaches and application such as direct patterning, hard masking, or sample functionalization.

Beyond nanopatterning, VELION FIB with its Liquid Metal Alloy Ion Sources (LMAIS) provides excellent ion beam imaging capabilities [2]. Lithium is the lightest ion for LMAIS available from periodic table and provides sub 2nm lateral image resolution. Latest results of 3D Mill&Image sample analysis will be presented utilizing the best depth milling resolution with Bismuth and superior lateral resolution with Lithium ions.

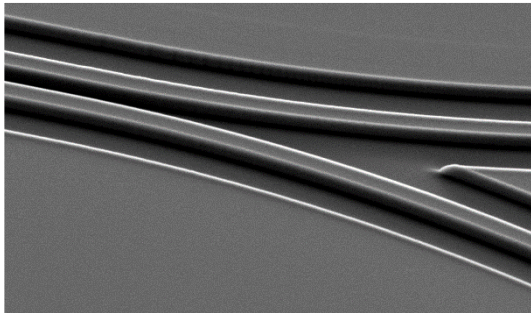
[1] J. Gierak, P. Mazarov, L. Bruchhaus, R. Jede, L. Bischoff, Review of electrohydrodynamical ion sources and their applications to focused ion beam technology, JVSTB 36, 06J101 (2018).

[2] N. Klingner, G. Hlawacek, P. Mazarov, W. Pilz, F. Meyer, and L. Bischoff, Imaging and milling resolution of light ion beams from helium ion microscopy and FIBs driven by liquid metal alloy ion sources, Beilstein J. Nanotechnol. 11, 1742 (2020)

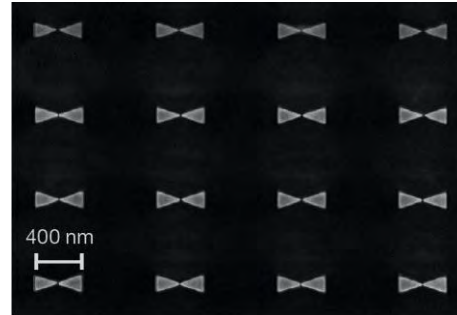




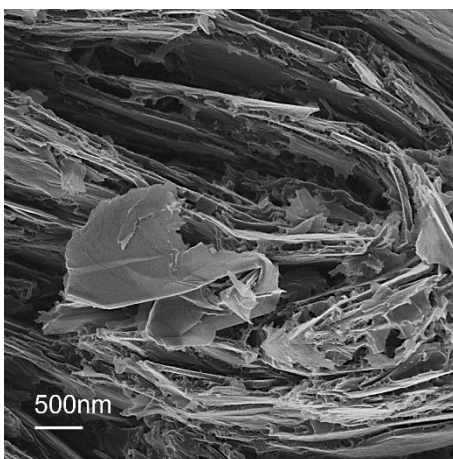
*Left: General VELION setup with vertical FIB column on Laser Interferometer Stage and SEM  
Right: Multi ion species FIB from Liquid Metal Alloy Ion Sources.*



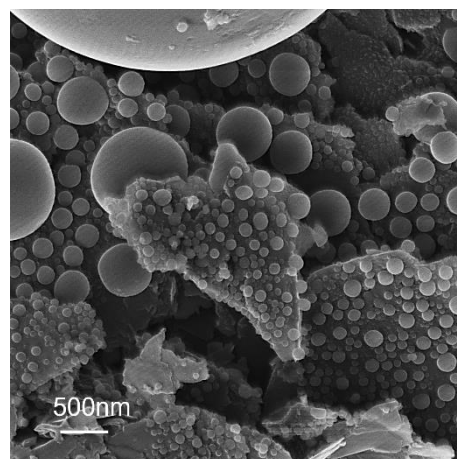
*Waveguide coupler*



*Stepwise fabrication of nano bowties with Bismuth and Lithium ions*



*Lithium-ion image of graphite*



*Lithium-ion image of Sn/C*

# Advanced microstructure analysis using cutting edge multiple ion species plasma FIB

Min Wu

Thermo Fisher Scientific, Eindhoven, The Netherlands

E-Mail: min.wu@thermofisher.com

Additive particles and agglomerates serve multiple functions in tires such as antioxidants, heat resisting elements, binders and others. The morphology, size and chemical distribution of these additive materials determine overall tire materials properties such as strength, elasticity, fuel efficiency, wear resistance and wet grip, etc. Meanwhile, since construction materials such as steel wires are used for reinforcement in tires, the microstructure of metal cords and adjacent rubber interface has been in significant ongoing research interests because gradual degradation of polymer metal interface fundamentally affects tire lifetime.

In this abstract we present the results of two multi scale electron microscopic characterizations on tire materials using cutting edge instruments. In the first dataset we investigated the 3D morphology and chemical distribution of additive particles in tire rubber volume using advanced multiple ion species plasma focused beam system integrated with femtosecond laser beam, the Helios Laser Hydra. The cut face quality on tire rubber and additive particles using different ion species with various beam parameters is also compared and analyzed. In the second dataset the polymer metal interface microstructure has been characterized using Helios Hydra system. A piece of lamella was extracted from the interface and subsequently analyzed using transmission electron microscopy (TEM) equipped with energy dispersive X-ray spectroscopy (EDS).

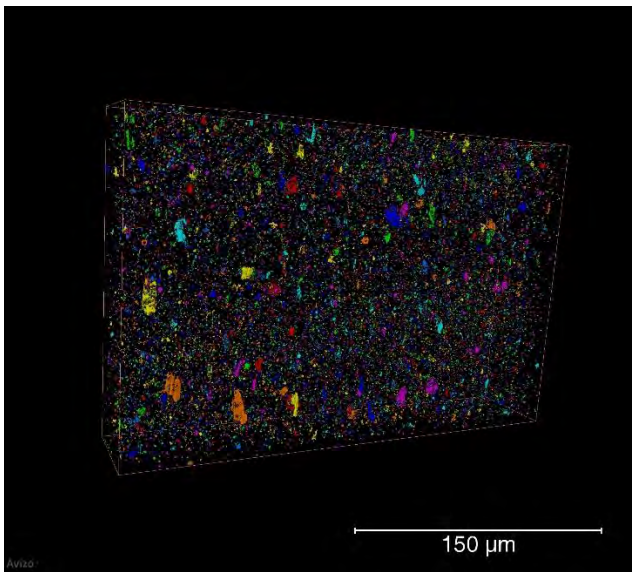


Figure 1: 3D reconstruction of particle analysis in tire materials.



**PELIICAEN setup status: Performances and new developments for elaboration and  
characterization of materials at nanoscale**

Mathieu Lalande <sup>1,2</sup>, Pierre Salou <sup>1,2</sup>, Arnaud Houel <sup>2</sup>, Thierry Been <sup>1</sup>, Thierry Birou <sup>2</sup>, Charles Bourin <sup>2</sup>,  
Amine Cassimi <sup>1</sup>, Arthur Keizer <sup>2</sup>, Jean-Baptiste Mellier <sup>2</sup>, Jean-Marc Ramillon <sup>1</sup>, Anthony Sineau<sup>1</sup>,  
Anne Delobbe <sup>2</sup>, and Stéphane Guillous <sup>1</sup>

<sup>1</sup> CIMAP, UMR 6252 (CEA/CNRS/ENSICAEN/Université de Caen Normandie), Caen, France

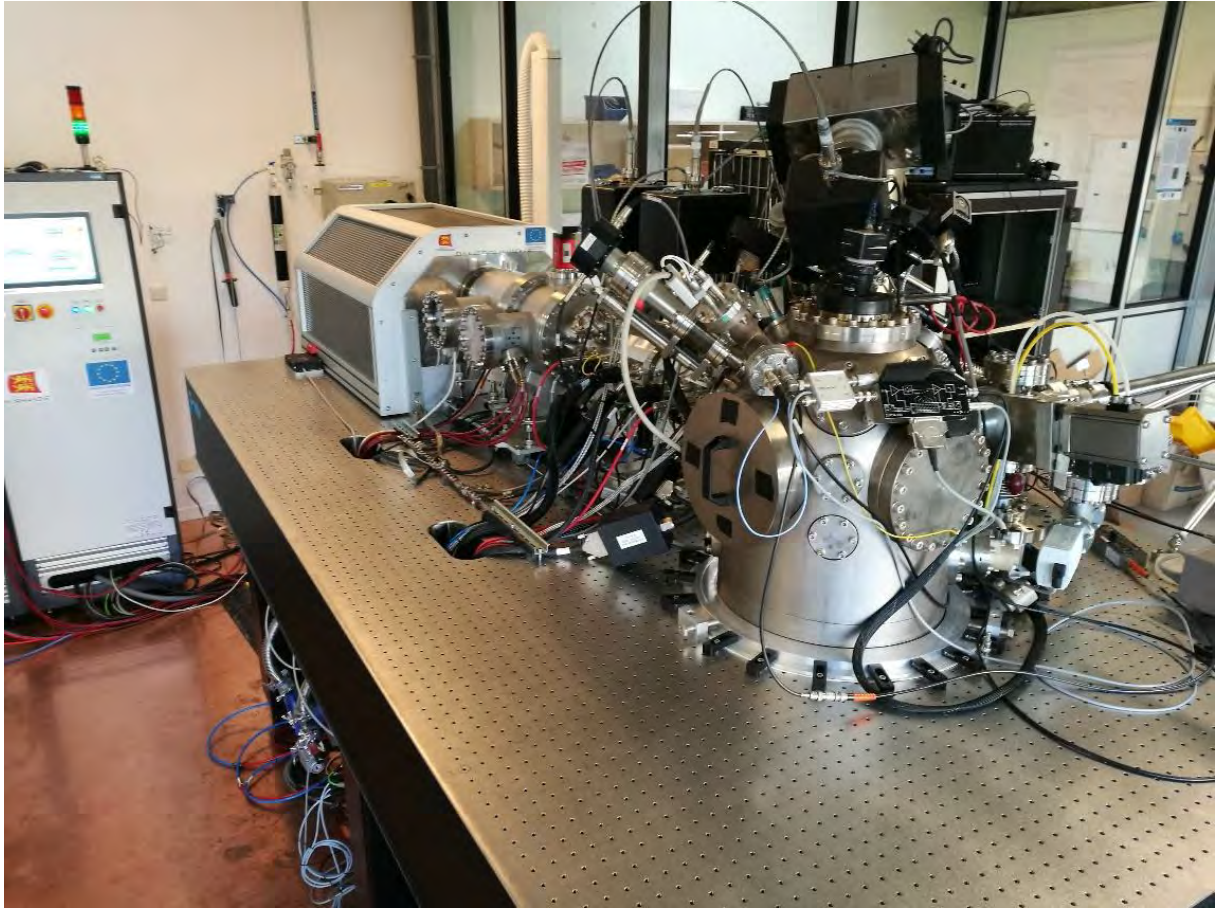
<sup>2</sup> Orsay Physics–Tescan Orsay Holding, Fuveau, France

E-Mail: (guillous@ganil.fr)

Since 2015, the PELIICAEN [1] (Platform for the Study of Ion Implantation Controlled and Analyzed at the Nanometric Scale) setup has demonstrated its capabilities to produce focused mono and multiply charged ions beam of sub-micron size on the ARIBE installation at GANIL (Grand Accélérateur National d'Ions Lourds). Recently, the setup has been upgraded to equip the platform with an ECRIS (Electron Cyclotron Resonance Ion Source) in order to make it autonomous and improve its performances [2]. The system can now provide mono and multiply charged ion beams of a broad range of species (H to Bi) and kinetic energies (from 2 to more than 500 keV), up to middle range charge states (Ar<sup>8+</sup>, Bi<sup>17+</sup>), focused down to a 100 nm spot size. Thus, we can now reach an image resolution of 25 nm and fluxes up to 10<sup>17</sup> ions/cm<sup>2</sup>/s. In addition, we developed an ultra-high-performance pulser that allows us to erase the beams in situ in less than 2 ns, without any tail, with repetition rates up to 1 MHz, thus enabling us to use these focused beams for time-of-flight chemical analysis such as for SIMS (Secondary Ion Mass Spectroscopy) and LEIS/MEIS (Low or Middle Energy Ion Scattering) or to be able to move towards single ion implantation at high repetition rates.

The apparatus also includes different types of in-situ microscopes such as a SEM (Scanning Electron Microscope) and a SPM (Scanning Probe Microscopies) in Ultra High Vacuum environment below 10<sup>-9</sup>mbar. The SPM will be upgraded this summer so to offer more possibilities of in-situ correlative physical property analysis such as mechanical, electrical or magnetical.

By using all these means, localized doping is possible for applications in quantronics and development of embedded sensors, localized 3D nano-structural modifications using non-contaminating beams ranging from milling to swelling, and localized multi-analysis with multiply charged ions (MC-TOF-SIMS, MC-LEIS/MEIS) coupled with SEM and SPM. Some results and examples of use will be presented showing the whole performance of PELIICAEN apparatus.



#### ACKNOWLEDGMENTS

Equipment for this study was funded by the French National Research Agency (ANR) in the Peliicaen Project (Grant No. ANR-12-NANO-008) and the LabCom CiCLOp (Grant No. ANR-18-LCV3-0005-01), by Région Normandie RIN Recherche and European Union ERDF funds (Grant No. EVOL-Peliicaen [17P04263]), and by the RADIATE project under the Grant Agreement No. 824096 from the EU Research and Innovation program HORIZON 2020.

#### REFERENCES

- [1] S. Guillous et al., "A new setup for localized implantation and live-characterization of keV energy multiply charged ions at the nanoscale," *Rev. Sci. Instrum.* 87, 113901 (2016).
- [2] Mathieu Lalande et al., "Nanoscale multiply charged focused ion beam platform for surface modification, implantation and analysis", *Rev. Sci. Instrum.* 93, 043703 (2022)



## Insulator on conductor ion source: first results and measurements

M. Laurencich<sup>1</sup>, L. Lapena<sup>1</sup>, M. Lagaize<sup>1</sup>, A. Houël<sup>2</sup>, A. Delobbe<sup>2</sup>, E. Salançon<sup>1</sup>

<sup>1</sup>CINaM, UMR 7325, campus de Luminy – case 913, 13288 Marseille cedex 9

<sup>2</sup>OrsayPhysics, Cht De L'arc, 95 AV des Monts Aurélien, 13710 Fuveau

E-Mail: (evelyne.salancon@univ-amu.fr)

An insulator on conductor structure has shown its ability to produce intense electric field [1]. Field emission and high brightness electron source has been developed in a new kind of point projection microscope [2]. Because the intense local field is proportional to the bias voltage applied, field ionization has been studied. Inserted in a field ion microscope, in a partial pressure of about  $P=10^{-3}$  mbar (Xenon or Argon), this structure made of a celadonite crystal deposited on a  $10\mu\text{m}$  carbon fiber has emitted ions. A localized emission has been stabilized during some hours. We have used a grid as extractor and observed a high contrast on the projected image. The intensity of emission has reached some nA for a bias voltage applied on the emitter of about  $V=10\text{kV}$ . Lifetime of this ion source has not yet been studied but the emission intensity decreases after some  $I(V)$  measurements having been made in few hours. The support of the source appears completely sputtered after ion emission. Nevertheless, these preliminary results give a good hope concerning the field ionization with insulator on conductor structures.

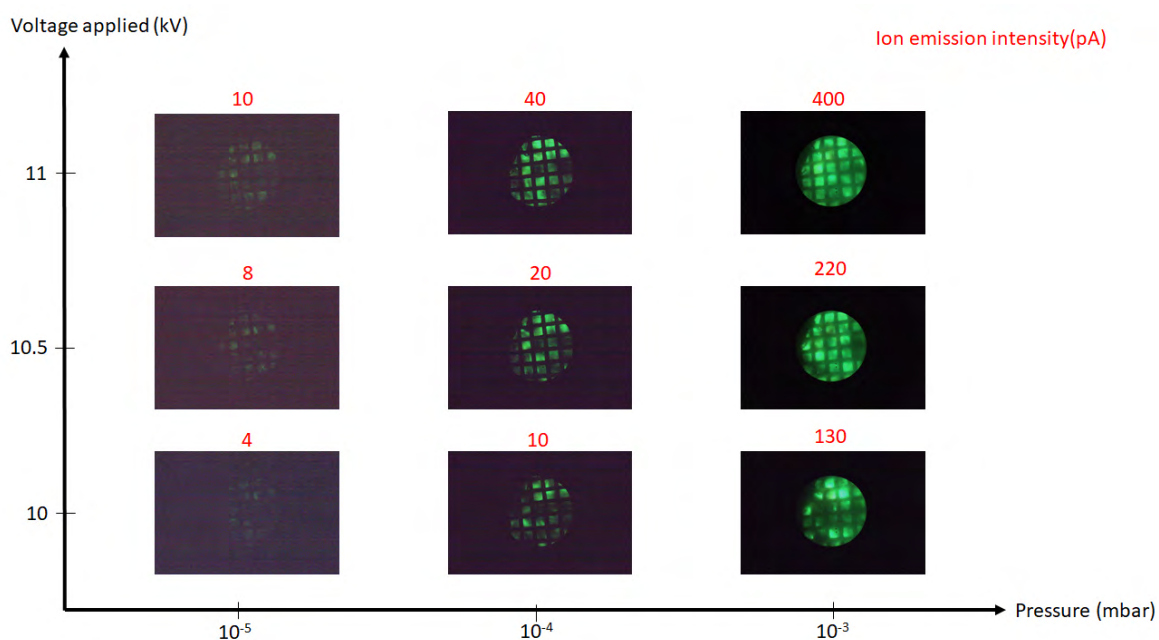


FIG. 1: Cartography  $I(P,V)$  of field ion emission produced with an insulator on conductor structure. Ionized gas: Argon.

## References

- [1] Laurent Lapena, Alain Degiovanni, Victoria Tishkova, and Evelyne Salançon "Low-macroscopic field emission structure: Using the shape of the conductor to identify a local difference in electric potential", Journal of Vacuum Science & Technology B 40, 024004 (2022) <https://doi.org/10.1116/6.0001716>
- [2] Evelyne Salançon, Alain Degiovanni, Laurent Lapena, Mehdi Lagaize, Roger Morin, "A low-energy electron point-source projection microscope not using a sharp metal tip performs well in long-range imaging", Ultramicroscopy 200, 125-131 (2019), <https://doi.org/10.1016/j.ultramic.2019.02.022>.



## Laser-cooled Cs<sup>+</sup> source meets magnetic sector SIMS: a unique platform for highest sensitivity nano-analytics

O. De Castro<sup>1</sup>, J. N. Audinot<sup>1</sup>, Chérif Coulbary<sup>1</sup>, Hung Quang Hoang<sup>1</sup>, Olivier Bouton<sup>2</sup>, Rachid Barahma<sup>2</sup>, Brenton Knuffman<sup>3</sup>, Adam Steele<sup>3</sup> and T. Wirtz<sup>1</sup>

<sup>1</sup>Advanced Instrumentation for Nano-Analytics (AINA), MRT Department, Luxembourg Institute of Science and Technology, 41 rue du Brill, L-4422 Belvaux, Luxembourg.

<sup>2</sup>Prototyping, MRT Department, Luxembourg Institute of Science and Technology, 41 rue du Brill, L-4422 Belvaux, Luxembourg.

<sup>3</sup>ZeroK NanoTech, 401 Professional Dr, Suite 125, Gaithersburg, Maryland, MD 20879, USA.

E-Mail: olivier.decastro@list.lu

In recent years, compact magnetic sector secondary ion mass spectrometry (SIMS) systems have been successfully deployed on different focused ion beam (FIB) platforms, so called FIB-SIMS, using He<sup>+</sup>, Ne<sup>+</sup> [1,2] and Ga<sup>+</sup> beams [3]. These FIB-SIMS platforms allow sub-20 nm resolution chemical imaging at excellent sensitivity. A further increase of the sensitivity of the analysis can be reached by exposing the sample to reactive species, i.e., oxygen for enhancing the emission of positive ions and cesium for increasing the negative ionization probability. While exposing the sample to oxygen is routinely done by injecting low amounts of oxygen gas into the analysis chamber via a leak valve, Cs gas flooding has also been successfully demonstrated but is more complex from a technical point of view [4,5]. Therefore, performing SIMS with a Cs<sup>+</sup> primary ion beam remains the most straightforward approach if extremely high sensitivity in the negative SIMS mode is required.

In this context, we coupled the afore mentioned compact magnetic sector SIMS system with the low temperature ion source (LoTIS) technology [6], which allows producing Cs<sup>+</sup> ion beams with a probe size of 2 nm. Here, we will present the newly developed instrument called SIMS:ZERO, discuss its performance and show application results in materials science and life sciences.

An example of an application case is shown in Figure 1, where diatoms have been imaged in Cs<sup>+</sup> induced secondary electron mode and correlated with SIMS images taken from the same region of interest in negative mode. The Si<sup>-</sup> SIMS image (Figure 1b) is representative for the skeleton structure of the imaged diatoms and the C<sub>2</sub><sup>-</sup> SIMS image (Figure 1c) can be seen as a fingerprint for organic matter residues.

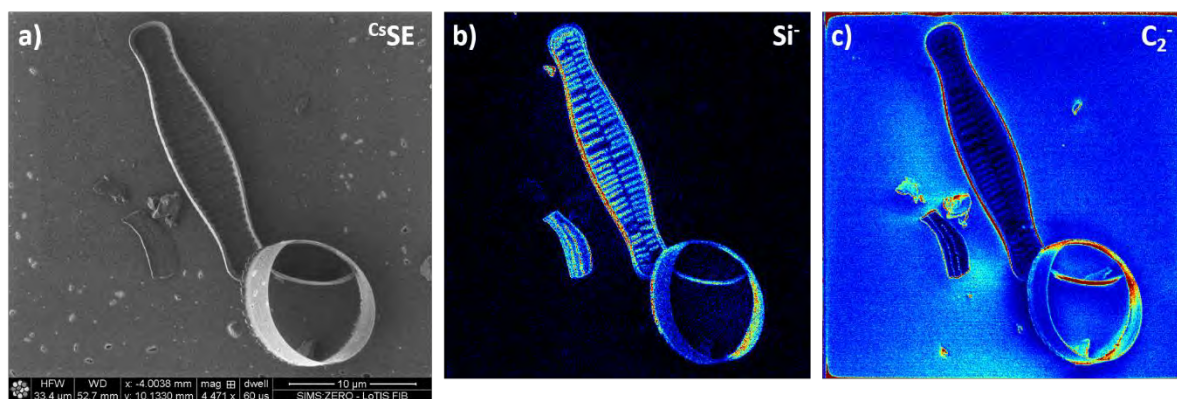


**Figure 1:** Correlative imaging of diatoms using the SIMS:ZERO instrument: a) Secondary electron image; b) Si<sup>-</sup> SIMS image; c) C<sub>2</sub><sup>-</sup> SIMS image. (Field of view: 33.4x33.4 μm<sup>2</sup>; Cs<sup>+</sup>: 16 keV, 7.4 pA).



- [1] J. N. Audinot et al.; Highest resolution chemical imaging based on Secondary Ion Mass Spectrometry performed on the Helium Ion Microscope. *Reports Prog. Phys.* **2021**, *84*, 105901, p. 1 - 41. <https://iop-science.iop.org/article/10.1088/1361-6633/ac1e32>
- [2] O. De Castro et al.; npSCOPE: A New Multimodal Instrument for In Situ Correlative Analysis of Nanoparticles. *Anal. Chem.* **2021**, *93* (43), 14417–14424. <https://doi.org/10.1021/acs.analchem.1c02337>
- [3] T. Wirtz et al.; Multimodal characterisation on FIB instruments combining nano-scale SIMS and SE imaging. *Microscopy and Microanalysis* **2021**, *27* (S1), p. 1008 – 1010. [https://www.cambridge.org/core/product/identifier/S1431927621003810/type/journal\\_article](https://www.cambridge.org/core/product/identifier/S1431927621003810/type/journal_article)
- [4] P. Philipp, T. Wirtz, H. Migeon, H. Scherrer; Important increase of negative secondary ion sensitivity during SIMS analysis by neutral cesium deposition. *Applied Surface Science* **2006**, *252* (19), p. 7205-7207. <https://linkinghub.elsevier.com/retrieve/pii/S0169433206004223>
- [5] L. Pillatsch, N. Vanhove, D. Dowsett, S. Sijbrandij, J. Notte and T. Wirtz; Study and optimisation of SIMS performed with He<sup>+</sup> and Ne<sup>+</sup> bombardment. *Applied Surface Science* **2013**, *282*, p. 908-913. <https://linkinghub.elsevier.com/retrieve/pii/S0169433213011999>
- [6] A. V. Steele et al.; High-brightness Cs focused ion beam from a cold-atomic-beam ion source. *Nano Futures* **2017**, *1* (1), p. 15005. DOI: 10.1088/2399-1984/aa6a48

## **Ion yields enhancement in FIB-TOF-SIMS by fluorine gas coinjection - A comprehensive study of 41 pure elements and multicomponent samples**

K. Wieczerek<sup>1</sup>, M. Wątroba<sup>1</sup>, J. Michler<sup>1</sup>

<sup>1</sup>Empa, Swiss Federal Laboratories for Materials Science and Technology, Laboratory for Mechanics of Materials and Nanostructures, CH-3602 Thun, Switzerland

E-Mail: krzysztof.wieczerek@empa.ch

High vacuum-compatible time-of-flight secondary ion mass spectrometry (TOF-SIMS) detectors are gaining in popularity, due to their easy integration to existing focused ion beam (FIB) instruments. Compared to dedicated TOF-SIMS systems, this solution is not only cost-effective but enables conducting correlative and/or complementary studies with other techniques, such as scanning electron microscopy, energy dispersive spectroscopy (EDS), wavelength dispersive spectroscopy (WDS), electron backscatter diffraction (EBSD), atomic force microscopy (AFM), and Raman spectroscopy without breaking vacuum conditions. FIB-TOF-SIMS can be applied for the chemical characterization of a wide range of organic and inorganic materials with parallel mass detection of all elements in a sputtered volume. However, a primary Ga<sup>+</sup> beam, typical for FIB systems, is less effective for the production of secondary ions compared to dedicated instruments equipped with reactive sources, such as O<sub>2</sub><sup>+</sup> or Cs<sup>+</sup>. To overcome this limitation, we propose modifying the samples' surface with fluorine to facilitate secondary ion generation.

In this talk, the practical aspects of FIB-TOF-SIMS analysis enhanced by fluorine gas will be discussed. We will show that fluorine-assisted FIB-TOF-SIMS measurements yield up to several orders of magnitude higher SIMS signals due to chemically improved ionization probability of various elements. This will be evidenced by results obtained during the analysis of high-purity single elements and multicomponent alloys with heterogeneous microstructures. Our studies indicate that the presence of fluorine gas reduces the negative effect of preferential reoxidation of the sample's surface. In turn, this decreases the probability of oxygen-enhanced ionization that would normally dominate the secondary ion signal, enabling to attain high lateral resolution FIB-TOF-SIMS maps.

# Combining cryo-FIB milling with cryo-electron tomography enables macromolecular insights into biological samples

Gregor L. Weiss

Institute of Molecular Biology and Biophysics, ETH Zurich, 8093, Zurich, Switzerland

E-Mail: gregor.weiss@mol.biol.ethz.ch

Imaging flash-frozen biological samples by cryo-electron tomography (cryoET) has become a powerful method for different research fields in biology. CryoET is a modality of cryo-electron microscopy and resolves macromolecular complexes in their native cellular context and at several nanometer of resolution.

However, cryoET is limited to samples that have a thickness well below 800 nm. For thicker samples, cryo-thinning techniques must be applied to overcome this limitation. While cryo-sectioning could generate some insights, the technique is challenging, cannot be automated and introduces artifacts that prevent high-resolution imaging approaches. The adaptation of cryo-focused ion beam (FIB) milling to prepare thin electron-transparent lamellae through biological samples enabled a multitude of groundbreaking insights into the structure and function of cells – from bacterial to eukaryotic model organisms. The throughput of cryo-FIB milling for biological samples was very low at the beginning and required a large amount of user input. To tackle this bottleneck, we developed in collaboration with Zeiss a procedure to automate the processes to sequentially mill multiple targets, which significantly increased the throughput. The thinning of well-established model organisms using cryo-FIB milling for subsequent cryoET studies is nowadays routine and is becoming more and more popular. However, the application of this thinning technique to more complex and large samples, such as environmental or clinical samples, remains challenging.

During my talk, I will present our latest efforts in applying a combined imaging workflow to more complex biological samples, with a specific focus on clinical samples such as body fluids or tissue biopsies. In this approach we use cryo-light microscopy to target rare events for subsequent correlated cryo-FIB milling for sample thinning, cryo-volume imaging for the integration of imaging datasets across scales and cryoET for high-resolution structural analysis.

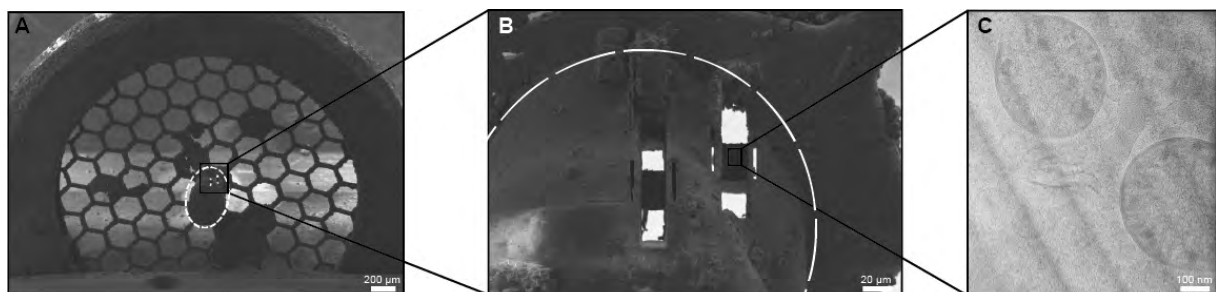


**Figure 1:** Towards the analysis of clinical samples and biopsies with a cryo-FIB milling and cryo-electron tomography imaging workflow. **(A)** SEM image of high-pressure frozen mouse biopsy (circled by dashed white line) on EM grid. **(B)** Two cryo-FIB milled lamellae through frozen biopsy. **(C)** 2D cryoTEM image of lamella shows fully vitrified cellular features like mitochondria. In collaboration with R. Irobalieva, ETH Zürich.

# High-throughput direct writing of metallic micro- and nanostructures by focused Ga<sup>+</sup> beam irradiation of palladium acetate films

Alba Salvador-Porroche<sup>1,2</sup>, Lucía Herrer<sup>1,2</sup>, Soraya Sangiao<sup>1,2</sup>, Patrick Philipp<sup>3</sup>, Pilar Cea<sup>1,2</sup>, and José María de Teresa<sup>1,2</sup>.

<sup>1</sup> Instituto de Nanociencia y Materiales de Aragón (INMA), CSIC-Universidad de Zaragoza, 50009, Zaragoza, Spain.

<sup>2</sup> Laboratorio de Microscopías Avanzadas (LMA), Universidad de Zaragoza, 50018, Zaragoza, Spain.

<sup>3</sup> Luxemburg Institute of Science and Technology (LIST), L-4422, Belvaux, Luxembourg.

E-Mail: asalvador@unizar.es

Nowadays, the fabrication of metallic nanopatterns is of great interest in applications that exploit the electrical conduction at the nanoscale, such as in interconnects, electrical nanocontacts and small gaps between metallic pads. Mature techniques such as optical lithography, electron beam lithography, or nanoimprint lithography are commonly used for metal patterning with high resolution and throughput but with the main disadvantage of being multi-step resist-based techniques. Furthermore, direct-write techniques such as focused ion beam or scanning probe lithography show high-resolution capabilities, but at the expense of low throughput.

Previous studies described the fabrication of metallic Pd nanostructures with the use of post-treatment steps [1,2]. In this work, we present the efficient decomposition of Pd<sub>3</sub>(OAc)<sub>6</sub> spin-coated films by means of focused Ga<sup>+</sup> beam irradiations which leads to metallic Pd deposits avoiding subsequent pre or post-treatment steps (Figure 1a). After optimizing the growth parameters, we found that using a low dose as 20 μC/cm<sup>2</sup> is sufficient to create deposits with a high palladium content (>50%) and with a resistivity as low as 70 μΩ·cm (Figure 1b). The low processing time together with the good electrical conductivity make these Pd deposits very interesting for a wide variety of applications. As a proof of concept, three different applications are demonstrated in the present work. Firstly, these deposits are used as metallic contacts to measure Pt nanowires. Secondly, two large structures are fabricated faced each other separated by only 40 nm for possible application in molecular electronics. Finally, the construction of large-area meshes with additional physical properties such as optical transparency is also demonstrated.

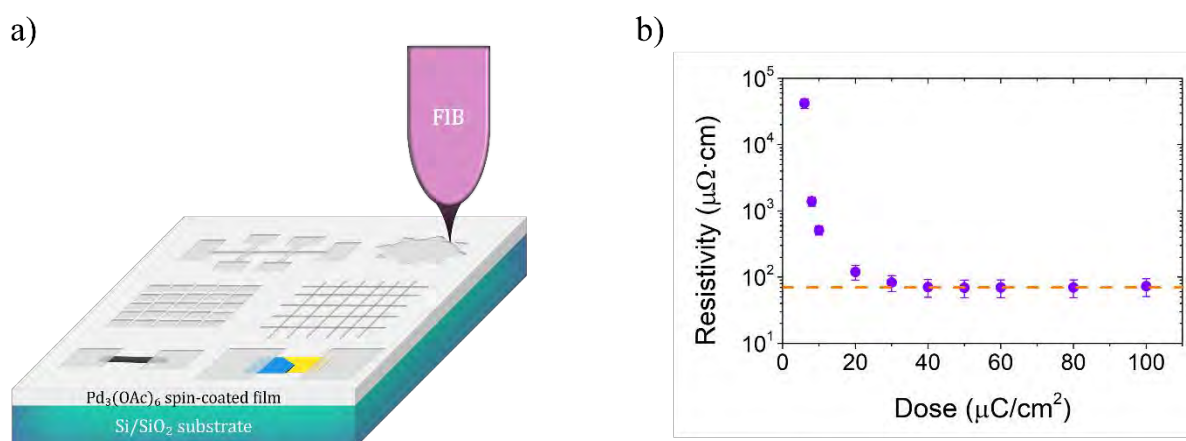


**Figure 1.** a) Scheme illustrating the formation of Pd deposits through the decomposition of an organometallic spin-coated film with the use of a focused ion beam. b) Electrical resistivity of Pd deposits as a function of the ion dose.

**References:**

1. L. R. Harriott, K. D. Cummings, M. E. Gross and W. L. Brown, *Appl. Phys. Lett.*, **49** (1986), 1661–1662.
2. M. E. Gross, W. L. Brown, L. R. Harriott, K. D. Cummings, J. Linnros and H. Funsten, *J. Appl. Phys.*, **66** (1989), 1403–1410.

**Acknowledgements:**

Authors acknowledge grants PID2019-105881RB-I00 and PID2020-112914RB-I00 funded by MCIN/AEI/ 10.13039/501100011033 and PIE 202060E187 funded by CSIC.

## Selection of coordination compounds for the study of interactions with a focused ion beam

K. Madajska<sup>1</sup>, A. Butrymowicz<sup>1</sup>, I. B. Szymańska<sup>1</sup>

<sup>1</sup> Faculty of Chemistry, Nicolaus Copernicus University in Toruń, Gagarina 7, 87-100 Toruń, Poland

E-mail: pola@umk.pl

Focused ion beam induced deposition (FIBID) is a technique based on the local dissociation of the adsorbed precursor molecules on the substrate upon irradiating with an ion beam. This method can be used for making 2D and 3D nanostructures of metals and composites. An important issue is finding precursors for metals that currently cannot be deposited with the FIBID method. Due to the precursors dedicated to this method should have adequate volatility, CVD and ALD precursors are still inspirations [1]. However, the effective interactions with ions or secondary electrons are equally important.

Here we report the procedure of the potential precursor selection. A number of methods were used, such as electron impact mass spectrometry (EI MS), variable temperature infrared spectroscopy (VT IR), thermal analysis, and sublimation experiments have been used to confirm that the studied compounds can be a source of metal carriers in the gas phase. The sensitivity of complexes to the high-energy electron beam has been taken into account; therefore, observations were made using scanning (SEM, 20 keV) and transmission (TEM, 200 keV) electron microscope. Finally, the thin films of compounds suitable for FIB experiments were fabricated based on sublimation data. For the first experiments two copper(II) complexes have been selected  $[Cu_2(\mu_3-O_2C^tBu)_2(\mu_2-O_2C^tBu)_2]_n$  [2] and b)  $[Cu_2((NH=)NH_2CR_f)_2(\mu-O_2CC_2F_5)_4]$ ,  $R_f = C_2F_5$  [3].

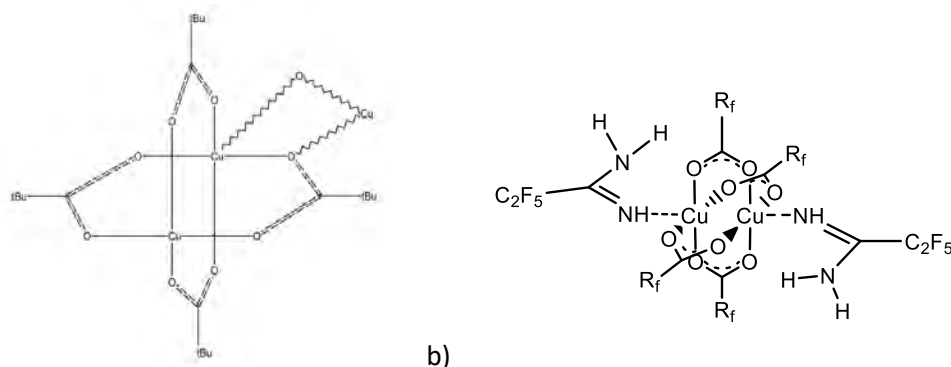


Fig. 1: The structures of potential copper FIBID precursors a)  $[Cu_2(\mu_3-O_2C^tBu)_2(\mu_2-O_2C^tBu)_2]_n$  [2], b)  $[Cu_2((NH=)NH_2CR_f)_2(\mu-O_2CC_2F_5)_4]$ ,  $R_f = C_2F_5$  [3].

Acknowledgments: The authors thank Nicolaus Copernicus University in Torun for the financial support (PDB no.103).

[1] I. Utke, P. Swiderek, K. Höflich, K. Madajska, J. Jurczyk, P. Martinović, I.B. Szymańska, Coordination and organometallic precursors of group 10 and 11: Focused electron beam induced deposition of metals and insight gained from chemical vapour deposition, atomic layer deposition, and fundamental surface and gas phase studies, *Coord. Chem. Rev.* 458 (2022) 213851. <https://doi.org/10.1016/j.ccr.2021.213851>.

[2] Il'ina E.G., Troyanov S.I., Dunaeva K.M., *Koordinatsionnaia khimiia*, 18 (1992) 18.

[3] K. Madajska, I.B. Szymańska, New volatile perfluorinated amidine-carboxylate copper(II) complexes as promising precursors in CVD and FEBID methods, *Materials (Basel)*. 14 (2021) 3145. <https://doi.org/10.3390/ma14123145>.

## New Cu Precursors for Ion Beam Induced Deposition under Gallium FIB

B.R. Jany<sup>1</sup>, K. Madajska<sup>2</sup>, A. Butrymowicz<sup>2</sup>, I.B. Szymańska<sup>2</sup>, and F. Krok<sup>1</sup>

<sup>1</sup> Institute of Physics, Jagiellonian University in Krakow, Lojasiewicza 11, 30-348 Krakow, Poland

<sup>2</sup> Faculty of Chemistry, Nicolaus Copernicus University in Torun, Gagarina 7, 87-100 Torun, Poland

E-Mail: [benedykt.jany@uj.edu.pl](mailto:benedykt.jany@uj.edu.pl)

Copper is commonly used metal for the electronics applications due to its properties like high thermal and electrical conductivity. Among the copper precursors tested in metal lithographic deposition under electron or ion beam so far, the highest metal content of 26 At. % was obtained for Cu(tbaoac)<sub>2</sub> (tbaoac- tert-butylacetoacetate) [1].

We tested two new Cu coordination compounds as potential precursors [Cu<sub>2</sub>(NH<sub>2</sub>NHCC<sub>2</sub>F<sub>5</sub>)<sub>2</sub>(O<sub>2</sub>CC<sub>2</sub>F<sub>5</sub>)<sub>4</sub>] and [Cu<sub>2</sub>(O<sub>2</sub>C<sup>t</sup>Bu)<sub>4</sub>] for the applications in Ion Beam Induced Deposition (IBID) under Gallium FIB. The first one was synthesized by the direct reaction of copper(II) pentafluoropropionate with amidine [2] and the second one in reaction of copper(II) nitrate with sodium pivalate [3]. Later, the precursors layers of thickness of ~6-8 μm were deposited on the silicon substrate under reduced pressure (10<sup>-4</sup> mbar), by sublimation. Precursor layer decomposition experiments were performed using Gallium FIB in FEI's Quanta 3D FEG dual beam SEM/FIB microscope. The decomposition process of the precursor layer results in the formation of isolated structures with a morphology dependent on the fluence of the incident Ga FIB beam. The relative changes in the stoichiometry of the modified layers were monitored by determining the change in the BSE SEM signal intensity, which is proportional to the average atomic number. Chemical quantification of the degraded precursors was performed using Machine Learning decomposition of SEM EDX measurement data by blind source separation (BSS) using non-negative matrix factorization (NMF) [4]. This method allows to separate the signal of the investigated structures from the signal coming from the silicon matrix. Next, the separated signals were quantified by the EDX ZAF method. The resulted copper content of the final structures was in the range of ~22-33 At. %. The IBID results were also compared with Electron Beam Induced Deposition (EBID) results obtained with the same fluence/current parameters of SEM electron beam as for the IBID under FIB.

K.M. and A.B. acknowledge funding from IDUB project 4101.00000070.

[1] a) I. Utke, P. Swiderek, K. Höflich, K. Madajska, J. Jurczyk, P. Martinović, I. B. Szymańska, *Coord. Chem. Rev.*, (2022) 458; b) S. Barth, M. Huth, F. Jungwirth, *J. Mater. Chem. C*, 8 (2020) 15884–15919.

[2] K. Madajska and I. B. Szymańska, *Materials*, 14 (2021) 3145.

[3] Guan X., Yan R., Synlett, 31 (2020) A-D.

[4] B.R. Jany et al., *Nano Letters*, Volume 17, Issue 11, 6507-7170 (2017).

# Additive nano-manufacturing of advanced superconductors, and devices using focused ion beam technology

R. Córdoba

Institute of Molecular Science (ICMol), University of Valencia, 46980 Paterna, Spain

E-Mail: rosa.cordoba@uv.es

Superconducting materials are dissipationless carriers of electric current and provide macroscopic and robust quantum coherence. These properties render them highly valuable as parts for electrical generators, magnetic sensors, and powerful magnets. To achieve the required performance employed in those applications, bulk superconductors often need nanoengineering. Moreover, when these materials are reduced to the nanoscale becoming nano-superconductors, exciting new physical phenomena emerge. This has encouraged the study of their performance as 1D quantum oscillators and Josephson junction arrays as essential elements to be implemented in circuits.

Ground-breaking proposals have taken advantage of the third dimension (3D) for the development of advanced electronic components, opening fascinating novel routes in the fields of material science, physics and nanotechnology. Thus, advanced nano-superconductors in the three dimensions could be implemented in future highly-efficient electronic elements. However, their fabrication and characterization remain a challenge.

In this contribution, we present a direct-write additive nano-manufacturing method based on focused ion beam technologies to fabricate advanced nano-superconductors at-will. This technique called focused ion beam induced deposition (FIBID) is based on a CVD process assisted by an ion beam focused to a few nanometers.

We have written 3D superconducting hollow nanocylinders with controllable inner and outer diameters (down to 32 nm)<sup>[1,2]</sup>, nanohelices with at-will geometries<sup>[3]</sup> and also nanospirals<sup>[4]</sup>, by decomposing a precursor with a He<sup>+</sup> FIB. These nanostructures become superconducting at 7 K and show large critical magnetic field and critical current density. Remarkably, these nanohelices display superconductivity up to 15 T depending on the direction of the field with respect to the nanohelix axis. This suggests that their helical 3D geometry and their orientation in a magnetic field play a significant role in the superconducting phase transition. Moreover, fingerprints of vortex and phase-slip patterns are also experimentally identified and supported by numerical simulations based on the time-dependent Ginzburg-Landau equation.

Furthermore, we present experimental outcomes on the modulation of the superconductivity induced by electric fields in nanowires fabricated with Ga<sup>+</sup> FIB<sup>[5]</sup> and He<sup>+</sup> FIB<sup>[6]</sup>. A theoretical model based on the GL theory explains this modulation by the squeezing of the superconducting state by the electric field.

## References

- [1] R. Córdoba, A. Ibarra, D. Mailly, J. M. De Teresa, *Nano Lett.* 2018, 18, 1379.
- [2] R. Córdoba, A. Ibarra, D. Mailly, I. Guillamón, H. Suderow, J. M. De Teresa, *Beilstein J. Nanotechnol.* 2020, 11, 1198.
- [3] R. Córdoba, D. Mailly, R. O. Rezaev, E. I. Smirnova, O. G. Schmidt, V. M. Fomin, U. Zeitler, I. Guillamón, H. Suderow, J. M. J. M. De Teresa, *Nano Lett.* 2019, 19, 8597.
- [4] A. Arroyo, G. Hlawacek, R. Córdoba, Manuscript in preparation.
- [5] P. Orús, V. M. Fomin, J. M. De Teresa, R. Córdoba, *Sci. Rep.* 2021, 11, 17698.
- [6] A. Arroyo, M. Pérez, G. Hlawacek, R. Córdoba, Manuscript in preparation.



## Comparison of Electron- and Ion-Induced Chemistry in FEBID/FIBID Precursors

J.-C. Yu<sup>1</sup>, A. Chaudhary<sup>1</sup>, M. K. Abdel-Rahman<sup>2</sup>,

D. H. Fairbrother<sup>2</sup>, and L. McElwee-White<sup>1</sup>

<sup>1</sup>Department of Chemistry, University of Florida, Gainesville, Florida 32611-7200, USA

<sup>2</sup>Department of Chemistry, Johns Hopkins University, Baltimore, Maryland 21218-2685, USA

E-Mail: [lmwhite@chem.ufl.edu](mailto:lmwhite@chem.ufl.edu)

Focused electron beam-induced deposition (FEBID) and focused ion beam-induced deposition (FIBID) are direct write fabrication techniques that use focused beams of charged particles (electrons or ions) to create 3-D metal-containing nanostructures by decomposing organometallic precursors onto substrates in a low-pressure environment. For many applications, it is important to minimize contamination of these nanostructures by impurities from incomplete ligand dissociation and desorption. We use ultra high vacuum (UHV) surface science studies to obtain mechanistic information on electron and ion-induced processes in organometallic precursor candidates [1,2]. The results are used for the mechanism-based design of custom precursors for FEBID and FIBID [3,4].

Differences in the results from FEBID and FIBID will be presented using examples taken from deposition of Ru and Pt. For example, electron irradiation of  $\text{Ru}(\text{CO})_4\text{I}_2$  yields  $\text{RuI}_2$ , while ion-induced fragmentation of the same precursor affords pure Ru. These results led to a re-examination of the Pt FEBID precursors  $\text{MeCpPtMe}_3$ ,  $\text{Pt}(\text{CO})_2\text{Cl}_2$  and  $\text{Pt}(\text{CO})_2\text{Br}_2$  to determine if these precursors, which undergo incomplete ligand desorption during FEBID, would yield higher metal content material upon a switch to FIBID due to the balance between ion-induced deposition and preferential sputtering of impurity atoms during FIBID. Results of ion-irradiation of the three Pt precursors will be discussed.

References:

- [1] R. M. Thorman, S. J. Matsuda, L. McElwee-White, and D. H. Fairbrother, *J. Phys. Chem. Lett.* 11 (6), 2006 (2020).
- [2] E. Bilgiliyoy, R. M. Thorman, J.-C. Yu, T. B. Dunn, H. Marbach, L. McElwee-White, and D. H. Fairbrother, *J. Phys. Chem. C* 124, 24795 (2020).
- [3] W. G. Carden, H. Lu, J. A. Spencer, D. H. Fairbrother, and L. McElwee-White, *MRS Commun.* 8 (2), 343 (2018).
- [4] J.-C. Yu, M. K. Abdel-Rahman, D. H. Fairbrother, and L. McElwee-White, *ACS Appl. Mater. Interfaces* 13 (41), 48333 (2021).

## Ion Induced Decomposition of Iron Pentacarbonyl

P. Nag<sup>1</sup>, L. Sala<sup>1</sup>, K. Grygoryeva<sup>1</sup>, B. Sedmidubská<sup>1</sup>, J. Fedor<sup>1</sup>, J. Kočíšek<sup>1</sup>,  
S. Indrajith<sup>2</sup>, P. Rousseau<sup>2</sup>, B. A. Huber<sup>2</sup>, Ch. Nicolafrancesco<sup>2</sup> and  
A. Domaracka<sup>2</sup>

<sup>1</sup>J. Heyrovský Institute of Physical Chemistry of CAS, Dolejškova 3, 18223 Prague, Czech Republic

<sup>2</sup>Normandie Univ., ENSICAEN, UNICAEN, CEA, CNRS, CIMAP, 14000 Caen, France

E-Mail: pamir.nag@jh-inst.cas.cz

Iron pentacarbonyl is a widely used organometallic precursor for direct writing of nanostructures using charged particle beams [1]. It consists of a central iron atom surrounded by five CO ligands, which secure its volatility. In the deposition process, the ligands are removed by action of a primary charged particle beam, secondary electrons, photons or heat to produce an iron deposit on the substrate. While the principle is the same also for other organometallic precursors, the underlying elementary processes are under debate.

A significant amount of research has been devoted to focused electron beam induced deposition (FEBID). Particularly explored was the role of secondary electrons produced in the substrate and deposit, which causes broadening of deposits [2]. It has been shown that electrons in a wide range of energies can effectively strip the CO ligands from the iron pentacarbonyl.[3-6]

Here, we focus on the processes induced by primary particles during focused ion beam induced deposition (FIBID).[7] In this technique, He<sup>+</sup> and Ga<sup>+</sup> ions at energies around 30 keV are usually used for direct writing of nanostructures, since He<sup>+</sup> and Ga<sup>+</sup> sources are common in the existing ion microscopes. However, also other projectiles were used to elucidate fundamental processes during the deposition. [8] This is also the present case, where we employed ARIBE facility at GANIL infrastructure to prepare a variety of projectile types and charge states as depicted in Fig. 1. These enable direct as well as long range charge transfer interactions between the ions and iron pentacarbonyl molecules isolated in vacuum. Energies of the projectiles ranged from 3keV to 255keV to enable interactions dominated by electronic or nuclear excitations. The matrix of measurements enabled identification of the most important parameters for ion induced decomposition of organometallics such as iron pentacarbonyl. The detailed analysis of the fragment kinetic energies then illuminates the dissociation dynamics of singly and multiply charged iron pentacarbonyl. In the present contribution, the study of an isolated molecule [9] will be discussed in connection with the ongoing studies of ion interaction with iron pentacarbonyl clusters.

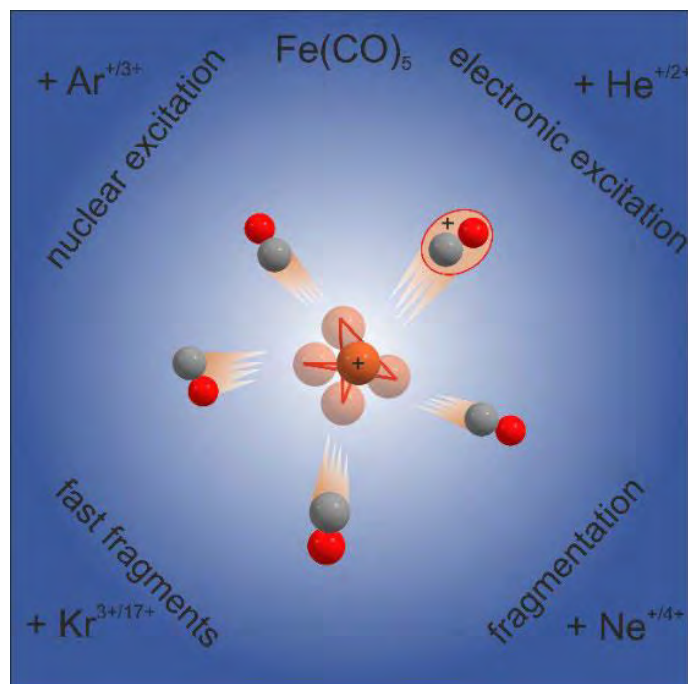


Fig.1 Dynamics of iron pentacarbonyl dissociation process upon interaction with various ions resulting in fast CO and CO+ fragments and slow “encaged” Fe+ ions. The various projectiles used in the study are shown in corners together with corresponding elementary processes.

Acknowledgement: This work was supported by European Regional Development Fund; OP RDE; Project “CARAT” no. CZ.02.1.01/0.0/0.0/16\_026/0008382.

- [1] Utke, I. et al., J. Vac. Sci.Tech. B 26 (2008) 1197
- [2] Schmied, R. Beilstein J. Nanotechnol. 6 (2015) 462
- [3] Massey, S. et al. J. Phys. Chem. C 119 (2015) 12708
- [4] Lengyel, J. et al. J. Phys. Chem. C 120 (2016) 7379
- [5] Allan, M. et al. PCCP 17 (2018) 11692
- [6] Lacko, M. et al., EPJD 69 (2015) 84
- [7] Stanford, M.G. et al. J. Vac. Sci.Tech. B 35 (2017) 030802
- [8] Bilgilişoy, E. et al., J. Phys. Chem. C 125 (2021) 17749
- [9] Indrajith, S. et al. J. Phys. Chem. C 123 (2019) 10639





# **POSTER CONTRIBUTIONS**



## Coaxial ion source: characterization of field ionization under gas flow

D. Bedrane<sup>1</sup>, M. Lagaize<sup>1</sup>, A. Houël<sup>2</sup>, A. Delobbe<sup>2</sup>, E. Salançon<sup>1</sup>

<sup>1</sup>CINaM, UMR 7325, campus de Luminy – case 913, 13288 Marseille cedex 9

<sup>2</sup>OrsayPhysics, Cht De L'arc, 95 AV des Monts Aurélien, 13710 Fuveau

E-Mail : (djouher.berane@cnsr.fr)

An ion source with a coaxial structure [1] comprises an ultrafine tungsten tip introduced into a stainless-steel capillary that joins a "high pressure" chamber (up to 1000mbar) and a very low-pressure chamber ( $<10^{-4}$ mbar). After characterizing behavior of molecular flows obtained in this structure [2], we estimated that ion source had an apparent source-size  $<2$ nm [3] and that, under all flow conditions and regimes. Today, we are interested by emitted intensities and brightness of ion source for all flow regimes and for different gases: argon, hydrogen, helium, xenon... Due to residual vapor pressure of water during injection, the tip is morphologically transformed, tungsten is corroded under the electric field. Traces of water are measured by mass spectrometry and confirm these results. The intensity of emitted current as a function of the voltage depends strongly on the tip shape. The monitoring of the characteristics  $I(V)$  as a function of the size of the tip will be presented. This approach allows a better understanding of the mechanisms involved to model the supply function in this system.

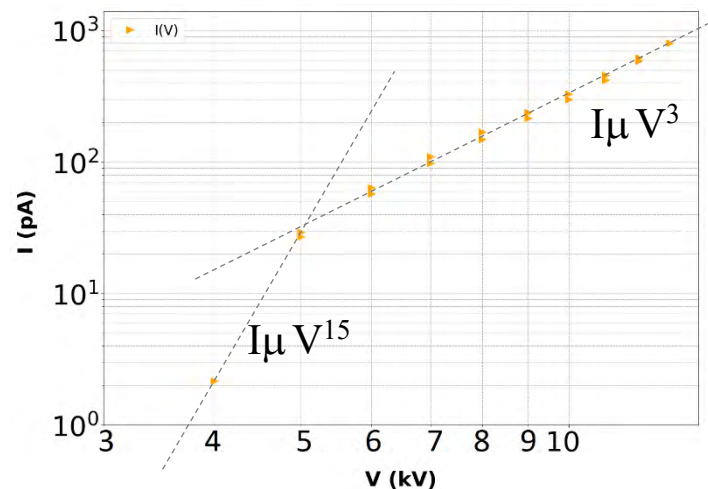
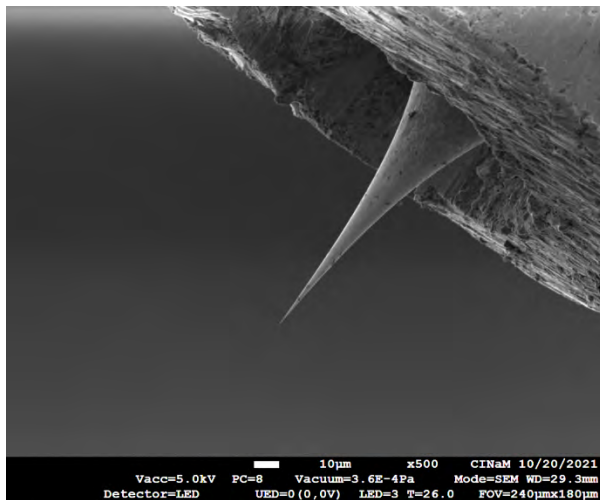


FIG. 1: Left : Coaxial ion source observed under scanning electron microscope. Right: Ionization intensity versus voltage characteristic obtained for  $P=10^{-5}$ mbar in the low pressure chamber.

## References

- [1] E. Salançon, Z.Hammadi, R.Morin, A new approach to gas field ion sources, *Ultramicroscopy* 95, 183-188 (2003)
- [2] M. Descoins, Z.Hammadi, R.Morin Local supply of gas in vacuum: application to a field ion source, *Journal of Vacuum Science & Technology A* 26, 1331 (2008)
- [3] L. Lapena, D. Bedrane, A. Dediiovanni, E. Salançon bright sources under the projection microscope: using an insulating crystal on a conductor as electron source, *The European Physical Journal Applied Physics* 97, 13 (2022)

# Application of FIB/SEM tomography for the advanced microstructural characterization of solid oxide fuel cells.

Katarzyna Berent<sup>1\*</sup>, Grzegorz Brus<sup>2</sup>, Tomasz Prokop<sup>2</sup> and Janusz Szmyd<sup>2</sup>

<sup>1</sup> AGH University of Science and Technology, Academic Centre for Materials and Nanotechnology, 30 Mickiewicza Ave., 30-059 Krakow, Poland

<sup>2</sup> AGH University of Science and Technology, Department of Fundamental Research in Energy Engineering, 30 Mickiewicza Ave., 30-059 Krakow, Poland

\* corresponding author email: kberent@agh.edu.pl

Tomography using a focused ion beam (FIB) combined with a scanning electron microscope (SEM) is a valuable approach for three-dimensional (3D) imaging that opens new possibilities to expand morphological context description and analysis into the third dimension. However, performing FIB/SEM tomography on poorly conducting materials which are solid oxide fuel cells remains challenging. The porous structure exposes subsurface areas of the planar cross-section surface, presenting an additional challenge to image processing and segmentation.

This work presents an investigation of the performance of the Ni-YSZ anodes from the SOFC stack before and after a prolonged period of operation. The analysis of the spatial distribution of different phases and porosity in SOFC anode provides an understanding of the structural influence on the transport properties [1-2]. Afterwards, a detailed three-dimensional (3D) image analysis enables the comprehensive quantitative evaluation of the morphological parameters such as average grain size, phase volume fraction, phase tortuosity factor and the triple phase boundary (TPB).

SOFC fragments were embedded into epoxy resin under vacuum conditions to infiltrate pores. The samples were coated with a thin conductive layer (10 nm Pt). FIB-SEM tomography was performed using an FEI Versa 3D dual beam scanning electron microscope (SEM) and Auto Slice and View (ASV) software. The observation was conducted under a low voltage in the range of 0.7–1kV. A typical series of alternating FIB milling and SEM imaging steps was used to produce a set of SE images from a volume of interest. Avizo software was used to stack and segment the SE images yielding a three-dimensional reconstruction and to quantify the microstructure. The phase volume fraction was measured by counting the number of voxels corresponding to Ni, YSZ and pores. The sample average TPB length was calculated using the volume expansion method, as implemented by Iwai, et al. [3]. The use of the FIB/SEM technique for the analysis of the SOFC anode microstructure allowed us to obtain significant insight into the estimation of transport properties resulting from changes in the microstructural parameters occurring after the ageing experiment.

[1] T. Prokop, K. Berent, H. Iwai, J. Szmyd, G. Brus; *Microscale, three-dimensional analysis of electrochemical energy conversion in SOFC anode using electron nanotomography and mathematical modeling*; International Journal of Hydrogen Energy (2018); doi.org/10.1016/j.ijhydene.2018.04.023

[2] T. A. Prokop, K. Berent, M. Moździerz, J. S. Szmyd, G. Brus, *A three-dimensional microstructure-scale simulation of a solid oxide fuel cell anode – the analysis of stack performance enhancement after a long-term operation*, Energies 12 (2019) 4784; doi:10.3390/en12244784

[3] H. Iwai, N. Shikazono, T. Matsui, H. Teshima, M. Kishimoto, R. Kishida, D. Hayashi, K. Matsuzaki, D. Kanno, M. Saito, H. Muroyama, K. Eguchi, N. Kasagi, H. Yoshida, *Quantification of sofc anode microstructure based on dual beam FIB-SEM technique*, Journal of Power Sources 195 (2010), 955–961





# New gold(I) and gold(II) complexes with amidinates as potential precursors for vapor deposition methods

A. Butrymowicz<sup>1</sup> and I. B. Szymańska<sup>1</sup>

<sup>1</sup>Faculty of Chemistry, Nicolaus Copernicus University in Toruń, 87-100, Toruń, Poland

E-mail: aleksandra.butrymowicz@doktorant.umk.pl

The direct deposition techniques for nanofabrication FEBID and FIBID require volatile and sensitive to the electron/ion beam compounds, capable of producing 2D and free-standing 3D structures. Research on finding new precursors and investigating the thermal decomposition mechanisms and the efficiency of induced dissociation processes is a crucial issue for the future. An important fact is that there is still a lack of appropriate stable and user-friendly compounds to obtain gold deposits with a defined 2D and 3D shape and without post-deposition purification [1]. One group of volatile coordination compounds is non-fluorinated amidinates, used as precursors in atomic layer deposition (ALD) and chemical vapor deposition (CVD). They have not been tested for their applicability in electron or ion-driven processes. On the other hand, fluorinated substituents are increasing the volatility of compounds. Among the fluorinated amidinates are known only:  $[\text{Ag}_2((\text{NH})_2\text{CCF}_3)_2]$ ,  $[\text{Ag}_2((\text{NH})_2\text{CC}_2\text{F}_5)_2]$ , and  $[\text{Hg}((\text{NH})_2\text{CC}_2\text{F}_5)_2]$  [2]. However, no evaporation experiments, CVD, and ALD tests have been carried out. Additionally, copper(II) complexes with perfluorinated amidine and carboxylate were described:  $[\text{Cu}_2(\text{NH}_2(\text{NH}=\text{CC}_2\text{F}_5)_2(\mu\text{-O}_2\text{CR}_F)_4]$ , where  $\text{R}_F = \text{CF}_3, \text{C}_2\text{F}_5, \text{C}_3\text{F}_7, \text{C}_4\text{F}_9$  and were used as Cu CVD precursors [3].

Here we report new, stable on air, and user-friendly gold(I) and gold(II) complexes with perfluorinated amidinate ligands:  $[\text{Au}_2((\text{NH})_2\text{CC}_2\text{F}_5)_2]$ ,  $[\text{Au}_2((\text{NH})_2\text{CC}_2\text{F}_5)_2\text{Cl}_2]$ , and  $[\text{Au}_2((\text{NH})_2\text{CCF}_3)_2\text{Cl}_2]$ . The thermal decomposition mechanism has been studied based on variable temperature infrared spectroscopy VT IR ( $10^{-1}$  mbar) supported with TGA/DTA. The occurrence of the  $[\text{Au}_2((\text{NH})_2\text{CC}_2\text{F}_5)_2]$  and  $[\text{Au}_2((\text{NH})_2\text{CCF}_3)_2\text{Cl}_2]$  complexes in the gas phase was found in the temperature range of 100–180°C, confirming that they are a metal source under reduced pressure. Experimental data confirm that the new gold(I) and gold(II) compounds sublime at 100–150°C and  $10^{-4}$  mbar. In addition, interactions with high-energy electrons were investigated to test the possibility of their use as FEBID precursors.

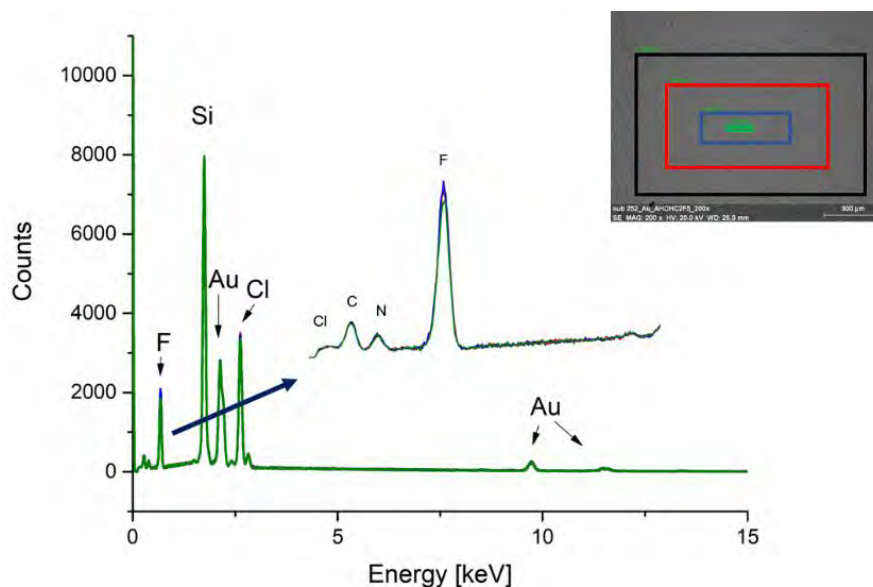


**Figure 1.** A thin layer of the  $[\text{Au}_2((\text{NH})_2\text{CC}_2\text{F}_5)_2\text{Cl}_2]$  sublimated on a silicon substrate and exposed to a beam of high-energy electrons (SEM,  $E = 20$  keV).

Acknowledgments:

The financing of this work was by Nicolaus Copernicus University in Torun (PDB no. 103).

References:

- [1] Utke, I.; Swiderek, P.; Höflich, K.; Madajska, K.; Jurczyk, J.; Martinović, P.; Szymańska, I.B., *Coord. Chem. Rev.* **2022**, *458*, doi:10.1016/j.ccr.2021.213851.
- [2] Reilly, W.L.; Brown, H.C., *J. Am. Chem. Soc.* **1956**, *78*, 6032–6034, doi:10.1021/ja01604a021.
- [3] Madajska, K.; Szymańska, I.B., *Materials*. **2021**, *14*, 3145, doi:10.3390/ma14123145.

# Innovative and Minimally Invasive Therapy for Melanoma using a Hybrid Nanosystem Combined with NIR Laser Irradiation

J. Lopes<sup>1</sup>, T. Ferreira-Gonçalves<sup>1</sup>, I. V. Figueiredo<sup>2,3</sup>, C. Rodrigues<sup>1</sup>, H. Ferreira<sup>4</sup>,  
D. Ferreira<sup>5</sup>, A. S. Viana<sup>6</sup>, P. Faísca<sup>7</sup>, M. Gaspar<sup>1</sup>, J. Coelho<sup>4</sup>,  
C. O. Silva<sup>1</sup>, and C. P. Reis<sup>1,4</sup>

<sup>1</sup> Research Institute for Medicines (iMed.Ulisboa), Faculty of Pharmacy, Universidade de Lisboa, Av. Professor Gama Pinto, 1649-003 Lisboa, Portugal.

<sup>2</sup> Pharmacology and Pharmaceutical Care Laboratory, Faculty of Pharmacy, University of Coimbra, Azinhaga de Santa Comba, 3000-548 Coimbra, Portugal.

<sup>3</sup> Institute for Clinical and Biomedical Research (iCBR), Faculty of Medicine, University of Coimbra, Azinhaga de Santa Comba, 3000-548 Coimbra, Portugal

<sup>4</sup> Instituto de Biofísica e Engenharia Biomédica, Faculdade de Ciências, Universidade de Lisboa, Campo Grande, 1749-016 Lisboa, Portugal.

<sup>5</sup> Comprehensive Health Research Centre (CHRC), Departamento de Desporto e Saúde, Escola de Saúde e Desenvolvimento Humano, Universidade de Évora, Largo dos Colegiais, 7004-516 Évora, Portugal.

<sup>6</sup> Centro de Química Estrutural, Faculdade de Ciências, Universidade de Lisboa, Campo Grande, 1749-016 Lisboa, Portugal.

<sup>7</sup> Faculty of Veterinary Medicine, ULHT, Campo Grande 376, 1749-024 Lisboa, Portugal.

\* E-Mail: [catarinareis@ff.ulisboa.pt](mailto:catarinareis@ff.ulisboa.pt)

The global impact of cancer emphasizes the importance of developing innovative, effective and minimally invasive therapies. In the context of superficial cancers, the development of a hybrid nanosystem activated by a near-infrared laser (NIR) and its in vitro and in vivo safety and efficacy characterization are, herein, proposed as schematically represented in Figure 1.

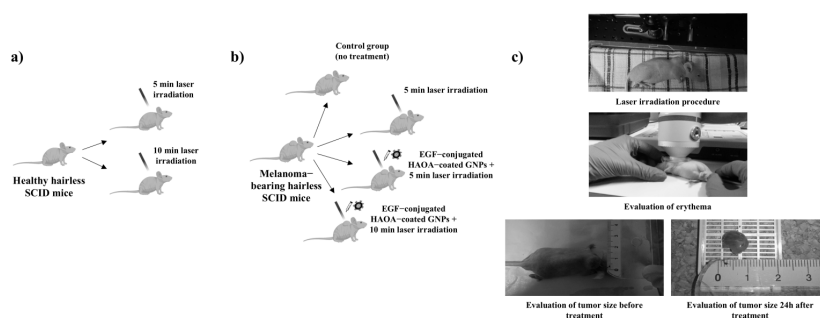


Figure 1. Illustrative representation of the different groups created to assess: (a) the safety of the laser exposure; and (b) the anti-cancer efficacy of the treatments. (c) Experimental setup.

This nanosystem consists of gold nanoparticles coated with polymeric and lipid-based material, and functionalized with epidermal growth factor (EGF), with mean size from 150 to 200 nm, negative surface charge, and spherical morphology. Two microscopic techniques confirmed the presence of this nanosystem in the cells (Figure 2 and 3), which suggests either their internalization or their binding to the surface. To evaluate the potential cytotoxicity, MTT assays were performed on healthy human keratinocytes (HaCat), human melanoma cells (A375) and murine melanoma cells (B16F10). The core proved to be safe in all cell lines. When coated and bioconjugated with EGF, the nanosystem showed a higher impact in all cell lines, promoting, in most cases, a reduction of cell viability when compared to uncoated and non-functionalized nanoparticles.

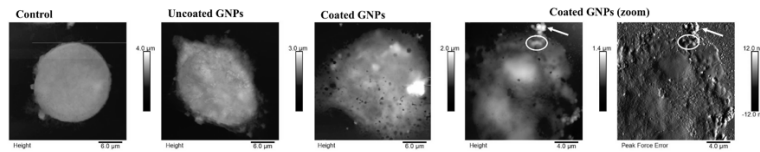


Figure 2. AFM height images of A375 cells alone (control) and after 4 h of incubation with different formulations. Additional height and peak force error images showed with more detail cells incubated with the nanosystem leading to hypothesize the presence of particle aggregates in the surface (arrow) as well as inside of the cell (circle).

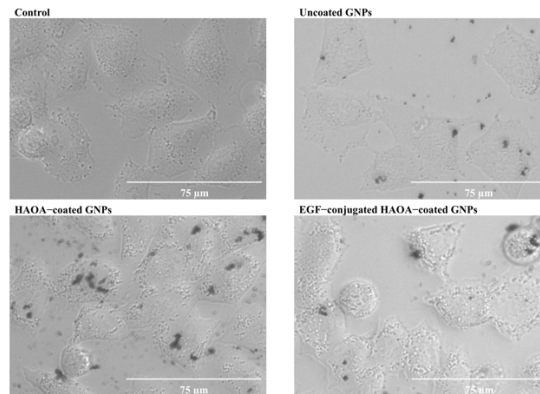


Figure 3. Representative images of A375 cells alone (control) and after 4 h of incubation with different formulations at 40x magnification. This nanosystem appeared highly aggregated as darker structures, which seem to be in the surface (arrow) as well as inside of the cell (circle). Scale bar, 75 μm.

Finally, hairless immunocompromised mice were selected for a xenograft model upon inoculation of A375 human melanoma cells. Treatment with near-infrared laser irradiation for five minutes combined with in situ administration of the nanoparticles showed a tumor volume reduction of approximately 80% and, in some cases, led to the formation of several necrotic foci, observed histologically. No significant skin erythema at the irradiation zone was verified, nor other harmful effects on the excised organs. This therapeutic approach did not show evidence of causing damage to normal skin structure, which indicates the nanoparticle system selectivity towards the melanoma tissues, although further research is necessary to clarify the molecular mechanism underpinning this system and cell-nanoparticle interaction using Focused Ion Technology.

Funding: The authors would like to thank to Fundação para a Ciência e Tecnologia (FCT) for the essential financial support under the project's references PTDC/BBB-BMC/0611/2012, UIDB/00645/2020, UIDB/04138/2020 and UIDP/04138/2020 as well as for the PhD fellowships SFRH/BD/148044/2019 and SFRH/BD/147306/2019.

Acknowledgments: The authors would like to thank to Professor Jesús Molpeceres from University of Alcalá, Professor Patrícia Rijo from Universidade Lusófona de Humanidades e Tecnologias, Professor Pedro Vieira from Faculdade de Ciências e Tecnologia of the Universidade Nova de Lisboa, Fernando Monteiro, Ana Gabriel and Ricardo Gomes, all from the Faculdade de Ciências of the Universidade de Lisboa, and Vanda Marques from Faculdade de Farmácia of the Universidade de Lisboa for their assistance to this work.

## Transfer of knowledge of new techniques based on Focused Electron/Ion Beam Induced Deposition (FEBID/FIBID)

A.T. Escalante-Quiceno<sup>1</sup>, A. Salvador-Porroche<sup>1,2</sup>, P. Orús<sup>1</sup>, J. Pablo-Navarro<sup>1,2</sup>, S. Sangiao<sup>1,2</sup>, F. Sigloch<sup>1</sup>, M. Barrado<sup>2</sup>, P. Cea<sup>1,2,3</sup>, C. Magén<sup>1,2</sup>, J.M. De Teresa<sup>1,2</sup>

1. Instituto de Nanociencia y Materiales de Aragón (INMA), CSIC-Universidad de Zaragoza, 50009 Zaragoza, Spain

2. Laboratorio de Microscopías Avanzadas (LMA), Universidad de Zaragoza, 50018 Zaragoza, Spain

3. Departamento de Química Física, Facultad de Ciencias, Universidad de Zaragoza, 50009 Zaragoza, Spain

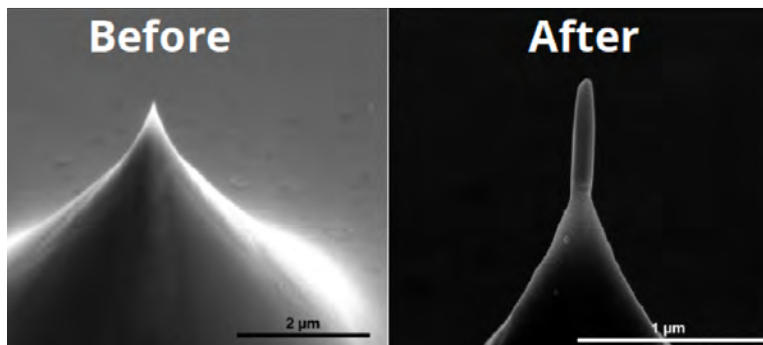
E-Mail: deteresa@unizar.es

Focused Electron/Ion Beam Induced Deposition is a direct-write, resist-free nanolithography technique that enables the growth of high-resolution nano- and micro-structures. This technique uses a gas precursor, which is injected into the area of interest. It is then decomposed by an electron/ion beam producing the dissociation of the gas molecules and subsequent deposition of the solid material of interest onto the substrate. High lateral resolution sub-100 nm, in some cases reaching 10 nm, can be achieved with this technique. We present here new techniques based on FEBID/FIBID, developed by our team, with the aim of transferring knowledge to companies.

One of them is Focused Ion Beam Induced Deposition under cryogenic conditions (Cryo-FIBID), in which the gas precursor is condensed on the surface substrate due to the low temperature. The development of this technique has allowed the deposition of W-C [1], Pt-C [2], and Co [3] nanostructures with liquid nitrogen as a cooling agent, as well as cryo-deposition of W-C using a thermoelectric plate [4]. This new approach has a higher efficiency than the room-temperature FIBID in terms of resolution, irradiation dose and processing speed [5]. It also provides deposits with high metal content and low resistivity for applications in circuit editing, electrical contacts, and mask repair.

Another new approach presented here is the development of 3D magnetic nanowires by Focused Electron Beam Induced Deposition (FEBID) for application in MFM measurements. These magnetic nanowires can be used for simultaneous topographic and magnetic measurements with significant advantages over commercial magnetic tips due to their high-aspect-ratio and good magnetic behaviour. The main advantages are the decreased non-magnetic tip-sample interaction, high lateral resolution, and high coercive field of the tips [6-8], as well as the capability to be used in liquid environment [9], for potential application in the investigation of magnetic biological samples.

### **a) Growth of magnetic tips by FEBID**



### **b) Growth of electrical contacts by Cryo-FIBID**

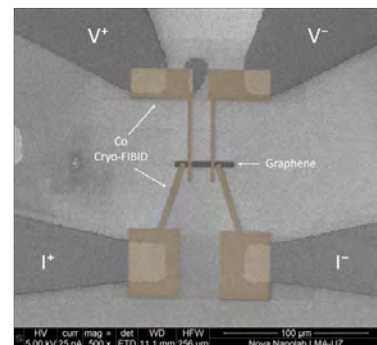


**Fig. 1.** a) Growth by FEBID technique of an Fe-based magnetic tip onto a cantilever for MFM; b) Cobalt-based electrical contacts onto graphene ribbons by Cryo-FIBID.

## References

- [1] R. Cordoba, P. Orús, S. Strohauser, T. Torres, J.M. De Teresa, "Ultra-fast direct growth of metallic micro- and nano-structures by Focused Ion Beam Irradiation" *Sci. Rep.* **9**, 14076 (2019)
- [2] A. Salvador-Porroche, S. Sangiao, P. Philipp, P. Cea, J.M. De Teresa, "Optimization of Pt-C deposits by cryo-FIBID: Substantial growth rate increase and quasi-metallic behaviour" *Nanomaterials* **10**, 1906 (2020)
- [3] A. Salvador-Porroche, S. Sangiao, C. Magén, M. Barrado, P. Philipp, D. Belotckerkovtceva, M.V. Kamalakar, P. Cea, J.M. De Teresa, "Highly-efficient growth of cobalt nanostructures using Focused Ion Beam Induced Deposition under cryogenic conditions: Application to electrical contacts on graphene, magnetism and hard masking" *Nanoscale Adv.* **3**, 5656-5662 (2021)
- [4] P. Orús, F. Sigloch, S. Sangiao, J.M. De Teresa, "Cryo-Focused Ion Beam-Induced Deposition of tungsten-carbon nanostructures using a thermoelectric plate" *Appl. Sci.* **11**, 10123 (2021)
- [5] J.M. De Teresa, P. Orús, R. Córdoba, P. Philipp, "Comparison between Focused Electron/Ion Beam-Induced Deposition at room temperature and under cryogenic conditions" *Micromachines* **10**, 799 (2019)
- [6] J. Pablo-Navarro, S. Sangiao, C. Magén, J.M. De Teresa, "Magnetic functionalization of scanning probes by Focused Electron Beam Induced Deposition technology" *Magnetochemistry* **7**, 140 (2021)
- [7] C. Magén, J. Pablo-Navarro, J.M. De Teresa, "Focused-Electron-Beam engineering of 3D magnetic nanowires" *Nanomaterials* **11**, 402 (2021)
- [8] H. Mattiat, N. Rossi, B. Gross, J. Pablo-Navarro, C. Magén, R. Badea, J. Berezovsky, J.M. De Teresa, M. Poggio, "Nanowire Magnetic Force Sensors Fabricated by Focused-Electron-Beam-Induced Deposition" *Phys. Rev. Applied* **13**, 044043 (2020)
- [9] M. Jaafar, J. Pablo-Navarro, E. Berganza, P. Ares, C. Magén, A. Masseboeuf, C. Gatel, E. Snoeck, J. Gómez-Herrero, J.M. De Teresa, A. Asenjo, "Customized MFM probes based on magnetic nanorods" *Nanoscale* **12**, 10090 (2020)

# Electron and ion beam deposited nanowires as probes for atomic force microscopy

E. Gacka<sup>1</sup>, B. Pruchnik<sup>1</sup>, T. Gotszalk<sup>1</sup>, and I.W. Rangelow<sup>2</sup>

<sup>1</sup> Department of Nanometrology, Wrocław University of Science and Technology, 50-372, Wrocław, Poland

<sup>2</sup> Group of Nanoscale Systems, Technische Universität Ilmenau, 98693, Ilmenau, Germany

E-Mail: ewelina.gacka@pwr.edu.pl

Focused electron beam induced deposition (FEBID) and focused ion beam induced deposition (FIBID) are promising technologies for nanoprototyping and for integrating fabricated nanodevices with microelectromechanical systems (MEMS). This technology allows 2D and 3D structures to be fabricated at the nanoscale in a single step (direct writing), inside the vacuum chamber of a scanning electron microscope with ease comparable to the rapid prototyping methods. Therefore, efforts are being undertaken to use it for prototyping nanodevices, including probes for scanning probe microscopy (SPM). Functionalisation of the probes provides various enhancements and new applications, thus their modifications are sought, including the diamond microparticles [1] or nitride-gallium microrods [2]. Mounting piece of material with use of FEBID/FIBID is one possibility, however the materials themselves also may offer exceptional properties.

In this paper we report the fabrication, application and comparison of FEBID and FIBID platinum-carbon (Pt(C)) nanowires as tips for conductive atomic force microscopy (C-AFM) (Fig. 1) with use of MeCpPtMe<sub>3</sub>, which is the most widely used precursor. After calibration of the Pt(C) nanowire growth, the nanowires were deposited on top of standard conductive silicon cantilevers with PtIr coating (model). The modified probes were used to perform measurements of the HOPG sample using a self-designed C-AFM system [3]. The investigations enabled simultaneous determination of the electrical (operation in conductive AFM mode) and mechanical (measurement in contact mode) properties of the fabricated probes as well as description of the topography and conductivity map of the HOPG surface (Fig. 2). Measurements were carried on with load forces no greater than 5 nN. Surface was polarised with 0.5 V.

Gathered information in form of topography and current maps show great distinction between FEBID and FIBID nanowires. Data acquired with those measurements present clearly, that functionalization of tips solely with focused beam material creates unique tool for both examination of material itself, nanowires and high resolution conductive atomic force microscopy.

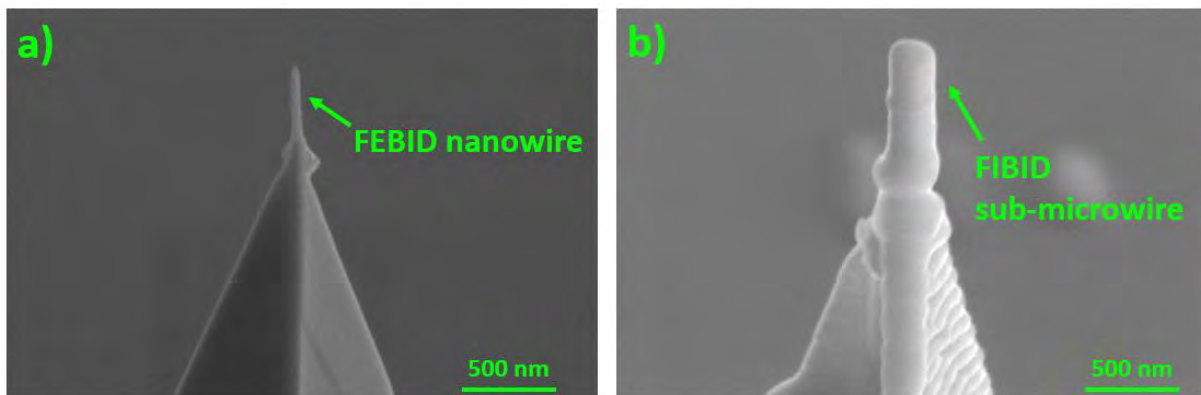


Fig. 1: SEM images of a modified silicon tip with nanowires fabricated by: a) focused electron beam induced deposition(FEBID) process; b) focused ion beam induced deposition (FIBID) process.



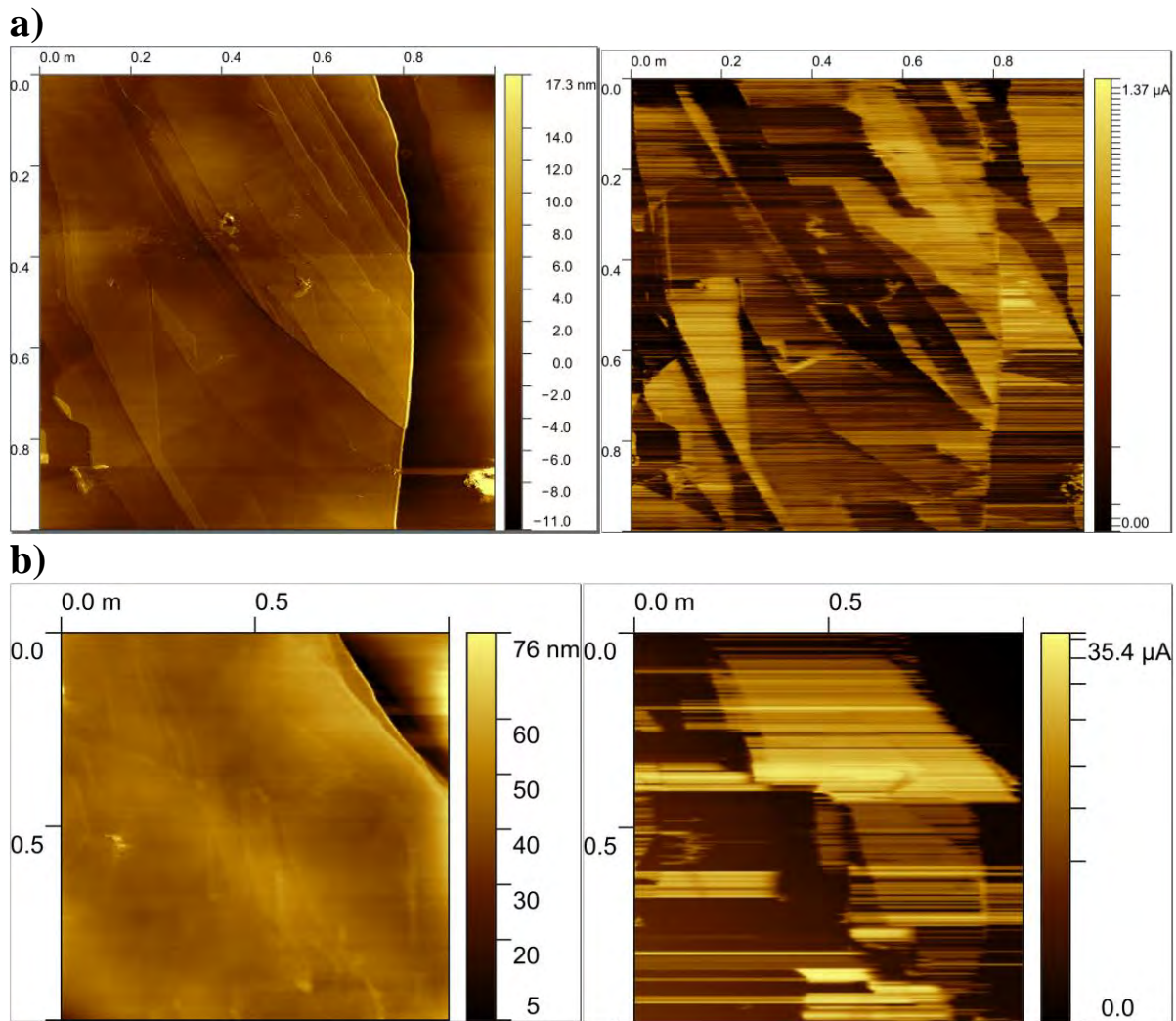


Fig. 2: Conductive AFM maps acquired with cantilevers equipped with nanowire-tips: a) focused electron beam induced deposition (FEIBID) tip topography and current map; b) focused ion beam induced deposition (FIBID) tip topography and current map.

#### References:

- [1] E. Gacka, P. Kunicki, A. Sikora, R. Bogdanowicz, M. Ficek, T. Gotszalk, I.W. Rangelow, K. Kwoka, Focused ion beam-based microfabrication of boron-doped diamond single-crystal tip cantilevers for electrical and mechanical scanning probe microscopy, *Measurement*. 188 (2022) 110373. <https://doi.org/10.1016/j.measurement.2021.110373>
- [2] M. Behzadirad, M. Nami, A.K. Rishinaramagalam, D.F. Feezell, T. Busani, GaN nanowire tips for nanoscale atomic force microscopy, *Nanotechnology*. 28 (2017) 20LT01. <https://doi.org/10.1088/1361-6528/aa6c0b>
- [3] D. A. Kopiec, W. Majstrzyk, B. Pruchnik, E. Gacka, D. Badura, A. Sierakowski, P. Janus, T. Gotszalk Metrology and control of electromagnetically actuated cantilevers using optical beam deflection method. *Metrology and Measurement Systems*. 28 (2021) <https://doi.org/10.24425/mms.2021.137698>

#### Acknowledgments

This work was supported by the National Science Centre, Poland, OPUS grant [“Nanometrology of Nottingham cooling effect using operational microelectromechanical systems”, grant number: 2020/37/B/ST7/03792]

## Fabrication of nanostructured van der Waals heterostructures using He ion beam patterning

Khairi F. Elyas<sup>1</sup>, Johanna Richter<sup>3</sup>, Kirill Bolotin<sup>3</sup>, Hannah C. Nerl<sup>2</sup> and Katja Höflich<sup>1</sup>

<sup>1</sup>Ferdinand-Braun-Institut gGmbH, Leibniz-Institut für Höchstfrequenztechnik, 12489 Berlin, Germany

<sup>2</sup>Humboldt Universität zu Berlin, Institute of Physics, 12489 Berlin, Germany

<sup>3</sup> Freie Universität Berlin, Institute of Experimental Physics, 14195 Berlin, Germany

E-Mail: ([Khairi.Elyas@fbh-berlin.de](mailto:Khairi.Elyas@fbh-berlin.de))

Polaritons in two-dimensional (2D) materials can lead to significantly enhanced light-matter interactions making them interesting for highly-confined and low-loss light transport. A polariton is a quasiparticle that couples a photon to a dipole-carrying excitation in matter and strongly depends on the materials' type and geometry. When combining different 2D materials, the different polaritonic modes may hybridize to combine the strong localization of plasmonic excitations with the long propagation distances of phonon modes [1]. Here, we report on the tuning of hybrid polaritonic modes by modifying the geometry of van der Waals (vdW) heterostructures at the nanoscale.

In this project, heterostructures from single-crystalline gold flakes, (semi-) metallic graphene and the wide-bandgap material hexagonal boron (hBN) nitride are fabricated using dry transfer methods with polydimethylsiloxane (PDMS) and poly(propylene) carbonate (PPC). Next, patterning is performed using He and/or Ne ion beam milling in a Zeiss Orion Nanofab microscope (cf. Figure 1). The spectral positions and mode profiles of polaritonic modes strongly depend on the geometry but also on the quality of the materials. Thus, a maximum of control over both, the beam parameters and its path is needed in order to obtain the highest shape fidelity combined with the lowest possible ion-induced damage. An important step in the study is therefore to systematically investigate different currents, acceleration voltages, and ion types with regard to damaging effects on the patterned structures. Furthermore, the geometrical pattern routines are being optimized using FIB-o-Mat providing ultimate control over the beam path [2].

The optical properties of the fabricated heterostructures are then mapped using monochromated low-loss scanning transmission electron microscopy (STEM) electron energy-loss spectroscopy (EELS) [3] and outcomes compared to optical methods.

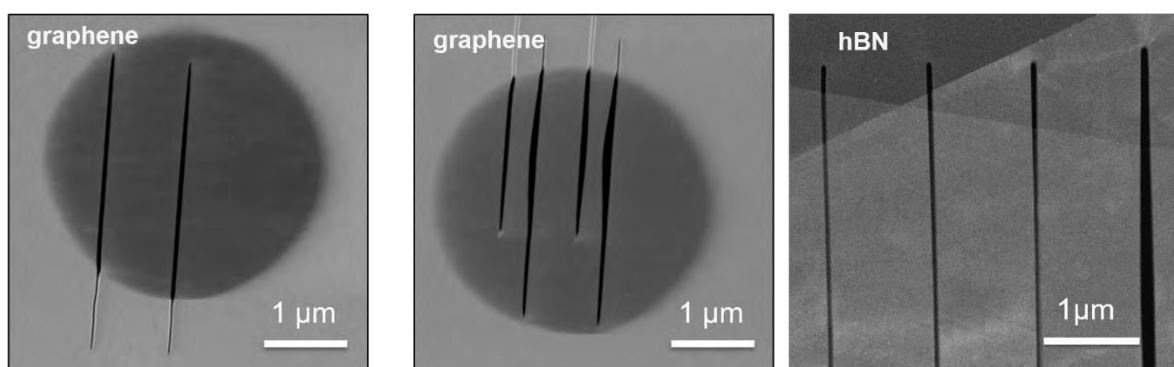


Figure (1): SEM image of an example graphene flake and hBN flake after using ion beam patterning to cut lines with different doses.

- [1] A. Woessner, M. B. Lundeberg, Y. Gao, A. Principi, P. Alonso-gonzález, M. Carrega, K. Watanabe, T. Taniguchi, G. Vignale, M. Polini, J. Hone, R. Hillenbrand, and F. H. L. Koppens, *14*, 421 (2015).
- [2] V. Deinhart, L. Kern, J. N. Kirchhof, S. Juergensen, J. Sturm, E. Krauss, T. Feichtner, S. Kovalchuk, M. Schneider, D. Engel, B. Pfau, B. Hecht, K. I. Bolotin, S. Reich, and K. Höflich, *Beilstein J. Nanotechnol.* *12*,304(2021).
- [3] O. L. Krivanek, N. Dellby, J. A. Hachtel, J. Idrobo, M. T. Hotz, N. J. Bacon, A. L. Bleloch, G. J. Corbin, M. V Hoffman, C. E. Meyer, and T. C. Lovejoy, *Ultramicroscopy* *203*, 60 (2019).

# Development and biological assessment in terms of cytotoxicity and hemolytic effect of hyaluronic acid (HA) based electrospun nanofibers

A.-T. Iacob<sup>1</sup>, O.M. Ionescu<sup>1</sup>, and L. Profire<sup>1</sup>

<sup>1</sup>Department of Pharmaceutical Chemistry, University of Medicine and Pharmacy, 700115, Iasi, Romania

E-mail: [panzariu.andreea.teodora@gmail.com](mailto:panzariu.andreea.teodora@gmail.com)

**Purpose.** The aim of this paper is the formulation of novel electrospun nanofibers based on hyaluronic acid and polyethylene oxide (HA/PEO) incorporating as active substances: propolis (P), insulin (I) and infusion of *Calendula officinalis flos* (C) as new dressing materials in the treatment of wounds.

**Materials and methods:** The preparation of HA/PEO matrices was carried out in three stages: (i) the dissolving of HA and PEO in physiological brine by stirring at room temperature (rt), then, (ii) the active substances were added and stirred until a homogeneous solution is obtained [1]; for the last step (iii) an INOVENSO nanospinner was used and then different values of flow-rate, applied voltage and also different distances from the tip of the syringe to the collecting plate were applied [2]. The 3 nanofibrous matrices developed were: HA/PEO/P (A); HA/PEO/PI (B); HA/PEO-PC (C) as seen in the SEM micrographs represented in the Fig. 1. After the formulation was optimized the polymeric formulations were subjected to the determination of the cytotoxicity by MTS assay on normal dermal fibroblast cells and the evaluation of hemolytic effect by the capacity of human erythrocyte membrane stabilization on hypotonicity-induced lysis [2].

**Results:** All the formulations were not cytotoxic at concentrations up to 500 µg/mL and regarding the hemolytic effect this is below 4%, which demonstrates a good bio-compatibility for the wound dressings designed.

**Conclusions:** After analyzing the data obtained, it was concluded that nanofibers with propolis and *Calendula officinalis flos* infusion obtained the best results by stimulating normal fibroblasts' proliferation by 21% at concentrations of 250 µg/mL and by 37% at 500 µg/mL and also by the smallest hemolytic index of 2.8%.

**Acknowledgments:** Scientific research funded by the national research Project entitled "Development of new bioactive and biomimetic polymeric nanostructures for wound healing applications", code PN-III-P4-ID-PCE-2020-2687.

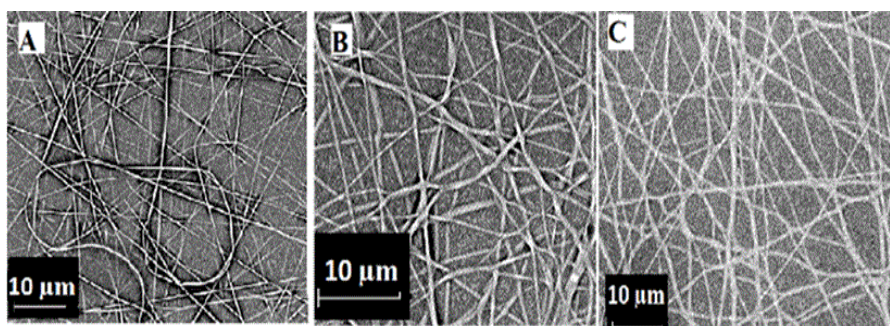


Fig. 1: SEM micrographs for HA/PEO/P (A); HA/PEO/PI (B); HA/PEO-PC (C)

## References

- [1] O.M. Ionescu, A. Mignon, A.T. Iacob, N. Simionescu, L.G. Confederat, C. Tuchilus, L. Profire; *Polymers* (2021) 13, 129.
- [2] J.J. Ahire, D.D. Robertson, A.J. Van Reenen, L.M.T. Dicks; (2017) 86, 143–148.

## POLYETHYLENE OXIDE-HYALURONIC ACID-BASED ELECTROSPUN NANOFIBERS: IN VITRO AND IN VIVO STUDIES

Oana M. Ionescu<sup>1</sup>, Andreea T. Iacob<sup>1</sup>, Arn Mignon<sup>2</sup>, Natalia Simionescu<sup>3</sup>, Ioannis Gardikiotis<sup>4</sup>, Irina-Draga Caruntu<sup>5</sup>, Simona Eliza Giusca<sup>5</sup>, Sandra Van Vlierberghe<sup>6</sup>, Lenuța Profire<sup>1</sup>

<sup>1</sup>University of Medicine and Pharmacy “Grigore T. Popa” of Iasi, 16 University Street, 700115, Iasi, Romania;

<sup>2</sup>Smart Polymeric Biomaterials, Surface and Interface Engineered Materials, Campus Group T, KU Leuven, Andreas Vesaliusstraat 13, 3000 Leuven, Belgium;

<sup>3</sup>Centre of Advanced Research in Bionanoconjugates and Biopolymers, “Petru Poni” Institute of Macromolecular Chemistry, 41A Grigore Ghica Voda Alley, 700487, Iasi, Romania;

<sup>4</sup>Advanced Centre of Research and Development in Experimental Medicine, “Grigore T. Popa” University of Medicine and Pharmacy of Iasi, 16 University Street, Iasi 700115, Romania;

<sup>5</sup>Department of Morphofunctional Sciences, Faculty of Medicine, “Grigore T. Popa” University of Medicine and Pharmacy of Iasi, 16 University Street, Iasi 700115, Romania;

<sup>6</sup>Polymer Chemistry and Biomaterials Group, Centre of Macromolecular Chemistry, Department of Organic and Macromolecular Chemistry, Ghent University, Krijgslaan 281, S4-bis, 9000 Ghent, Belgium

ionescu\_mariuca@yahoo.com

The development of advanced wound dressing materials is a major concern in the biomedical field. Nanofibers (NFs) are relatively new porous materials which can act as excellent extracellular matrices by enhancing tissue formation [1, 2]. The present study focuses on the development of new wound dressings, NFs type, based on hyaluronic acid (HA) and polyethylene oxide (PEO), including also different active compounds (ACs). More exactly, we report here the preparation, characterization and in vitro and in vivo biological evaluation of HA-PEO based NFs, enriched with Manuka honey, propolis, *Calendula officinalis* and L-arginine, as ACs.

To prepare the electrospinning solutions, HA was added to the initial PEO solution and after 24 h of stirring, homogeneous polymeric solutions were obtained. A total polymer concentration was kept at 12.5% (wt/wt). Afterwards, different ACs, such as Manuka honey (M), propolis (P), and L-arginine (L), *Calendula officinalis* were added to the obtained polymeric solutions. The electrospinning was carried out using an INOVENSO nanospinner with different values of parameters (flow-rate, voltage and tip-to-collector) [3]. The NFs were characterized in terms of morphology and fiber diameter as well cytocompatibility degree and wound healing potential.

Following the electrospinning process, new HA/PEO/ACs based nanomaterials were developed. The developed NFs showed a good vapour transmission rate that means a good capacity of maintaining a moist environment proper for healing process as well as a good biocompatible degree and healing effects.

The results of our study suggest that the developed porous matrices had a synergistic effect on behalf of the ACs, especially for the propolis-*Calendula officinalis* combination, that also promoted cellular proliferation.

This work was supported by a grant of the Romanian Ministry of Education and Research, CNCS-UEFISCDI, project number PN-III-P4-ID-PCE-2020-2687 (contract nr. 244/2021), within PVCDI III and AUF-IFA 2019-2020 (contract no. 28/2019).

### References:

[1] Veith A. P., Henderson K., Spencer A., Sligal A.D., Baker, A. B., *Adv. Drug Deliv. Rev.* 146, 97–125 (2019).

[2] Weng L., Xie J., *Curr. Pharm. Des.*, 21, 1944-1959 (2015).

[3] Rieger K.A., Birch N.P., Schiffman, J.D. *Carboh. Polym.* 139, 131-138 (2016).

# Focused ion beam-fabricated thin film phase masks for electron lens aberration correction and structured illumination electron ptychography

P.-H. Lu<sup>1</sup>, M. Kruth<sup>1</sup>, and R. E. Dunin-Borkowski<sup>1</sup>

<sup>1</sup> Ernst Ruska-Centre for Microscopy and Spectroscopy with Electrons and Peter Gruenberg Institute, Research Centre Juelich, 52425 Juelich, Germany

E-Mail: p.lu@fz-juelich.de

Approximately 75 years ago, Boersch proposed several devices that could produce a desired phase shift between a direct electron beam and scattered electrons to enhance phase contrast in transmission electron microscopy (TEM) [1]. One of these devices, which later became known as a Zernike phase plate, makes use of the inner electrostatic potential of a thin film to introduce a phase shift to scattered electrons, while the direct beam passes through a central hole without undergoing a phase change. Similar to this, by sculpting a thin film with a designed spatially-resolved thickness profile at nanometer precision using advanced nanofabrication techniques such as focused ion beam [2], one can create a refractive or diffractive phase mask and hence shape the electron wavefunctions in-line or off-axis, respectively [3]. As an example, this presentation will show how such an approach could be applied to spherical aberration correction [4] (Figure 1a-d) and structured illumination ptychographic imaging [5] (Figure 1e-h) in transmission electron microscopy, which gives access to otherwise invisible features at better spatial resolution or with enhanced contrast.

## Acknowledgement

The author acknowledges the funding from the European Union's Horizon 2020 research and innovation programme under grant agreement No. 823717 (ESTEEM 3) and No. 856538 (3D MAGiC). The authors are grateful to R. Shiloh, R. Remez, D. Roitman, A. Arie (Tel Aviv, Israel), F. Allars, S. You, A. M. Maiden, J. M. Rodenburg (Sheffield, UK) for the fruitful collaboration and great contributions to those work.

## References

- [1] H. Boersch, *Zeitschrift fur Naturforschung A* 2, 615 (1947).
- [2] R. Shiloh\*, P.-H. Lu\*, R. Remez\* et al., *Physica Scripta* 94, 034004 (2019)
- [3] D. Roitman, R. Shiloh, P.-H. Lu et al., *ACS Photonics* 8, 3394 (2021)
- [4] R. Shiloh\*, R. Remez\*, P.-H. Lu\* et al., *Ultramicroscopy* 189, 46 (2018)
- [5] F. Allars\*, P.-H. Lu\*, M. Kruth et al., *Ultramicroscopy* 231, 113257 (2021)



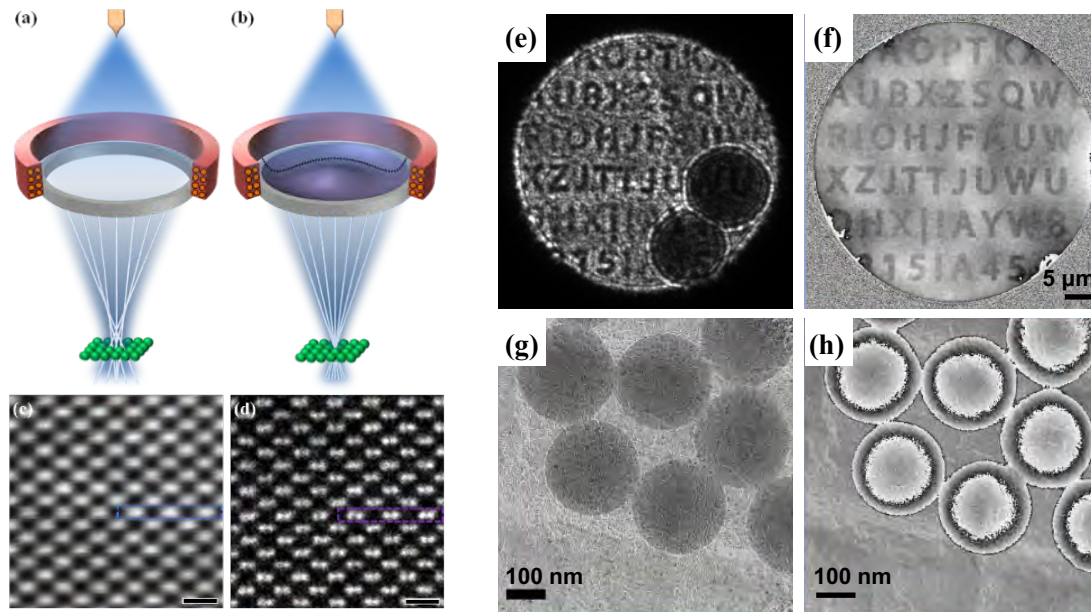


Figure 1.

(a-d) Thin-film spherical aberration corrector. (a-b) Schematic diagrams of the setup for spherical aberration correction using a thin film corrector. (c-d) HAADF-STEM images of a Si  $\langle 110 \rangle$  crystal imaged (c) without and (d) using a thin film corrector. Si  $\langle 110 \rangle$  dumbbells with 136 pm separation can only be resolved after correction. The scale bars in (c) and (d) are 500 pm. Reproduced from Ref [4].

(e-h) Structured illumination near-field electron ptychography. (e) An example near-field diffraction pattern. (f) Reconstructed phase image of the diffuser. (g-h) Reconstructed amplitude (g) and phase (h) image of the latex sphere on carbon/Au nanoparticle substrate, reconstructed from only nine diffraction patterns. Reproduced from Ref [5].

## Binuclear rhenium(III) complexes with amidinate and amidate. Volatility and electron interaction studies

K. Madajska<sup>1</sup>, I. B. Szymańska<sup>1</sup>

<sup>1</sup>Faculty of Chemistry, Nicolaus Copernicus University in Toruń, Gagarina 7, 87-100 Toruń, Poland

E-Mail: pola@umk.pl

Focused electron beam induced deposition (FEBID) is a direct maskless nanolithography technique based on the local dissociation of adsorbates upon the irradiation with an electron beam. It is used for making 2D and 3D nanostructures. The precursors dedicated to this method should have adequate volatility and interact with electrons [1–3].

Rhenium has the second-highest melting point (3185°C) among all metals, exceeded only by W (3422°C). Rhenium nanostructures can be used in electromechanical sensors, field emission devices, scanning probe microscopes and interconnects [4,5].

Here we report on our study of new binuclear rhenium(III) complexes with perfluorinated amidinate and amidate:  $[\text{Re}_2\text{Cl}_2(\mu\text{-(NH)}_2\text{CR}_f)_4]$  (Fig. 1a) and  $[\text{Re}_2\text{Cl}_2(\mu\text{-O(NH)CR}_f)_4]$ , where  $\text{R}_f = \text{CF}_3, \text{C}_2\text{F}_5$ .

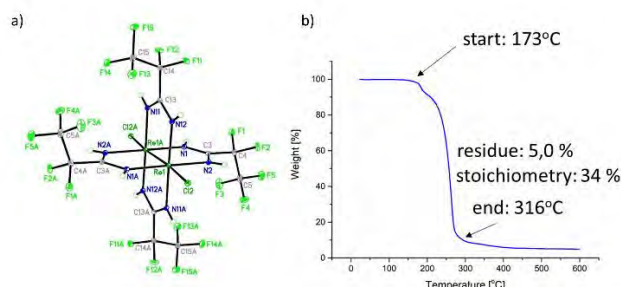


Fig. 1:  $[\text{Re}_2\text{Cl}_2(\mu\text{-(NH)}_2\text{CC}_2\text{F}_5)_4]$ : a) structures, b) thermal analysis.

Volatility studies such as electron ionization mass spectrometry, variable temperature infrared spectroscopy (VT IR), thermal analysis (Fig. 1b), and sublimation experiments have shown that the entire molecules of the compounds can be evaporated. To initially assess the sensitivity of complexes to the high-energy electron beam, observations were made using a scanning electron microscope (SEM, 20 keV) and a transmission electron microscope (TEM, 200 keV).

Acknowledgements: The financing of this work was by Nicolaus Copernicus University in Torun (PDB no.103).

[1] I. Utke and A. Götzhäuser, Small, Minimally Invasive, Direct: Electrons Induce Local Reactions of Adsorbed Functional Molecules on the Nanoscale, *Angewandte Chemie Int. Ed.* 49 (2010), 9328.

[2] D. Belić, M. M. Shawrav, E. Bertagnolli, H. D. Wanzelboeck, Direct writing of gold nanostructures with an electron beam: On the way to pure nanostructures by combining optimized deposition with oxygen-plasma treatment, *Beilstein J. Nanotechnol.* 8 (2017), 2530.

[3] I. Utke, P. Hoffmann, J. Melngailis, Gas-assisted focused electron beam and ion beam processing and fabrication, *J. Vac. Sci. Technol. B.* 26, 1197–1276 (2008).

[4] J. Bedia, L. Calvo, J. Lemus, A. Quintanilla, J.A. Casas, A.F. Mohedano, J.A. Zazo, J.J. Rodriguez, M.A. Gilarranz, Colloidal and microemulsion synthesis of rhenium nanoparticles in aqueous medium, *Colloids and Surfaces A: Physicochem. Eng. Aspects*, 469 (2015) 202–210.

[5] L. Philippe, Z. Wang, I. Peyrot, A. W. Hassel, J. Michler, Nanomechanics of rhenium wires: Elastic modulus, yield strength and strain hardening, *Acta Materialia*, 57 (2009) 4032–4035.



## Structure and morphology of the surface of cadmium sulfide thin films

L. Nykyruy<sup>1</sup>, R. Yavorskyi<sup>1</sup>, G. Wisz<sup>2</sup>, P. Sawicka-Chudy<sup>2</sup>, and B. Naidych<sup>1</sup>

<sup>1</sup> Department of Physics and Chemistry of Solids, Vasyl Stefanyk Precarpathian National University, 76018, Ivano-Frankivsk, Ukraine

<sup>2</sup> College of Natural Sciences, University of Rzeszów, 35-959, Rzeszów, Poland

[bohdana.naidych@pnu.edu.ua](mailto:bohdana.naidych@pnu.edu.ua)

Thin-film semiconductor structures occupy a leading position among high-efficiency solar energy conversion devices. Due to the small size of the structures, the final properties are influenced by both the composition of the material and the morphology of the surface. Cadmium chalcogenides have proven themselves well as photoelectric materials, so the analysis of structural parameters of cadmium sulfide thin films obtained by open evaporation in vacuum was carried out.

The synthesis of cadmium sulfide was performed in quartz ampoules by fusing elements of cadmium (CD0000) and sulfur (TV-4) taken in stoichiometric ratios, with an accuracy of  $10^{-4}$  g. The concentration of background impurities in the source components did not exceed  $10^{-5}$  wt.%.

CdS thin films were obtained by open evaporation in vacuo from pre-synthesized Cd-S compounds. Pre-chemically cleaned glass thin plates were used as substrates. The evaporator temperature was  $T_E = 880^\circ\text{C}$ , the substrate temperature was  $T_S = 200^\circ\text{C}$ , and the deposition time  $\tau = (60 - 90)$  sec.

The morphology of CdS thin films was studied on the basis of Scanning Electron Microscopy data. According to the data of phase analysis of CdS films, the contributions of the atomic masses of the elements are Cd  $\sim 55\%$  and S  $\sim 43\%$ . It is established that the deposited films are characterized by stoichiometric composition, regardless of the film thickness.

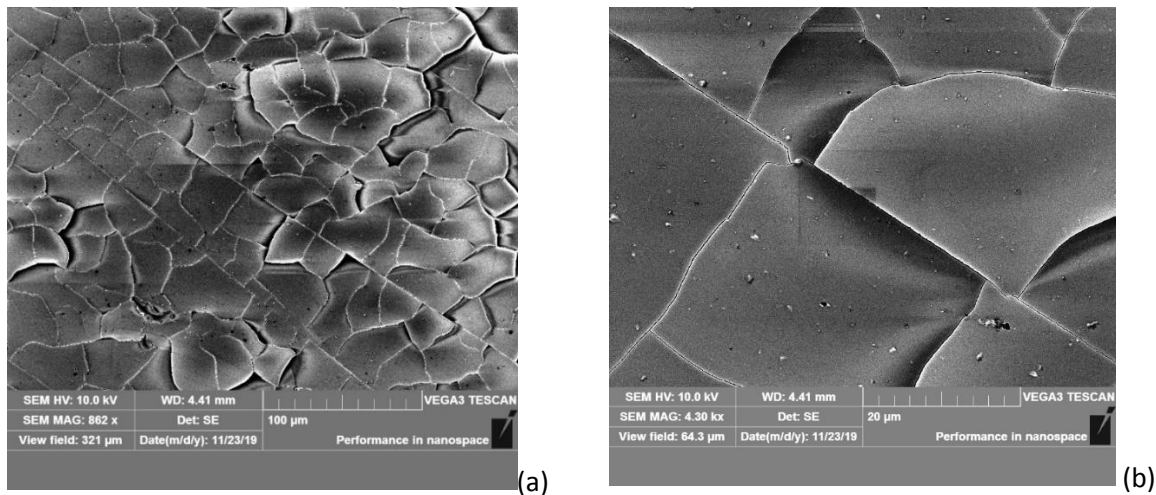


Fig. 1. The SEM image of the surface of CdS thin-film condensate obtained at substrate temperature  $T_S = 200^\circ\text{C}$ , evaporator temperature  $T_E = 880^\circ\text{C}$ , deposition time  $\tau = 60$  sec, film thickness  $d = 420$  nm with 862x (a) and 4300x (b) magnification.

Condensate in the form of separate plates forms on the surface of the films. The size of these plates and their presence is directly determined by the deposition time. As the deposition time increases, the plates merge and become more difficult to identify, and thicker films have a smoother surface. Increasing the temperature of the heater allows obtaining structures with a lamellar surface, and the deposition time determines the size and density of such formations.

## **Cobalt and Dysprosium Liquid Alloy Ion Sources for Magnetic Nanostructures**

P. Mazarov<sup>1</sup>, [W. Pilz](mailto:w.pilz@hzdr.de)<sup>2</sup>, F. Meyer<sup>2</sup>, L. Bischoff<sup>2</sup>, N. Klingner<sup>2</sup>, Kilian Lenz<sup>2</sup>, J. Lindner<sup>2</sup>

<sup>1</sup> Raith GmbH, Konrad-Adenauer-Allee 8, 44263 Dortmund, German

<sup>2</sup> Helmholtz-Zentrum Dresden-Rossendorf, Institute of Ion Beam Physics and Materials Research,  
Bautzner Landstrasse 400, 01328 Dresden, Germany

E-Mail: ([w.pilz@hzdr.de](mailto:w.pilz@hzdr.de), [Paul.Mazarov@raith.de](mailto:Paul.Mazarov@raith.de))

Focused Ion Beam (FIB) processing has been established as a well-suited and promising technique in R&D in many fields of nanotechnology. Here, direct maskless magnetic patterning and modification of ferromagnetic nanostructures is presented using Cobalt and Dysprosium Liquid Metal Alloy Ion Source (LMAIS). A CuDy based LMAIS in the Raith-FIB-System VELION was used for changing magnetic properties like damping in metallic alloys. Another LMAIS based on CoDy was used to implant a 300-nm-wide track of Co-ions. Structures as small as 30 nm can be implanted. Such lateral resolution is hard to reach for other lithographic methods. The changes of the magnetic damping were measured by ferromagnetic resonance spectroscopy, a standard tool for probing magnetic anisotropy and spin dynamics.



## Plasma treatment and electrowetting on polymer thin films and nanofiber membranes

Matthias Vesco<sup>1</sup>, Stefan del Rossi<sup>1</sup>, and Silvia Schintke<sup>1</sup>

<sup>1</sup> Laboratory of Applied NanoSciences (COMATEC-LANS), Department of Industrial Technologies, Haute Ecole d'Ingénierie et de Gestion du Canton de Vaud HEIG-VD / HES-SO // University of Applied Sciences and Arts Western Switzerland, CH-1401 Yverdon-les-Bains, Switzerland

E-Mail: [silvia.schintke@heig-vd.ch](mailto:silvia.schintke@heig-vd.ch)

Plasma surface treatment is used in industrial applications in order to improve the wettability of surfaces prior to painting, coating, or printing. However, in particular for polymer surfaces, the results cannot necessarily be predicted, as plasma surface interaction is complex. We therefore investigate the effect of the interaction of ions (plasma) on various hydrophilic polymer surfaces by studying the surface wettability as a function of plasma treatment parameters. Two polymers are polyvinylidene fluorid (PVDF) and polytetrafluorethylen (PTFE, Teflon). We furthermore compare the obtained effects of plasma treatment with the effects obtained in electrowetting experiments.

PVDF thin films were fabricated by semi-automated blade coating on glass, as well as on aluminum foil, PVDF fiber membranes were manufactured by electrospinning onto brass discs and on aluminum foils. Water contact angles of the hydrophobic PVDF samples were measured using an industrial camera with magnification lens and semi-automated image analysis.

One part of PVDF samples were then treated using low-pressure plasma treatment. Ion etching by plasma treatment (using air) was performed under low pressure for different durations (100 s, 1'000 s and 10'000 s), while another part of PVDF samples were left untreated for comparison (Figure 1).

Time-lapse imaging of the treated PVDF nanofiber samples shows absorption of water droplets, compared to water droplets staying stable on untreated PVDF essentially evaporating over time (Figure 2).

PTFE thin films (PTFE tape) were deposited onto copper plates and onto aluminum foils as substrate. Plasma treatment was performed during 100 s on part of the samples. Water contact angles were analyzed for treated and untreated samples.

We have constructed a set-up for the study of electrowetting. PTFE thin films show electrowetting. The obtained results are promising for dedicated surface modifications of wettability through a combination of local plasma ion etching and electrowetting.

This work has been performed in the research context of the Cost Action 19140 "Focused Ion Technology for Nanomaterials" (FIT4NANO); the work has been financially support by HES-SO, project NANOFIT IA-EXT20-103 – 107469.

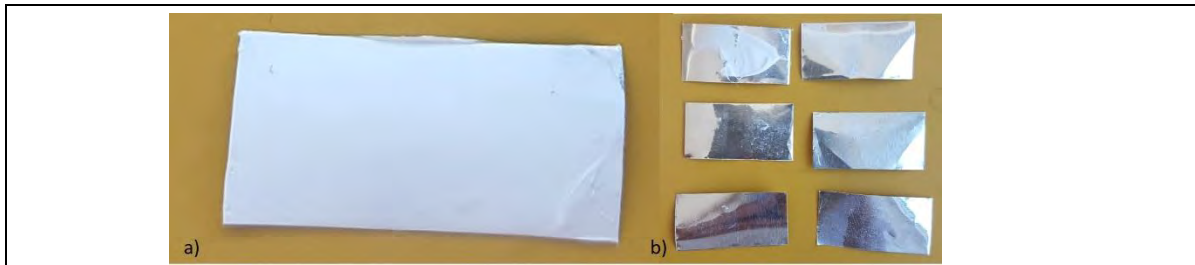


**Figure 1:** Representative example of an untreated PVDF nanofibers membrane on aluminum foil, as well as examples of samples that were plasma treated. Plasma treatment during 10'000 s led to complete etching of the nanofiber membrane, and thus cleaning of the aluminum foil substrate.

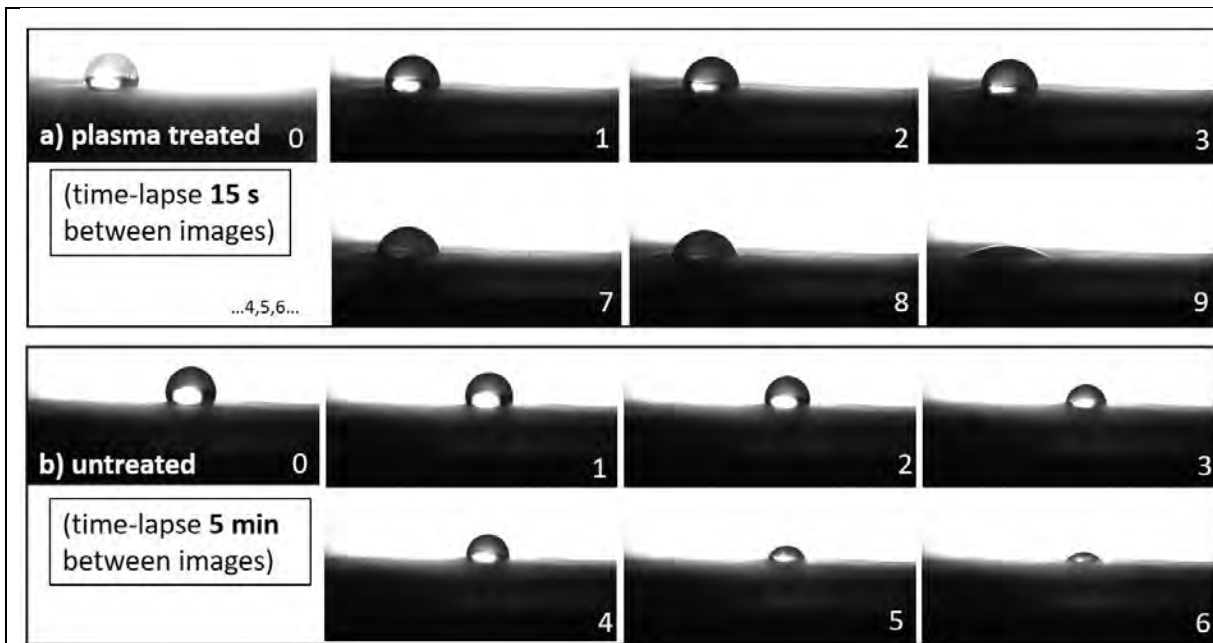


**Figure 2:** Time-lapse images of a water droplet:

a) on a plasma treated PVDF nanofiber membrane (upon 100 s plasma treatment), the water droplet is absorbed into the PVDF film after about 2 min 15s.

b) on an untreated PVDF nanofiber membrane, the water droplet volume shrinks over time, while the contact area of the droplet on the nanofiber membrane stays essentially constant. The droplet vanishes essentially by evaporation, over a long time scale of about 30 minutes.

## Direct Writing of Chiral and Nonlinear Plasmonic Devices

A. Tsarapkin<sup>1</sup>, V. Deinhart<sup>1</sup>, T. Feichtner<sup>2</sup> and K. Höflich<sup>1</sup>

<sup>1</sup> Ferdinand-Braun-Institut gGmbH Leibniz-Institut für Höchstfrequenztechnik, 12489 Berlin, Germany

<sup>2</sup> Experimental Physics 5, University of Würzburg, Am Hubland, 97074 Würzburg, Germany

E-Mail: aleksei.tsarapkin@fbh-berlin.de

The miniaturization of electrical and optical devices over the last decades has allowed for many technological and economic advancements. Devices that permit controlling the polarization of light are of crucial importance in telecommunication and quantum optics. Currently established solutions require bulky optical systems; however, we aim at designing a uniquely compact plasmonic converter and detector with a footprint of only a few  $\mu\text{m}$ . The device is based on a vertically oriented double helix coupled to a planar two-wire transmission line as shown in Fig. 1 (c). The helix acts as a sensitive antenna for circularly polarized light [1], and the transmission line guides plasmons on-chip [2].

Using numerical modelling, we show that antisymmetric modes can be excited in both parts of the device, specifically double helix and two-wire waveguide (see Fig. 1 b, d). The resonances of the plasmonic helix, the transmission line dispersion relation and their impedances strongly depend on the geometry of both structures. By adjusting their sizes one can finely maximize power transfer [3] to achieve the best coupling efficiency between helical antenna while also realizing linear-to-circular transformation.

The fabrication of the separate components has been accomplished. The helix can be directly written with a focused electron beam using Me<sub>2</sub>Au(acac) as a gold precursor. The beam path for the double helix was created with Fib-o-Mat [4]. It resembles a star-like jumping pattern (see Fig. 1 f) corresponding to a parallel printing approach that optimizes the growth rate and achieves the highest shape fidelity. The plasmonic waveguide can be cut from single-crystalline gold or silver flakes by means of focused ion beam milling. To fabricate waveguides with various geometries one can choose different types of ions, respectively helium, neon or gallium, depending on the desired gap size and shape. With a proper pattern it is possible to achieve gaps of several nanometers with helium ions [4]. However, helium ion beam milling is a very time-consuming process, thus, utilizing neon and gallium ions is preferable for larger gaps. Figures 1 (a) and (e) show scanning electron micrographs of the resulting structures.

[1] K. Höflich et al.; Resonant behavior of a single plasmonic helix; *Optica* 6, 1098 (2019).

[2] P. Geisler et al.; Multimode Plasmon Excitation and In Situ Analysis in Top-Down Fabricated Nanocircuits; *Phys. Rev. Lett.* 111, 183901 (2013).

[3] Jer-Shing Huang et al.; Impedance Matching and Emission Properties of Nanoantennas in an Optical Nanocircuit; *Nano Letters* 9, 1897 (2009).

[4] V. Deinhart et al.; The patterning toolbox FIB-o-mat: Exploiting the full potential of focused helium ions for nanofabrication; *Beilstein J. Nanotechnol.* 12, 304 (2021)

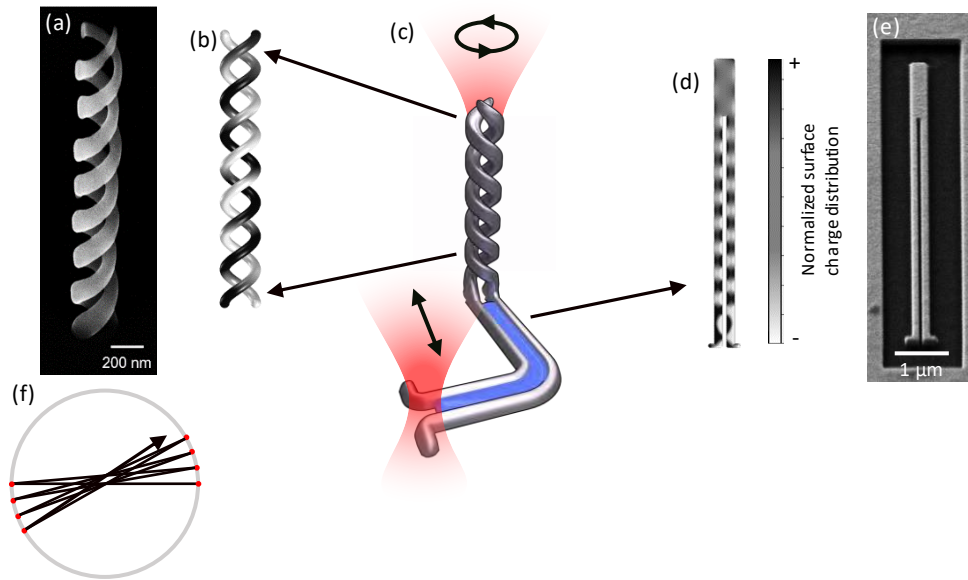


**Figure 1.** Artistic sketch of the proposed device, far-field polarizations depicted by black arrows (c); surface charge distributions of the double helix (b) and two-wire transmission line (d) show antisymmetric nature of according fundamental modes; scanning electron micrograph of the gold double helix (a) and scanning electron micrograph of the two-wire transmission line (e) [2], star-shaped beam path for double helix fabrication, created with Fib-O-Mat patterning toolbox [4] (f).

# Application of Fluorine Gas-Assisted FIB-TOF-SIMS for Chemical Characterization of Buried Thin Films and Quality Control of Deposition Process

A. Priebe, I. Utke, and J. Michler

Empa, Swiss Federal Laboratories for Materials Science and Technology, Laboratory for Mechanics of Materials and Nanostructures, Feuerwerkerstrasse 39, CH-3602 Thun, Switzerland

e-mail: agnieszka.priebe@empa.ch

Time-of-flight secondary ion mass spectrometry (TOF-SIMS)[1] is a powerful analytical technique, which allows material's chemical structure to be represented in 3D with nanoscale resolution. Furthermore, all generated ions (i.e. light and heavy ions, single ions and ionized molecules) can be detected and isotopes can be distinguished. This is a great advantage over commonly used scanning transmission electron microscopy, combined with energy-dispersive X-ray spectroscopy (STEM/EDX), which does not provide information of light elements, such as Li. The development of compact high vacuum (HV) compatible TOF detectors[2] opens new opportunities of upgrading focused ion beam scanning electron microscopy (FIB/SEM), the most frequently used tool in material science and nanotechnologies, into advanced chemical analysis stations. In the case of FIB-TOF-SIMS, a continuous (not pulsed) Ga<sup>+</sup> primary ion beam is used for both, sputtering and analysis, allowing for fast and efficient depth profiling of a sample. Furthermore, the novel combination of FIB-TOF-SIMS with *in situ* gas injection system (GIS)[3,4] provided significant enhancement of generated secondary ions, and consequently higher resolution and better quality of obtained 2D chemical maps. Remarkably, co-injection of fluorine gas during the experiment has potential of separating mass interference[5,6], which is one of the major drawbacks of the TOF-SIMS technique.

In this work, we present the application of gas assisted FIB-TOF-SIMS (Figure 1) for chemical characterization of various thin films buried deep (over 500 nm) under sample surface. The recently developed fabrication system, integrating *in situ* atomic layer deposition (ALD) and physical vapour deposition (PVD), was employed to obtain complex model multilayer systems comprised of alternating ceramic and metallic layers. This solution allowed a layer thickness to be precisely controlled within the range spanning from several nanometers to hundreds of nanometers. The high resolution and high sensitivity of fluorine gas-assisted FIB-TOF-SIMS are expected to play an important role in the quality control of nano- and microdevices as well as for the failure analysis of fabrication processes. Consequently, it can help develop microelectronics, next generation batteries and other thin film-based devices [7–10].



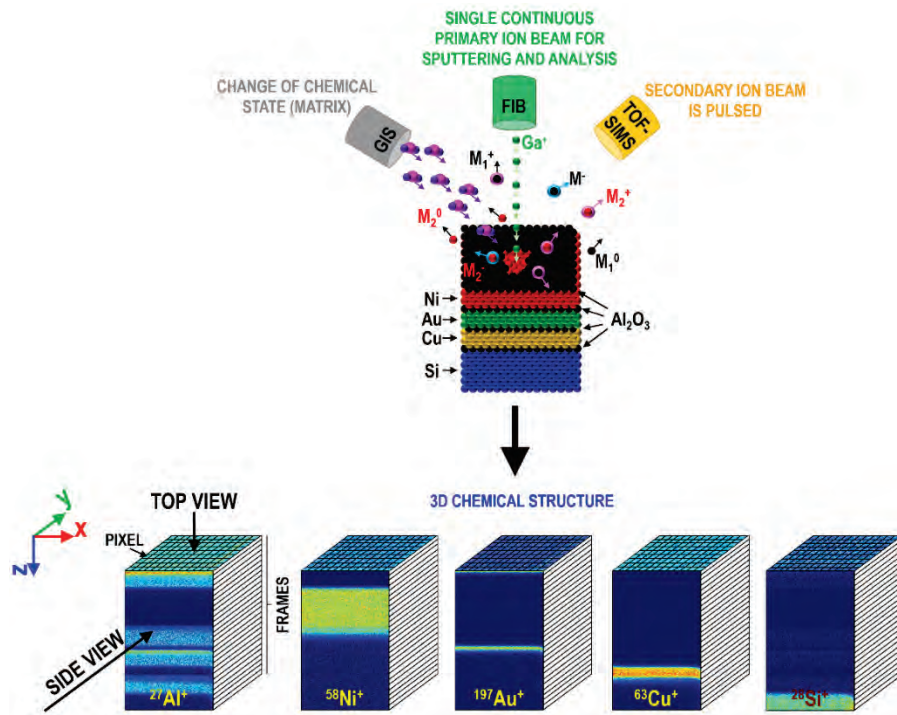


Figure 1. Gas assisted FIB-TOF-SIMS allows the chemical structure of complex buried thin films to be represented in 3D with nanoscale resolution.

- [1] Benninghoven A, Rudenauer F G and Werner H W 1987 Secondary ion mass spectrometry—basic concepts, instrumental aspects, applications and trends. *Surf. Interface Anal.* **10** 435
- [2] Whitby J A, Östlund F, Horvath P, Gabureac M, Riesterer J L, Utke I, Hohl M, Sedláček L, Jiruše J, Friedli V, Bechelany M and Michler J 2012 High spatial resolution time-of-Flight secondary ion mass spectrometry for the masses: A novel orthogonal ToF FIB-SIMS instrument with in situ AFM *Adv. Mater. Sci. Eng.* **2012** 1–13
- [3] Priebe A, Utke I, Pethö L and Michler J 2019 Application of a Gas-Injection System during the FIB-TOF-SIMS Analysis - Influence of Water Vapor and Fluorine Gas on Secondary Ion Signals and Sputtering Rates *Anal. Chem.* **91** 11712–22
- [4] Priebe A, Xie T, Pethö L and Michler J 2020 Potential of gas-assisted time-of-flight secondary ion mass spectrometry for improving elemental characterization of complex metal-based systems *J. Anal. At. Spectrom.* **35** 2997–3006
- [5] Priebe A, Pethö L and Michler J 2020 Fluorine Gas Coinjection as a Solution for Enhancing Spatial Resolution of Time-of-Flight Secondary Ion Mass Spectrometry and Separating Mass Interference *Anal. Chem.* **92** 2121–9
- [6] Priebe A, Huszar E, Nowicki M, Pethö L and Michler J 2021 Mechanisms of fluorine-induced separation of mass interference during TOF-SIMS analysis *Anal. Chem.* **93**, 29, 10261–10271.
- [7] Priebe A, Pethö L, Huszár E, Xie T, Utke I and Michler J 2021 High sensitivity of fluorine gas-assisted FIB-TOF-SIMS for chemical characterization of buried sublayers in thin films *ACS Appl. Mater. Interfaces*, **13**(13), 15890-15900
- [8] Priebe A, Sastre J, Futscher M H, Jurczyk J, Puydinger Dos Santos M V., Romanyuk Y E and Michler J 2021 Detection of Au<sup>+</sup> Ions During Fluorine Gas-Assisted Time-of-Flight Secondary Ion Mass Spectrometry (TOF-SIMS) for the Complete Elemental Characterization of Microbatteries *ACS Appl. Mater. Interfaces*, **13**(34), 41262-41274
- [9] Sastre J, Futscher M H, Pompizi L, Aribia A, Priebe A, Overbeck J, Stiefel M, Tiwari A N and Romanyuk Y E 2021 Blocking lithium dendrite growth in solid-state batteries with an ultrathin amorphous Li-La-Zr-O solid electrolyte *Commun. Mater.* **2**, 76
- [10] Dubey R, Sastre J, Cancellieri C, Okur F, Forster A, Pompizii L, Priebe A, Romanyuk Y E, Jeurgens L P H, Kovalenko M V. and Kravchuk K V. 2021 Building a Better Li-Garnet Solid Electrolyte/Metallic Li Interface with Antimony *Adv. Energy Mater.* **11** (39), 2102086.

# Study of Focused Rb<sup>+</sup> Ion Beam Applications

Y. Li<sup>1</sup>, S. Xu<sup>1</sup>, and E. J. D. Vredenburg<sup>1</sup>

<sup>1</sup>Department of Applied Physics, Eindhoven University of Technology, P.O. Box 513, 5600 MB Eindhoven, the Netherlands

E-Mail: (e.j.d.vredenburg@tue.nl)

Focused ion beams (FIBs) are important tools for materials science and the semiconductor industry. With their applications in milling and material deposition, FIBs enable circuit editing and mask repair during device development and failure analysis in wafer processing. Here a prototype Rb FIB system is presented. The essential innovation is the use of a cold-atom ion source<sup>[1]</sup> based on photoionization of a laser-intensified and cooled atomic Rb beam. The whole source is mounted onto a commercial FIB column for milling and deposition experiments<sup>[2-3]</sup>.

Stable performance of the Rb<sup>+</sup> beam enabled beam profiling using a knife-edge method. Working at 8.5 keV and 6 pA, the beam was determined to have a  $d_{50}$  of 160 nm. After optimization, a  $d_{50}$  of a few nm and a predicted reduced brightness of near  $1 \times 10^6$  A/(m<sup>2</sup>·sr·eV) should be achievable, which is comparable with that of the commercial Ga<sup>+</sup> LMIS. Different energies and currents are also available with the beam.

Milling performance is firstly studied using several standard substrates. The experimental results show that Rb<sup>+</sup> has good sputter yield ability in most substrates used, such as B, Diamond, Cu, Au, GaAs, and InP as shown in Fig.1, even compared to 30 keV Ga<sup>+</sup>. It should be noted that the Rb FIB system uses 8.5 keV beam energy, which can have the advantage of a short ion projection range due to the low beam energy. A further study has shown that the Rb staining in the Si substrate is limited to 5.1% in atomic concentration.

Focused-ion-beam-induced deposition (FIBID) was achieved by introducing a precursor gas to the vicinity of the ion beam scanning area. For Pt deposition, (MeCp)Pt(Me)<sub>3</sub> was used as the precursor. Fig.2 contains a Rb<sup>+</sup> induced Pt bar on Si with the inset showing a 225×122.5 nm<sup>2</sup> area of the deposition cross section. The thickness of the deposition is indicated by the groove made using a Ga FIB, and the granularity of the deposited material can be seen in the inset. Characterization results of FIBID Pt are included in Table 1. These results reveal that the deposition induced by the Rb<sup>+</sup> has a smaller primary ion content and a lower resistivity than that induced by the Ga<sup>+</sup> under similar circumstances

[1] J. J. McClelland *et al*; *Bright focused ion beam sources based on laser-cooled atoms*; Applied Physics Reviews 3 (2016), 011302

[2] G. ten Haaf; *Ultracold Rb Focused Ion Beam*; PhD thesis, Eindhoven University of Technology (2017)

[3] G. ten Haaf *et al*; *Measurements of the energy distribution of a high brightness rubidium ion beam*; Ultramicroscopy 190 (2018), 12



 **Kraków**

**FEBIP 2022**  
8<sup>th</sup> Workshop on **Focused**  
**Electron Beam Induced**  
**Processing**



13<sup>th</sup> – 15<sup>th</sup> of July 2022





The event is organized under  
the **Honorary Patronage**  
of AGH UST Rector  
Prof. dr hab. inż. Jerzy Lis



#### Local Organizing Committee:

Dr. Aleksandra Szkudlarek (ACMiN)  
Dr. Ivo Utke (EMPA)  
Dr. Katarzyna Berent (ACMiN)  
Dr. Kamilla Kollbek (ACMiN)  
Dr. Sylwia Klejna (ACMiN)  
Prof. Angelika Kmita (ACMiN)  
Krzysztof Maćkosz (EMPA)  
Anna Sikora (ACMiN)  
Prof. Marcin Sikora (ACMiN)  
Prof. Marek Przybylski (ACMiN)

#### Scientific Committee:

Dr. Cornelis W. Hagen (Delft University of Technology)  
Dr. Klaus Edinger (SMT Carl Zeiss)  
Dr. Gian Carlo Gazzadi (CNR Institute Nanoscience Modena)  
Prof. Michael Huth (Goethe University Frankfurt)  
Prof. Harald Plank (Graz University of Technology)  
Prof. Masayuki Shimojo (Shibaura Institute of Technology)  
Prof. José Maria de Teresa (ICMA Zaragoza)  
Prof. Milos Toth (University of Technology Sidney)  
Dr. Ivo Utke (EMPA Thun)  
Prof. Heinz Wanzenböck (Vienna University of Technology)

#### Organizers:



#### Sponsors:



Seeing beyond



#### Partners:





FEBIP 2022 Program Overview	
Tuesday 12/07/2022	
19:00	Welcome Reception
Wednesday 13/07/2022	
8:45	OPENING ADDRESS
Session 1: Nanofabrication with FIB/FEB	
9:00	<b>R. Cordoba (invited, fit4nano):</b> FIBID of $W(CO)_6$
9:30	<b>Stephen T. Kelly (Zeiss):</b> The importance of data representivity in the analysis of modern battery materials: Why FIB tomography voxel size is critical?
9:50	<b>L. McElwee-White:</b> Comparison of Electron- and Ion-Induced Chemistry in FEBID/FIBID Precursors
10:10	<b>P. Nag:</b> Ion Induced Decomposition of Iron Pentacarbonyl
10:30	Coffee Break
Session 2: FIBIP	
11:00	<b>M. Toth (invited):</b> Nanofabrication and knock-on doping using an inert plasma FIB and solid/gaseous precursors
11:30	<b>M. Wu (Thermofisher):</b> Femtosecond laser integrated multiple species ion plasma FIB and its interaction with soft and hard materials
11:50	<b>P. Le Gal:</b> Comparative study of copper contents obtained by focused electron & ion beam induced deposition ( $Ga^+$ , $Xe^+$ ) with $Cu(II)(hfac)_2 \cdot xH_2O$
12:10	<b>M. Huth:</b> Locally selective magnon excitation in FEBID/FIBID nanostructures
12:30	Lunch
Session 3: FIBID/FEBID & Fundamentals	
14:00	<b>J. M. De Teresa (invited):</b> Recent advances in superconducting FIBID nanostructures and Cryo-FIBID
14:30	<b>H. Fairbrother (invited):</b> Electrons/Ions Stimulated Surface Reactions of Organometallic Precursors
15:00	<b>J. Jurczyk:</b> Modeling ligand co-deposition in selective electron-driven deposition with metalorganic molecules
15:20	<b>A. Kuprava:</b> Effective simulation of the FEBID process
15:40	Coffee Break
16:10	Poster Slam 11x5 min
17:10	Poster session



Thursday 14/07/2022	
Session 4: Fundamentals	
9:00	<b>S. Barth (invited):</b> Precursors for direct-write nanofabrication with electrons
9:30	<b>I. B. Szymańska:</b> How coordination chemistry limits new FEBID precursors development?
9:50	<b>L. Amiaud:</b> Electron induced decomposition – toward quantitative data
10:10	<b>P. Martinović:</b> Electron-Induced Decomposition of Different Silver(I) Complexes: Implications for the Design of Precursors for Focused Electron Beam Induced Deposition
10:30	Coffee Break
Session 5: 3D FEBID	
11:00	<b>H. Plank (invited):</b> 3D printed nanostructures with focused electron beams
11:30	<b>C. W. Hagen:</b> Direct Fabrication of 3D Hollow Nano-cones
11:50	<b>L. M. Seewald:</b> Advancing Design Possibilities during 3D Nanoprinting
12:10	<b>A. Weitzer:</b> On the Route towards Precision - 3D-Nanoprinting of Closed Structures via FEBID
12:30	Lunch
Session 6: Metallic Nanostructures	
14:00	<b>K. Höflich (invited):</b> Direct electron beam writing of metallic nanostructures and insight gained from surface deposition techniques
14:30	<b>A. Salvador-Porroche:</b> Nanofabrication of Metallic Palladium Deposits by a Direct Electron Beam Irradiation Process Free of Post-Treatments Steps
4:50	<b>A. Tsarapkin:</b> Direct Writing of Chiral and Nonlinear Plasmonic Devices
15:10	Coffee Break
15:30	Trip to Wieliczka (visiting at 17:10 )
20:30	Conference Dinner

Friday 15/07/2022	
Session 7: Perspectives	
9:00	<b>S. George (invited):</b> Electron-enhanced atomic layer deposition
9:30	<b>A. Han:</b> Injecting Energetic Electrons into CO <sub>2</sub> Ice
9:50	<b>C. Glessi:</b> Water-Assisted FEBID/FEBIE for the Deposition of High Purity Noble Metal Nanostructures
10:10	<b>H. Marbach:</b> Pushing the Limits of EUV Mask Repair: Addressing Sub-10 nm Defects with the Next Generation Ebeam-based Mask Repair Tool
10:30	Coffee Break
Session 8: Application of FEBIP/FIBIP	
11:00	<b>O. Dobrovolskiy (invited):</b> Hybrid superconductor/ferromagnetic structures
11:30	<b>A. Fernández-Pacheco (invited):</b> Layer by Layer FEBID 3D Printing and its Applications to Nanomagnetism
12:00	<b>D. Kuhness:</b> Plasmonic On-Demand Design via 3D Nanoprinting
12:20	<b>CLOSING REMARKS</b>
12:40	Lunch





**Oral** presentations



# Nanofabrication and Knock-on Doping Using an Inert Plasma FIB and Solid/Gaseous Precursors

Milos Toth<sup>1,2,\*</sup>

<sup>1</sup> School of Mathematical and Physical Sciences, University of Technology Sydney, New South Wales 2007, Australia

<sup>2</sup> ARC Centre of Excellence for Transformative Meta-Optical Systems, University of Technology Sydney, New South Wales 2007, Australia

\* email: [milos.toth@uts.edu.au](mailto:milos.toth@uts.edu.au)

Inert focused ion beam (FIB) techniques are appealing as they avoid implantation of reactive species such as Ga<sup>+</sup>. Here, I present two recent developments in inert-ion-beam processing: (1) A chemical approach for suppressing artifacts during FIB milling (Fig. 1a-c), and (2) A versatile method for dopant implantation (Fig. 1d-e) [1, 2].

**FIB milling:** Inert ion beams are appealing as they avoid staining by reactive ions which can radically alter functional properties of materials. However, the utility of inert FIB milling is limited by ion-induced crystal damage and surface coarsening. Sub-surface damage can be reduced or even eliminated by performing milling above the recrystallisation temperature of the milled material [3]. However, in this regime, surface coarsening is problematic because of high thermal mobilities of surface species (Fig. 1b). Here, I describe a chemical solution to this problem based on FIB milling in a hydrogen plasma delivered to a sample locally using a remote plasma source (Fig. 1a). Hydrogen immobilizes adatoms and surface vacancies, and thus suppresses surface coarsening (Fig. 1c). The method enables smooth, damage-free FIB milling of crystalline semiconductors under FIB conditions needed for practical nanofabrication. The approach, demonstrated here using Ge, GaAs and GaP, is applicable to a wide range of materials and enhances the utility of inert FIB systems for the milling of functional nanostructures.

**Knock-on doping:** Ion implantation is a powerful technique for doping of materials. Direct implantation by a FIB is particularly appealing as it eliminates the need for sample masking and associated steps employed in lithographic methods. However, the range of ions that can be implanted is limited by the species which can be generated in common ion sources. This limitation can be overcome by a well-known approach termed recoil-implantation (a.k.a. "knock-on doping"), whereby implantation is achieved via momentum transfer from energetic ions to atoms in a solid-state precursor (typically a thin film, see Fig. 1d). Here, I will demonstrate how this technique can be implemented on an inert ion FIB system, and used to dope diamond [1]. Moreover, I will demonstrate an analogous method using a gas phase precursor (Fig. 1e), thereby expanding the range of dopants accessible by this method [2].

[1] J.E. Fröch et al.; *Versatile direct-writing of dopants in a solid state host through recoil implantation*; Nature Communications 11, 5039 (2020)

[2] A. Gale et al.; *Recoil implantation using gas-phase precursor molecules*; Nanoscale 13, 9322 (2021)

[3] X. Ou et al.; *Reverse epitaxy of Ge: ordered and faceted surface patterns*; Phys. Rev. Lett. 111, 016101 (2013)

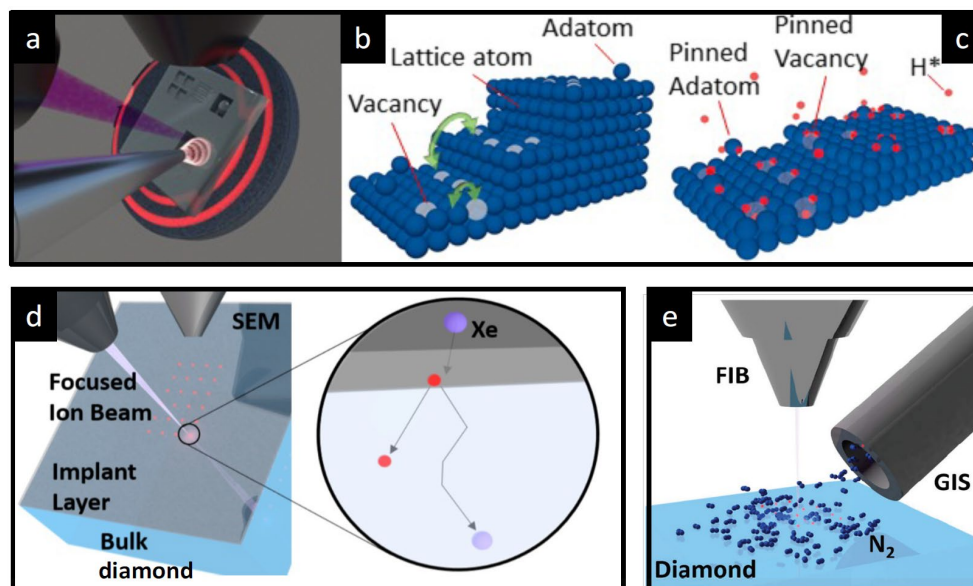


**Figure 1. Nanofabrication and knock-on doping using a focused ion beam.** (a) A sample on a heating stage of a FIB-SEM instrument. The sample is irradiated by a hydrogen plasma plume during ion beam (purple) milling. (b) Adatom and vacancy diffusion at a sample surface, resulting in terracing and surface coarsening. (c) Pinning of surface species by hydrogen, resulting in suppression of surface roughness. (d) Knock-on implantation of dopants into diamond from a solid state precursor ("implant layer") [1]. (e) Knock-on doping using a gas-phase precursor [2].

# Femtosecond laser integrated multiple species ion plasma FIB and its interaction with soft and hard materials

Min Wu<sup>1,\*</sup>

<sup>1</sup> Thermo Fisher Scientific, Eindhoven, The Netherlands

\* email: [min.wu@thermofisher.com](mailto:min.wu@thermofisher.com)

Femtosecond laser brings the new opportunities for large area materials ablation and volume recovery. Combined with multiple ion species plasma PFIB it is possible to investigate microstructure not only with ultrafast materials removal but also with superior high cut face quality and voxel resolution.

In this abstract we present the results of comparative studies of femtosecond laser enabled multiple species ion plasma FIB on both soft (tire polymer) and hard (additive manufacturing Ti64 alloys) materials. In the two datasets we investigated the cut face quality on tire polymer and Ti64 alloys using different ion species with various beam parameters, the effect of different ion species and slicing parameters on the tire materials is compared and analysed, respectively.

The slice surface quality using different ultra shot pulse laser wavelength and resulting periodic surface texture induced by laser is also discussed.



**Figure 1.** Tire polymer cut face from laser only, laser+Xe ion polishing and Laser+O ion polishing, respectively.



# Comparative study of copper contents obtained by focused electron & ion beam induced deposition ( $\text{Ga}^+$ , $\text{Xe}^+$ ) with $\text{Cu(II)(hfac)}_2 \cdot x\text{H}_2\text{O}$

Pierre Le Gal<sup>1,\*</sup>, Krzysztof Mackosz<sup>2</sup>, Ivo Utke<sup>2</sup> and Gregory Goupil<sup>1</sup>

<sup>1</sup> Orsay Physics, TESCAN Orsay, 95 Avenue des Monts Auréliens – ZA Saint-Charles 13710 Fuveau, France

<sup>2</sup> Empa, Swiss Federal Laboratories for Materials Science and Technology, Laboratory for Mechanics of Materials and Nanostructures, Feuerwerkerstrasse 39, 3602 Thun, Switzerland

\* email: [pierre.legal@orsayphysics.com](mailto:pierre.legal@orsayphysics.com)

Copper is widely used to make interconnections in complex high density 3D packaged electronic circuits. This metal presents the property to be a very good electrical conductor and can be easily deposited with the classically used semiconductor processes. Nevertheless, for circuit testing the copper hardwiring needs to be modified, meaning wires need to be cut and rewired to check the function of electrical units on the printed board.

In this contribution we will revisit focused electron and ion beam deposition (FEBID and FIBID) of copper lines with the copper-hexafluoroacetylacetonate precursor  $\text{Cu(II)(hfac)}_2 \cdot x\text{H}_2\text{O}$ . This precursor is known for its notoriously low copper content  $< \approx 10\text{at.}\%$  during room temperature FEBID deposition [1], which can only be marginally improved by vacuum annealing [2]. The FEBID material contained large amounts of carbon smaller amounts of oxygen and fluorine from the ligand. However, to realize an electrically conductive bond between two metallic lines, it is important to realize a precise, high metal content, and reliable deposition.

Particularly, in our study we were extending from FEBID to FIBID using not only gallium ion beams but also noble gas ions beams of xenon. Furthermore,  $\text{Cu(II)(hfac)}_2 \cdot x\text{H}_2\text{O}$  comes in hydrated form as can be witnessed by its color. The monohydrate ( $x=1$ ) is green while the dehydrated precursor is deep purple ( $x=0$ ). We found the metal content in deposited squares to be dependent on the type of focused charged particle beams used for deposition being highest for xenon and lowest for electrons,  $\text{Xe}^+ > \text{Ga}^+ > \text{e}^-$ . Morphological changes were observed in cross sections of Xe ion deposited squares pointing to a more granular structure, see **fig. 1a**. Similarly, a dependence on the hydration state of the precursor was observed, which could be mitigated by increasing the precursor flux of the dehydrated precursor by changing the temperature of evaporation, see **fig. 1b**. We will discuss the findings and propose a route for high copper content deposition using FEBID & FIBID.

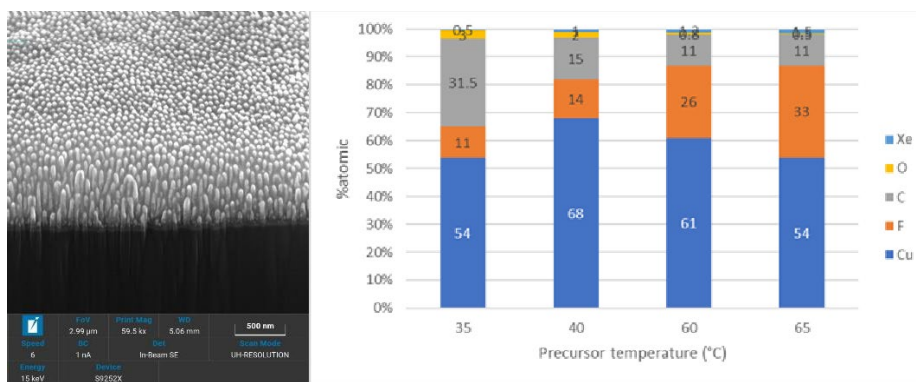


**Figure 1.** Xe plasma FIB deposits with  $\text{Cu(hfac)}_2$ . a) SEM image of cross section square deposit showing a grainy structure. b) EDX measured composition of deposited material as function of precursor temperature (precursor flux). Note the  $> 50\text{at.}\%$  Cu content which was achieved for the first time with a  $\text{Cu(II)}$  precursor

[1] I. Utke b, P. Swiderek, K. Höflich, K. Madajska, J. Jurczyk, P. Martinovic, I. B. Szymanska; *Organometallic precursors of group 10 and 11: Focused electron beam induced deposition of metals and insight gained from chemical vapour deposition, atomic layer deposition, and fundamental surface and gas phase studies*; Coordination Chemistry Reviews 458 (2022) 213851. DOI: 10.1016/j.ccr.2021.213851.

[2] M. V. Puydinger dos Santos, A. Szkudlarek, A. Rydosz, C. Guerra-Nuñez, F. Béron, K.R. Pirola1, S. Moshkalev, J. A. Diniz, I. Utke; Beilstein J. Nanotechnol. 2018, 9, 91–101. DOI: 10.3762/bjnano.9.11

# Locally selective magnon excitation in FEBID/FIBID nanostructures

M. Küß<sup>1</sup>, F. Porrati<sup>2</sup>, A. Hörner<sup>1</sup>, M. Weiler<sup>3</sup>, M. Albrecht<sup>4</sup>, M. Huth<sup>2,\*</sup> and A. Wixforth<sup>1</sup>

<sup>1</sup> University of Augsburg, Experimental Physics I, Institute of Physics, 86135 Augsburg, Germany

<sup>2</sup> Goethe University, Physics Institute, 60438 Frankfurt am Main, Germany

<sup>3</sup> Technical University Augsburg, Physics Department and OPTIMAS, 67663 Kaiserslautern, Germany

<sup>4</sup> University of Augsburg, Experimental Physics IV, Institute of Physics, 86135 Augsburg, Germany

\* email: [michael.huth@physik.uni-frankfurt.de](mailto:michael.huth@physik.uni-frankfurt.de)

Resonant coupling of surface acoustic waves (SAWs) to magnetic excitations in ferromagnets (spin waves, SWs) is the basis for an energy efficient approach towards SW generation and manipulation, see e.g. [1] for a recent review. In addition, SAW technology is extremely well developed and SAW-based devices are ubiquitous in mobile devices and other hf-based electronics.

Employing interdigital transducers (IDTs), i.e. comb-shaped metallic electrodes, on top of a piezoelectric substrate, SAWs can be effectively generated. By using tapered IDTs (TIDTs) on a Y-cut Z-propagating LiNbO<sub>3</sub> as substrate material, see Fig. 1 below, it is possible to fulfill the resonant coupling conditions with lateral control on the micron scale and thus specifically address magnetic micro-stripes with differing magnetic properties fabricated by means of focused electron (FEBID) or ion beam induced deposition (FIBID) employing HCo<sub>3</sub>Fe(CO)<sub>12</sub> as precursor [2].

In this contribution, we show results of magnetoacoustic SW excitation and characterization in the forward volume mode geometry. Based on magnetoacoustic transmission measurements employing TIDTs we demonstrate how resonant coupling can be locally confined so as to generate a SAW beam of about 8 μm width which is suitable to selectively excite SWs in magnetic micro-stripes with 20 x 40 μm<sup>2</sup> dimension.

By systematically varying the direction of the external magnetic field from normal (z) to in-plane orientation (xy) in three different azimuths a large set of transmission data was acquired for a systematic study of *k*-dependent SW excitation. By employing a recently developed semi-phenomenological model based on the Landau-Lifshitz-Gilbert equation including a magnetoacoustic driving field [3] generalized to arbitrary field orientation and to non-zero wave vector *k* [2] we are able to reproduce the transmission data via numerical simulation. Our results show that the ε<sub>zz</sub> strain component can result in enhanced SAW-SW coupling efficiency and SAW-SW helicity mismatch causing non-reciprocal SW propagation without the need of Dzyaloshinskii-Moriya-like, i.e. chiral, interactions.

[1] D. A. Bozhko et al.; *Magnon-phonon interactions in magnon spintronics (review)*; Low Temp. Phys. 46, 383 (2020).

[2] M. Küß et al.; *Forward volume magnetoacoustic wave excitation with micron-scale spatial resolution*; Appl. Phys. Lett. Mater., submitted (2022).

[3] M. Küß et al.; *Nonreciprocal Dzyaloshinskii-Moriya magnetoacoustic waves*; Phys. Rev. Lett. 125, 217203 (2020).

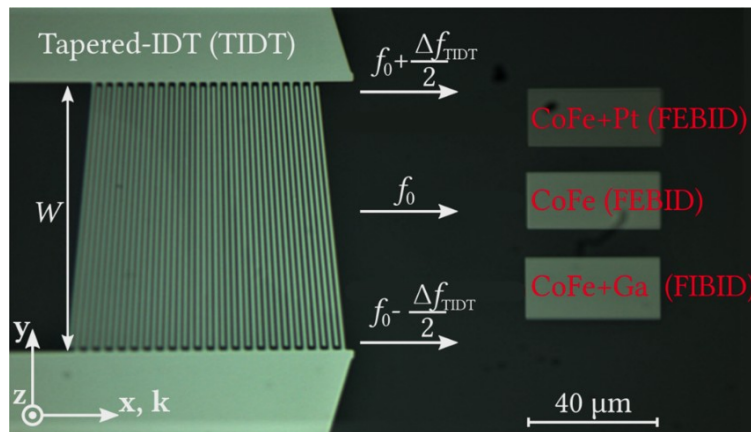


**Figure 1.** Optical microscopy image of tapered interdigital transducer with three magnetic micro-stripes fabricated by FEBID (top and middle) and FIBID (bottom), as indicated. See text for details.

# Recent advances in superconducting FIBID nanodevices and Cryo-FIBID

José María De Teresa<sup>1,2,\*</sup>, Alba Salvador-Porroche<sup>1</sup>, Fabian Sigloch<sup>1</sup>, Pablo Orús<sup>1</sup>, Alix Tatiana Escalante-Quiceno<sup>1</sup>, Soraya Sangiao<sup>1,2</sup>, Mariano Barrado<sup>2</sup>, Cesar Magén<sup>1,2</sup>, Pilar Cea<sup>1,2</sup>, Daria Belotcerkovtceva<sup>3</sup>, M. Venkata Kamalakar<sup>3</sup>, Patrick Philipp<sup>4</sup>

<sup>1</sup> Instituto de Nanociencia y Materiales de Aragón (INMA), CSIC-Universidad de Zaragoza, 50009 Zaragoza, Spain

<sup>2</sup> Laboratorio de Microscopías Avanzadas (LMA), Universidad de Zaragoza, 50018 Zaragoza, Spain

<sup>3</sup> Department of Physics and Astronomy, Uppsala University, Box 516, SE-751 20, Uppsala, Sweden

<sup>4</sup> Advanced Instrumentation for Nano-Analytics (AINA), MRT Department, Luxembourg Institute of Science and Technology (LIST), 41 rue du Brill, 4422 Belvaux, Luxembourg

\* email: [deteresa@unizar.es](mailto:deteresa@unizar.es)

Focused Ion Beam Induced Deposition (FIBID) is a relevant technique to directly pattern superconducting materials and build nanodevices, as recently reviewed by some of us [1]. This topic will be discussed in the first part of the talk; in particular, the use of FIBID for the growth of W-C nanoSQUIDs will be described in detail [2]. In the second part of the talk, the utilization of FIBID under cryogenic conditions (Cryo-FIBID), based on the formation of a condensed layer of the precursor material via substrate cooling, will be introduced. By using a cryogenic module based on liquid N<sub>2</sub>, we have applied Cryo-FIBID to grow W-C [3, 4], Pt-C [5] and Co [6] deposits, observing a few-hundred-times enhancement in the growth speed when compared to room-temperature FIBID. Applications of Cryo-FIBID to grow electrical contacts on micro-structures will be discussed, such as their use on graphene ribbons (Figure 1). Lastly, the perspectives opened by Cryo-FIBID processing will be presented, highlighting its successful application at -60°C making use of a thermoelectric plate [7].

[1] P. Orús, F. Sigloch, S. Sangiao, J. M. De Teresa; *Superconducting materials and devices grown by focused ion and electron beam induced deposition*; *Nanomaterials*, vol. 12, p.1367, 2022.

[2] F. Sigloch, S. Sangiao, P. Orús, J. M. De Teresa; *Large output voltage to magnetic flux change in nanoSQUIDs based on direct-write Focused Ion Beam Induced Deposition technique*; arXiv: 2203.05278.

[3] R. Córdoba, P. Orús, S. Strohauser, T.E. Torres, J. M. De Teresa; *Ultra-fast direct growth of metallic micro- and nanostructures by focused ion beam irradiation*; *Scientific Reports*, vol. 9, p.14076, 2019.

[4] J. M. De Teresa, P. Orús, R. Córdoba, P. Philipp; *Comparison between focused electron/ion beam induced deposition at room temperature and under cryogenic conditions*; *Micromachines*, vol. 10, p. 799, 2019.

[5] A. Salvador-Porroche, S. Sangiao, P. Philipp, P. Cea, J. M De Teresa; *Optimization of Pt-C deposits by Cryo-FIBID: substantial growth rate increase and quasi-metallic behavior*; *Nanomaterials*, vol. 10, p.1906, 2020.

[6] A. Salvador-Porroche, S. Sangiao, C. Magén, M. Barrado, P. Philipp, D. Belotcerkovtceva, M. V. Kamalakar, P. Cea, J. M De Teresa; *Highly-efficient growth of cobalt nanostructures using focused ion beam induced deposition under cryogenic conditions: application to electrical contacts on graphene, magnetism and hard masking*; *Nanoscale Advances*, vol. 3, p. 5656, 2021.

[7] P. Orús, F. Sigloch, S. Sangiao, J. M. De Teresa; *Cryo-Focused Ion Beam Induced Deposition of tungsten-carbon nanostructures using a thermoelectric plate*; *Applied Sciences*, vol. 11, p.10123, 2021.

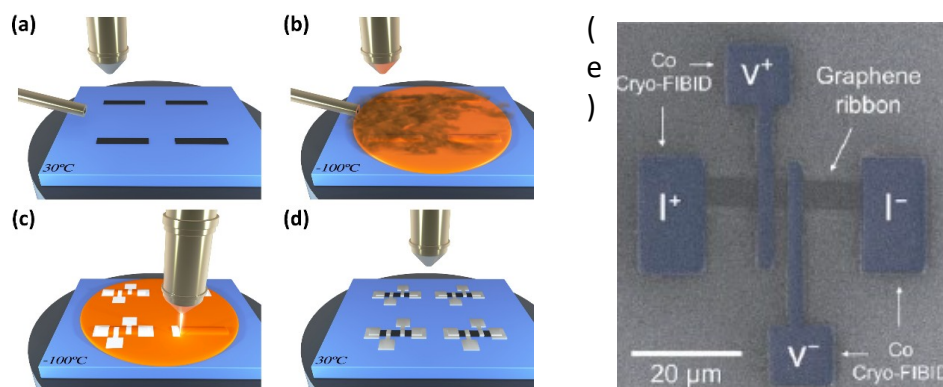


Figure 1. (a) to (d) the four steps of the Cryo-FIBID process, used to contact graphene ribbons (e), reprinted from [6]

# Surface Reactions of Organometallic Precursors with Ions and Electrons

Howard Fairbrother<sup>1,\*</sup>, Lisa McElwee White<sup>2</sup>, Mohammed Abdel-Rahmen<sup>1</sup>, Patrick Eckhert<sup>1</sup>, Jo-Chi Yu<sup>2</sup>

<sup>1</sup> Department of Chemistry, Johns Hopkins University, Baltimore, MD 21218, USA

<sup>2</sup> Department of Chemistry, University of Florida, Gainesville, Florida 32611-7200, USA

\* email: [howardf@jhu.edu](mailto:howardf@jhu.edu)

One of the biggest challenges with charged particle deposition techniques, focused electron beam-induced deposition (FEBID) and focused ion beam-induced deposition (FIBID), is the difficulty in controlling or predicting the composition of the deposits. Indeed, the creation of pure metal nanostructures in FEBID or FIBID is often a goal for optimizing materials properties, but is rarely realized in practice without postdeposition processing.

In FEBID and FIBID the initial molecular event involves a deposition step which converts the organometallic precursor into a non-volatile species. These molecular level processes can be studied by studying the effects of electron or ion irradiation on a nanometer thick film of precursor molecules is studied using analytical techniques, such as XPS, mass spectrometry and infrared spectroscopy [1, 2]. Results point to systematic and fundamental differences between electron and ion induced deposition processes. In electron mediated deposition, reactions occur from reactions initiated by low energy electrons, produced by the interaction of the primary electron beam with the substrate. In contrast, ion-induced reactions are consistent with energy transfer between the incident ion and the adsorbed precursor [3]. In both electron and ion induced reactions, the deposition step leads to ligand desorption from the organometallic precursor, although the extent of ligand desorption is invariably higher for ion-induced reactions. For example, in electron induced deposition of MeCpPtMe<sub>3</sub> leads to the loss of one CH<sub>3</sub> group as methane while ion-induced reactions are responsible for the desorption of all four CH<sub>3</sub> groups in the form of methane and ethane [4].

Subsequent reactions of the intermediate species produced by the precursor deposition step are varied and depend critically upon the chemical identity and structure of the intermediate and the deposition conditions. In FEBID the reactivity of the intermediate species reflects a balance between further electron beam induced reactions, which overwhelmingly lead to unwanted incorporation of organic contaminants in the deposits, and thermal reactions which promote further ligand desorption and improve metal content. In FIBID, the fate of the intermediate species is determined predominantly by sputtering of the deposited atoms, with organic contaminants undergoing preferential removal compared to deposited metal atoms. This balance between sputtering and deposition is manifested by the structural and compositional differences observed in the Pt-containing structures formed as a result of Ar<sup>+</sup> and He<sup>+</sup> mediated deposition of MeCpPtMe<sub>3</sub> in both precursor and ion-limited deposition regimes (Fig. 1).

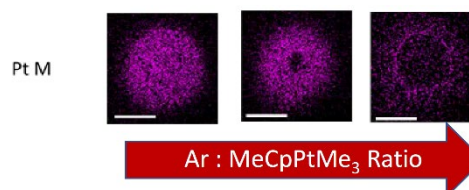


**Figure 1.** Effect of increasing Ar:MeCpPtMe<sub>3</sub> ratio on deposits formed by ion-induced deposition.

While these mechanistic underpinning can provide the basis to qualitatively understand the ultimate composition of deposits created by charged particles, the scientific literature reveals a wide range of reported compositions for structures created from the same precursor. This issue represents a severe obstacle towards progress in the field and I will discuss two of the most significant reasons for these inconsistencies; (i) the effect of contaminant gases on deposit composition and (ii) overreliance, inconsistency and lack of quantification associated with EDS data.

[1] J. C. Yu, M. K. Abdel-Rahman, D. H. Fairbrother, L. McElwee-White; *Charged Particle-Induced Surface Reactions of Organometallic Complexes as a Guide to Precursor Design for Electron- and Ion-Induced Deposition of Nanostructures*; ACS Applied Materials & Interfaces. 13: 48333-48348 (2021).

[2] M. Rohdenburg, P. Martinović, K. Ahlenhoff, S. Koch, D. Emmrich, A. Götzhäuser, P. Swiderek; *Cisplatin as a Potential Platinum Focused Electron Beam Induced Deposition Precursor: NH<sub>3</sub> Ligands Enhance the Electron-Induced Removal of Chlorine*; The Journal of Physical Chemistry C. 123: 21774-21787 (2019).

[3] R. M. Thorman, S. J. Matsuda, L. McElwee-White, D. H. Fairbrother; *Identifying and Rationalizing the Differing Surface Reactions of Low-Energy Electrons and Ions with an Organometallic Precursor*; Journal of Physical Chemistry Letters. 11: 2006-2013 (2020).

[4] J. D. Wnuk, J. M. Gorham, S. G. Rosenberg, W. F. van Dorp, T. E. Madey, C. W. Hagen, D. H. Fairbrother; *Electron Induced Surface Reactions of the Organometallic Precursor Trimethyl(methylcyclopentadienyl)platinum(IV)*; Journal of Physical Chemistry C. 113: 2487-2496 (2009).

# Modeling ligand co-deposition in selective electron-driven deposition with metalorganic molecules

Jakub Jurczyk<sup>1\*</sup>, Leo Brokhuis<sup>2</sup>, Luisa Berger<sup>2</sup>, Czesław Kapusta<sup>3</sup> and Ivo Utke<sup>2</sup>

<sup>1</sup> Institute of Nanoscience and Materials of Aragon – CSIC, Edif. I+D, C/ Mariano Esquillor Gómez, 50018 Zaragoza, Spain

<sup>2</sup> Empa - Swiss Federal Laboratories for Materials Science and Technology, Laboratory for Mechanics of Materials and Nanostructures, Feuerwerkerstrasse 39, CH - 3602 Thun, Switzerland

<sup>3</sup> AGH University of Science and Technology, Faculty of Physics and Applied Computer Science, Al. Mickiewicza 30, 30-059 Kraków, Poland

\* email: [jakub.jurczyk@unizar.es](mailto:jakub.jurczyk@unizar.es)

Focused electron beam induced deposition (FEED) is a promising candidate to be a reliable 3D nano printing method, as it combines high lateral resolution (down to single nanometres) with possibility of deposition of complex three-dimensional structures [1]. In most cases it is used to deposit metal-containing structures with various applications including amongst others photolithography mask repair [2], scanning probe tips production [3] and basic research in the fields of nanomagnetism and plasmonics [1]. It utilizes organometallic molecules to deliver them in gas phase over the substrate, where they adsorb and are dissociated by the electron beam.

One of the challenges of FEED remains a low metal content of the deposits. It is most frequently caused by presence of organic ligands, which can be incorporated into the deposit via incomplete dissociation or co-deposition of already dissociated ligands. As was shown before for various precursors, metal content of the structures highly depends on the parameters used for deposition, such as electron flux, substrate temperature or flux of precursor molecules [4]. To fully understand the relation between deposition parameters and metal content of the deposit it would be important to have a possibility to properly model all electron induced processes happening on the substrate. Unfortunately, current FEED models do not provide such an opportunity [5].

In presented contribution, we would like to show a possibility of modelling ligands' co-deposition process during FEED. The model bases on two differential equations, instead of one: first to analyse behaviour of nondissociated precursor molecules on the substrate's surface and the second one to analyse the electron-induced deposition of ligands, created due to dissociation of precursor molecules. Although the model is more complex than the one currently used, it allows for prediction of dependence between metal content of the deposit and applied deposition parameters and more accurately predict the growth rate of the deposit.

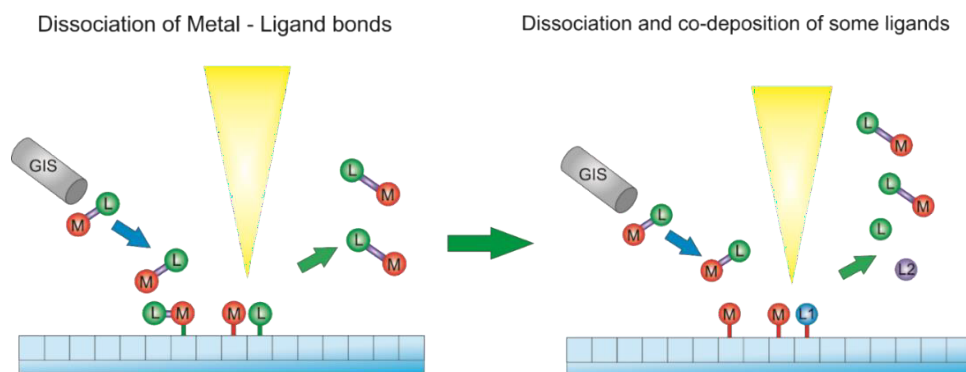


**Figure 1.** Schematic representation of the new FEED model: precursor molecule adsorb and can be dissociated, creating a metal atom and ligand, which can be dissociated further into volatile and non-volatile part.

[1] M. Huth, F. Porrati, and O. V. Dobrovolskiy; *Microelectronic Engineering* **185-186**, 9 (2018).

[2] T. Bret, T. Hofmann, and K. Edinger; *Applied Physics A: Materials Science & Processing* **117**, 1607 (2014).

[3] H. Plank, R. Winkler, C. H. Schwalb, J. Hütner, J. D. Fowlkes, P. D. Rack, I. Utke, and M. Huth; *Micromachines* **11** (2020).

[4] S. Barth, M. Huth, and F. Jungwirth; *Journal of Materials Chemistry C* **8**, 15884 (2020).

[5] D. Sanz-Hernández and A. Fernández-Pacheco; *Beilstein Journal of Nanotechnology* **8**, 2151 (2017)



# Effective simulation of the FEBID process

Alexander Kuprava<sup>1,\*</sup>, Michael Huth<sup>1</sup>

<sup>1</sup> Goethe University Frankfurt: Applied physics, Thin layers, Max-von-Laue Str. 1, 60438, Frankfurt a.M., Germany

\* email: [kuprava@physik.uni-frankfurt.de](mailto:kuprava@physik.uni-frankfurt.de)

Over the last decade focused electron beam induced deposition or FEBID has been shown as a promising technique for next generation nanofabrication. Unlike conventional lithography techniques, FEBID enables true free-form fabrication of 2D and 3D structures and opens a path for the development of nanomaterials, e.g. with exotic magnetic properties induced by curved geometries [1]. However, the shape-true transfer from a 3D CAD model to a deposit represents a serious challenge to a more widespread practical usage of the method. Different simulation approaches, e.g. [2, 4] and slicers or pattern optimizers have been reported, e.g. [3], addressing various aspects of the shape-true transfer. However, so far software capable of full growth simulation based on the approach described in [4] is not available in the public domain. We would like to present an effective hybrid Monte Carlo–continuum simulation of the FEBID process. Given the initial the parameters, it allows prediction and inspection of the resulting shape of the structure and, coupled with reference deposition experiments, enables a step-by-step determination of the key parameters such as surface diffusion coefficient or average residence time. The code of the simulation will be published as open-source and will be free for everyone to explore and develop further.

The simulation consists of two major modules: a Monte Carlo electron beam-matter interaction module and a deposition module based on a reaction-diffusion continuum model taking into account precursor adsorption, desorption, diffusion and dissociation. Each time a volume element within the simulation domain is filled or the beam moves to a new position, the Monte Carlo module is executed to obtain a spatially resolved surface secondary electron flux. Then, based on the obtained electron flux and surface precursor density, a miniscule amount of material is deposited as a result of the dissociation process and the surface precursor density is recalculated at a rate corresponding to a timestep  $\Delta t$ . The Monte Carlo module is based on the single scattering model with a Mott-fitted Rutherford formula for the total cross section and Bethe equation for continuous energy loss. Secondary electron emission is implemented according to a parametric model.

The developed software is primarily aimed to assist the laborious work of pattern file and parameter optimization during the fabrication of complex 3D structures. The model allows iterative deposition with different precursors and the resulting digital 3D model of the deposit can be easily sliced and inspected. Coupled with experiment, the simulation gives the opportunity to more precisely quantify ill-defined simulation parameters using a step-by-step approach. And finally, owing to the reasonable execution speed on a regular desktop, it exposes the features of a numerical simulation to the researchers without the need of an access to a computing cluster.

[1] O. Dobrovolskiy et al.; *Cherenkov radiation of spin waves by ultra-fast moving magnetic flux quanta*; Appl.Phys. Lett. 118, 132405 (2021).

[2] E. Mutunga et al.; *Impact of Electron-Beam Heating during 3D Nanoprinting*; ACS Nano 13, 5198–5213 (2019).

[3] L. Keller and M. Huth; *Pattern generation for direct-write three-dimensional nanoscale structures via focused electron beam induced deposition*; Beilstein Journal of Nanotechnology 9, 2581–2598 (2018).

[4] J. D. Fowlkes et al.; *Simulation-Guided 3D Nanomanufacturing via Focused Electron Beam Induced Deposition*; ACS Nano 10, 6163–6172 (2016).

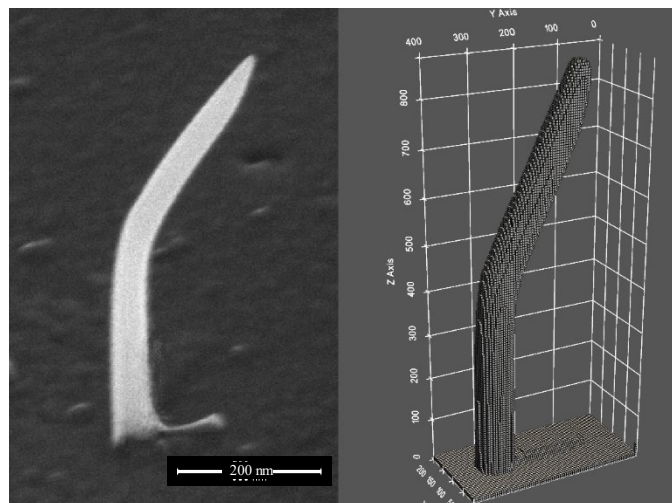


**Figure 1.** An exemplary ‘hockey stick’ structure fabricated by FEBID (left) and reproduced by the simulation (right)

# Precursors for Direct-Write Nanofabrication with Electrons

S. Barth<sup>1,\*</sup>, F. Jungwirth<sup>1</sup>, F. Porrati<sup>1</sup>, M. Huth<sup>1</sup>, D. Knez<sup>2</sup>, H. Plank<sup>2</sup>

<sup>1</sup> Physical Institute, Goethe University Frankfurt, Max-von-Laue-Str. 1, 60438 Frankfurt, Germany.

<sup>2</sup> Institute of Electron Microscopy and Nanoanalysis, Graz University of Technology, 8010 Graz, Austria.

\* email: [barth@physik.uni-frankfurt.de](mailto:barth@physik.uni-frankfurt.de)

Focused electron beam deposition (FEBID) allows the spatially controlled formation of nanoparticles, thin films, nanowires and free-standing complex nanoarchitectures on a wide range of substrate materials. Moreover, the method enables a growth on structured surfaces and the formation of predefined arrays by this maskless direct-write approach. However, the purity of the as-grown material is typically limited. According to the knowledge gained by considering surface science studies, several different reaction paths could be assigned according to the composition gained in FEBID experiments as summarized in **Fig. 1**. Therefore, the FEBID method requires precursor development to provide chemical impetus driving its broader applicability. This contribution will shortly summarize the state-of the art of precursors used, which has been described in a recent review [1]. Moreover, suggestions of necessary limitations or suggestions will be presented. The knowledge gained is applied to the synthesis procedures for metal silicide and alloy formation. Specific examples of precursors will be discussed and approaches for targeted binary compounds will be presented [2, 3].

Acknowledgment: S.B. acknowledges generous financial support from the Deutsche Forschungsgemeinschaft (DFG, German Research Foundation) project 413940754 and 413942347

[1] S. Barth, M. Huth, F. Jungwirth; *Precursors for direct-write nanofabrication with electrons*; J. Mater. Chem. C 8, 15884 (2020).

[2] F. Jungwirth, F. Porrati, A. G. Schuck, M. Huth, S. Barth; *Direct Writing of Cobalt Silice Nanostructures Using Single-Source Precursors*; ACS Appl. Mater. Interf. 13, 48252 (2021).

[3] F. Jungwirth, D. Knez, F. Porrati, A. G. Schuck, M. Huth, H. Plank, S. Barth; *Vanadium and Manganese Carbonyls as Precursors in Electron-Induced and Thermal Deposition Processes*; Nanomaterials 12, 1110 (2022).

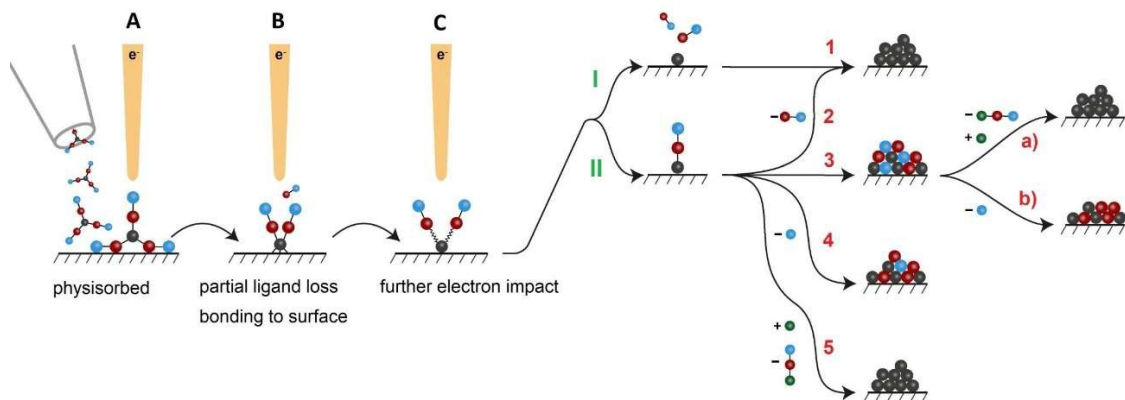


**Figure 1.** Schematic representation of different reaction paths during the FEBID process and resulting material composition.

# How coordination chemistry limits new FEBID precursors development?

Iwona B. Szymańska<sup>1,\*</sup>, Aleksandra Butrymowicz<sup>1</sup>, Katarzyna Madajska<sup>1</sup>

<sup>1</sup> Faculty of Chemistry, Nicolaus Copernicus University in Toruń, Gagarina 7, 87-100 Toruń, Poland

\* email: pola@umk.pl

Thanks to focused electron beam-induced deposition (FEBID), it is possible to obtain metallic nanostructures with complex shapes in a simple, one-step process. Therefore, the applications of the materials thus obtained are practically unlimited. In the case of the metals of 10 and 11 groups, they are concentrated in the field of a) micro- and nanoelectronics, b) plasmonics and formation of sensors, c) catalysis, and d) modification of AFM probes [1].

Precursors, which are sources of metal carriers in the gas phase, are one of the most important factors for the success of FEBID because their chemical nature and dissociation behavior determine the composition of the deposit [1-3]. Used coordination compounds should be volatile, sufficiently thermal stable, and electron sensitive. The crucial issue is clean decomposition induced by electrons to the expected material. Moreover, these complexes should be easily synthesized with high yield, cheap, user-friendly, etc. Therefore, designing and fabricating such coordination compounds remains a challenge. The more essential limits are connected with a coordination center (oxidation states and their stability in the gas and condensed phase; coordination numbers, affinity to solvents molecules) and ligands (type and number of donor atoms, polarizability, reactivity, the tendency to polymeric structure formation).

The factors that may cause copper(II) complexes with N, O- and N, N-, donor ligands demonstrated in **Figure 1** exhibit completely different sensitivity to electrons will be discussed.

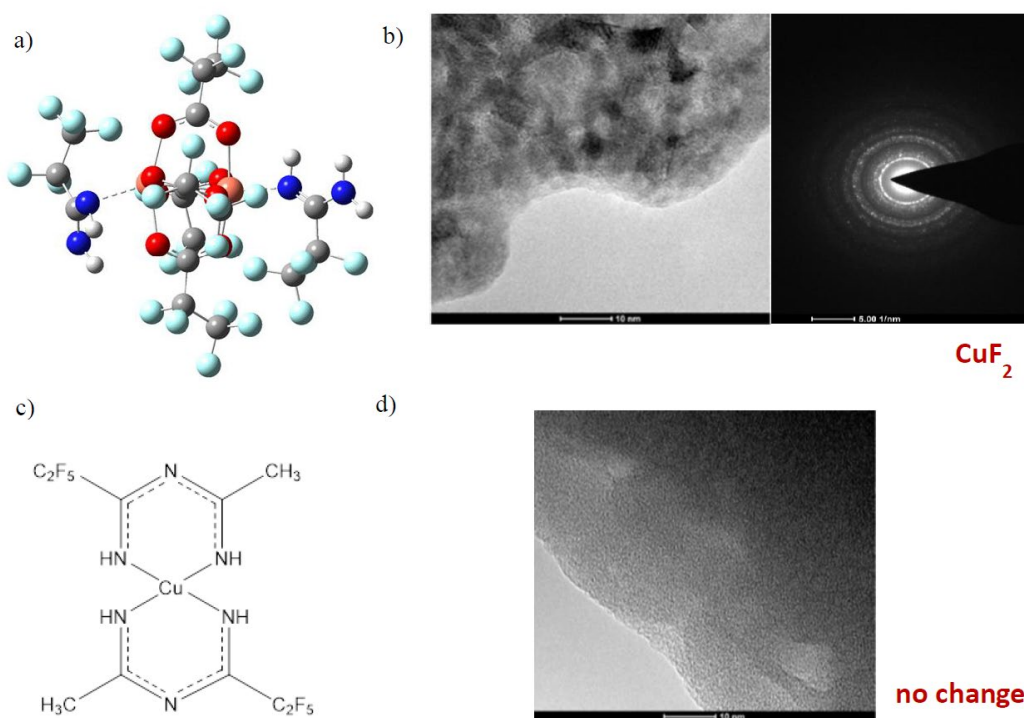


**Figure 1.** The heteroleptic dinuclear complex  $[\text{Cu}_2(\text{NH}_2(\text{NH})\text{CC}_2\text{F}_5)_2(\mu\text{-O}_2\text{CC}_2\text{F}_5)_4]$  a) the optimized structure confirming the =N-H amidine coordination, b) TEM observation (200keV): the image of the sample after a few seconds of interaction with electrons and diffraction pattern, which confirms crystallinity of the  $\text{CuF}_2$  deposit, on the base on [4]; The homoleptic mononuclear complex  $[\text{Cu}(\text{NHC}(\text{C}_2\text{F}_5)\text{NC}(\text{CH}_3)\text{NH})_2]$  c) structure, d) TEM observation (200keV): the image of the sample after a few seconds of interaction with electrons.

[1] I. Utke, P. Swiderek, K. Höflich, K. Madajska, J. Jurczyk, P. Martinović, I. B. Szymańska; *Coordination and organometallic precursors of group 10 and 11: Focused electron beam induced deposition of metals and insight gained from chemical vapour deposition, atomic layer deposition, and fundamental surface and gas phase studies*; Coordination Chemistry Reviews, 458, 213851 (2022).

[2] S. Barth, M. Huth, F. Jungwirth; *Precursors for direct-write nanofabrication with electrons*; J. Mater. Chem. C. 8, 15884 (2020).

[3] I. Utke, P. Hoffmann, J. Melngailis; *Gas-assisted focused electron beam and ion beam processing and fabrication*; J. Vac. Sci. Technol. B. 26, 1197 (2008).

[4] K. Madajska, I.B. Szymańska; *New Volatile Perfluorinated Amidine-Carboxylate Copper(II) Complexes as Promising Precursors in CVD and FEBID Methods*; Materials, 14, 3145 (2021). <https://doi.org/10.3390/ma14123145>



# Electron induced decomposition – toward quantitative data

Lionel Amiaud<sup>1,\*</sup>, Reza Tafrihi<sup>2</sup>, Daniela Torres-Diaz<sup>1</sup>, Oddur Ingolfson<sup>2</sup>, Anne Lafosse<sup>1</sup>

<sup>1</sup> Institut des Sciences Moléculaires d'Orsay, Université Paris-Saclay, CNRS, Orsay, France

<sup>2</sup> Science Institute and Department of Chemistry, University of Iceland, Reykjavik, Iceland

\* email: [lionel.amiaud@universite-paris-saclay.fr](mailto:lionel.amiaud@universite-paris-saclay.fr)

Focused Electron Beam Induced Deposition (FEBID) [1] and Extreme Ultra Violet light (EUV) [2] lithography involve the decomposition of molecular entities / films under irradiation by high-energy beams with energies well above any ionization thresholds. The large amounts of resulting secondary electrons, of low energies ( $0 \leq E \leq 20$  eV), contribute significantly to the lithographic processing. The design of the precursor molecular entities is a key element for an efficient decomposition, optimizing the overall process. Of particular interest are the characterization of the precursor chemical evolution, the understanding of the dominant underlying chemical processes including the low-energy electrons (LEE) contribution, and the quantitative characterization of decomposition pathways [3].

In the “electrons-solids” UHV setup at ISMO, thin films of precursors are submitted to high-energy (92 eV) vs. low-energy (< 15 eV) electron irradiation. Damages leading to the release of neutral volatile fragments are probed “in operando” during the electron irradiation by quadrupole mass spectrometry (Electron Stimulated Desorption studies). The film residues and pristine deposits are analyzed by Temperature Programmed Desorption (TPD). The experiments procedure is represented in **figure 1**. The decomposition of the compound during irradiation and resonant mechanisms can be observed. The effective cross sections at given incident energy can be determined from desorption evolution with time [4].

Electron irradiation at low-energy (1-16 eV) has been compared to electron irradiation at high-energy (92 eV) for thin molecular films of 2-(trifluoromethyl)acrylic acid (TFMAA, **figure 2**), a model halogenated unsaturated precursor [5] of potential interest for developing alternative EUV resists. The low energy experiments show a major decomposition channel via CO<sub>2</sub> formation at both ~1 eV incident energy, possibly associated to dissociative electronic attachment (DEA), and above the electronic excitation threshold (5.5 eV). At 12 eV, a resonance is observed, compatible with a two fold mechanism, first an ionization then an attachment of the near 0 eV electron produced. From the high energy experiments, we deduce the effective cross section for the desorption of volatile species and the limit dose for damaging the layer.

[1] I. Utke et al.; *Gas-Assisted Focused Electron Beam and Ion Beam Processing and Fabrication*; JVSTB, 26, 4 (2008), 1197.

[2] Thete et al. Proc. of SPIE (2015), Kozawa et al. Jap. J. App. Phys. 2010.

[3] Thorman et al. Beilstein J. Nanotechnology 2016, Böhler et al. Chem. Soc. Rev. 2013.

[4] L. Sala et al., Beilstein J. Nanotechnol. 9 (2018) 57; K. Landheer et al. J. Phys. Chem. C, 115, 35, (2011) 17452;

J. Wnuk et al. Surface Science 605 (2011) 257.

[5] R. Tafrihi et al., in preparation.

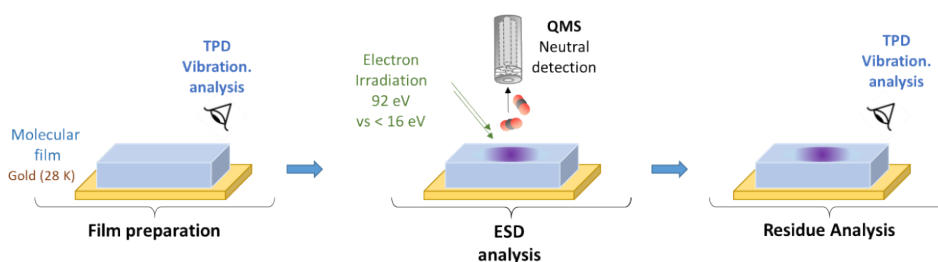


**Figure 1.** Principle of the analysis allowed with “electrons-solids” setup in ISMO

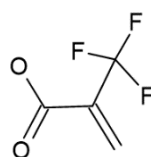


**Figure 2.** 2-(trifluoromethyl)acrylic acid

# Electron-Induced Decomposition of Different Silver(I) Complexes: Implications for the Design of Precursors for Focused Electron Beam Induced Deposition

Petra Martinović<sup>1</sup>, Markus Rohdenburg<sup>1,3</sup>, Aleksandra Butrymowicz<sup>2</sup>, Selma Sarigül<sup>1</sup>, Paula Huth<sup>3</sup>, Reinhard Denecke<sup>3</sup>, Iwona B. Szymańska<sup>2</sup>, and Petra Swiderek<sup>1,\*</sup>

<sup>1</sup> Institute for Applied and Physical Chemistry (IAPC), Fachbereich 2 (Chemie/Biologie), University of Bremen, Leobener Str. 5 (NW2), 28359 Bremen, Germany

<sup>2</sup> Nicolaus Copernicus University in Toruń, Faculty of Chemistry, Gagarina 7, 87-100 Toruń, Poland

<sup>3</sup> Wilhelm-Ostwald-Institute for Physical and Theoretical Chemistry (WOI), Leipzig University, Linnéstr. 2, 04103 Leipzig, Germany

\* email: [swiderek@uni-bremen.de](mailto:swiderek@uni-bremen.de)

Focused electron beam induced deposition (FEBID) is a versatile tool to produce nanostructures through electron-induced decomposition of metal-containing precursor molecules [1]. However, the metal content of the resulting materials is often low. Using different Ag(I) complexes, we show that the precursor performance depends critically on the molecular structure [2]. This includes Ag(I) 2,2-dimethylbutanoate, which yields high Ag contents in FEBID [3], as well as aromatic Ag(I) benzoate, and the acetylide Ag(I) 3,3-dimethylbutynyl (**Fig. 1a**). The compounds were sublimated on inert surfaces and the volatile products released from the samples upon electron irradiation were analysed by use of mass spectrometry (MS) in an electron-stimulated desorption (ESD) experiment. Reflection-absorption infrared spectroscopy (RAIRS) was employed to monitor chemical changes in the precursor layer upon electron exposure.

As a general guideline for the design of novel FEBID precursors, our results indicate that aliphatic carboxylate ligands are a preferential choice. Following electron ionization, the investigated Ag(I) carboxylates fragment by loss of volatile CO<sub>2</sub> (**Fig. 1b**). The remaining alkyl radical converts favourably to a stable and volatile alkene by loss of H. The decomposition is much less efficient for Ag(I) benzoate and Ag(I) 3,3-dimethylbutynyl. In the former, loss of H from the phenyl radical released upon expulsion of CO<sub>2</sub> would lead to a highly strained ring and is thus unfavourable. A more general explanation is provided by calculated average local ionization energies (ALIE). They reveal that ionization from unsaturated carbon units competes with ionization from the coordinate bond to Ag. In the case of Ag(I) 2,2-dimethylbutanoate, which contains only saturated side groups, the ALIE is lowest on the carboxylate group. Ionization thus preferably destabilizes the carboxylate group and triggers expulsion of CO<sub>2</sub>. In contrast, the unsaturated CC double or triple bonds, such as present in Ag(I) benzoate and Ag(I) 3,3-dimethyl-1-butynyl, represent alternative sites within the molecule where electron density can be easily removed. This, however, does not favour dissociation, rationalizing the slow decomposition of these precursors.

[1] I. Utke, P. Hoffmann, J. Melngailis; *Gas-assisted focused electron beam and ion beam processing and fabrication*; J. Vac. Sci. Technol. B Volume 26, 1197 (2008).

[2] P. Martinović, M. Rohdenburg, A. Butrymowicz, S. Sarigül, P. Huth, R. Denecke, I. B. Szymańska, P. Swiderek; *Electron-Induced Decomposition of Different Silver(I) Complexes: Implications for the Design of Precursors for Focused Electron Beam Induced Deposition*; *Nanomaterials*, accepted (2022).

[3] I. Utke, P. Swiderek, K. Höflich, K. Madajski, J. Jurczyk, P. Martinović, I. B. Szymańska; *Coordination and organometallic precursors of group 10 and 11: Focused electron beam induced deposition of metals and insight gained from chemical vapour deposition, atomic layer deposition, and fundamental surface and gas phase studies*; *Coord. Chem. Rev.* 458, 213851 (2022).

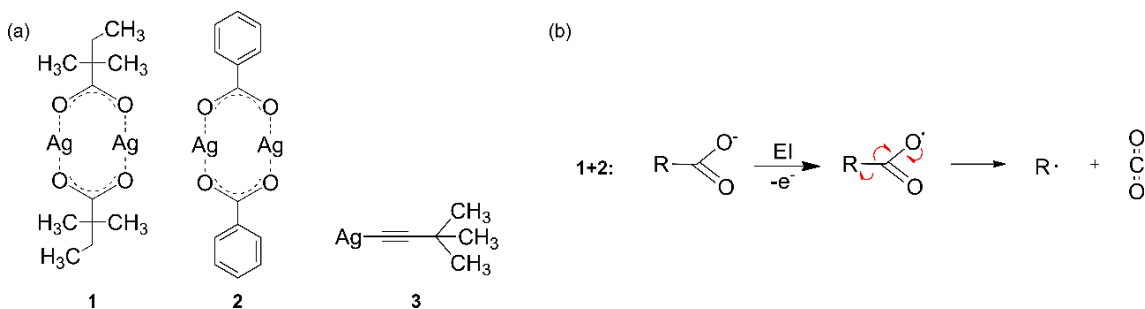


**Figure 1.** (a) Silver(I) complexes used in the present study: Ag(I) 2,2-dimethylbutanoate (1), Ag(I) benzoate (2), Ag(I) 3,3-dimethyl-1-butynyl (3). (b) Fragmentation of carboxylate ligands in complexes (1) and (2) following electron ionization (EI). Red arrows indicate the charge rearrangement that leads to release of CO<sub>2</sub> and an organic radical R•.

# 3D Nanoprinting via Focused Electron Beams: A Perspective

Harald Plank<sup>1,2,3,\*</sup>

<sup>1</sup> Graz University of Technology, Institute of Electron Microscopy, Steyrergasse 17, 8010 Graz, Austria

<sup>2</sup> Christian Doppler Laboratory for Direct-Write Fabrication of 3D Nanoprobes, Graz University of Technology, Steyrergasse 17, 8010 Graz, Austria

<sup>3</sup> Graz Centre of Electron Microscopy, Steyrergasse 17, 8010 Graz, Austria

\* email: [harald.plank@felmi-zfe.at](mailto:harald.plank@felmi-zfe.at)

During the past years, controlled 3D nanofabrication via focused electron beam induced deposition (FEBID) has made tremendous progress. While originally demonstrated around the millennium and explored in slight more detail about 5 years later, the full exploitation of that approach started around 2015. During that 10 years 'break', the joint efforts of the related community built up a deeper fundamental process understanding, which, together with new technical possibilities, laid the foundation for the successful revisit of true 3D nanofabrication, currently being one of the unique selling points of FEBID. During the past 7 years, further research was conducted by a number of research groups worldwide, which crucially improved the process understanding and impacted predictability, accuracy and reliability. That leveraged 3D-FEBID more and more into the status of a true 3D nanoprinting technology, which currently is barely surpassed by any other technology with the exception of its ion-beam sibling (focused ion beam induced deposition – FIBID). Although 3D FEBID is well matured so far, there are remaining questions, challenges and even clear demands to exploit the full potential of that approach for advanced applications in research and development beyond current possibilities.

In this contribution, we start with a brief introduction about the 3D FEBID working principle together with a critical view on general and current limitations. The latter also includes material-related aspects, which still is an ongoing research area due to the partly decisive character when aiming on specific applications. We then provide an overview on selected activities from different workgroups worldwide, ranging from fundamental work over technical implementations towards innovative application examples. Finally, we discuss a few application areas, which are rarely touched so far, although the unique 3D FEBID / FIBID capabilities could expand related possibilities. By that, the intention of this talk is to provide an overview about technologies, limitations, achievements and demands with emphasis on application areas where 3D FEBID not only acts as option but as enabling element for future concepts in research & development.

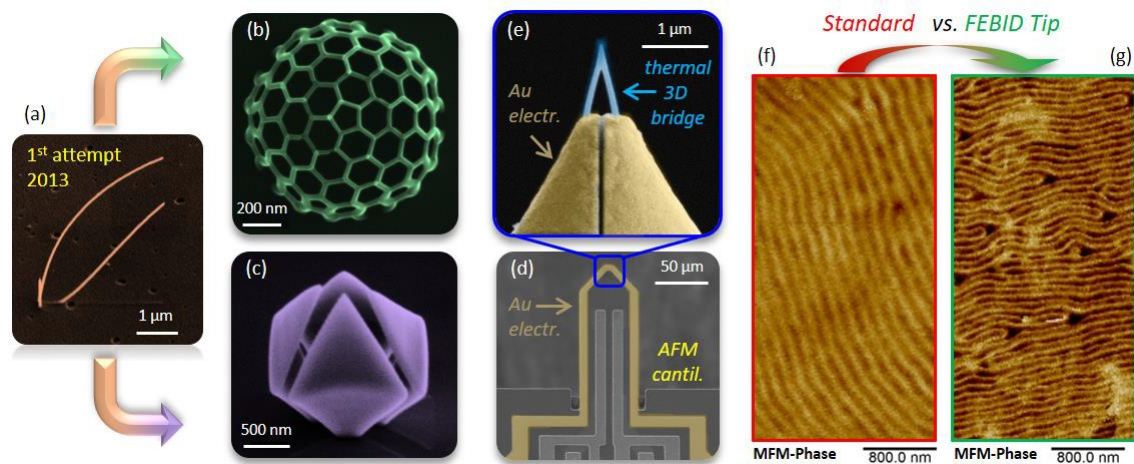


**Figure 1.** From an attempt towards applications. (a) shows the very first experiment of a tilted pillar, which was the starting point towards 3D nanofabrication activities in Graz. In the following years, the concept expanded towards complex, mesh-like (b) and sheet-like objects (c) in 3D space. As representative application, a pre-structured AFM cantilever is shown in (d), which can specifically be modified by different nanoprobe concepts, based on 3D FEBIDs design flexibility and direct-write character with nanometer resolution. An example is shown in (e), which is a thermal 3D nano-probe, consisting of a tetra-pod, which bridges two electrodes and responds on varying temperatures by a change of electrical resistance. To demonstrate the improved performance of 3D FEBID objects, a direct comparison of a CoPt multilayer sample is shown, using magnetic force microscopy (MFM). (f) shows the results with a commercially available MFM tip right next to a FEBID based, Co<sub>3</sub>Fe nanotip where the improved performance is obvious.

# Direct Fabrication of 3D Hollow Nano-cones

C. W. Hagen<sup>1,\*</sup>, A. Mahgoub<sup>1</sup>, L. van Kessel<sup>1</sup>, R. de Jong<sup>1</sup>, W. D. Laur<sup>1</sup> and P. Kruit<sup>1</sup>

<sup>1</sup> Delft University of Technology, Fac. Applied Sciences, Dept. ImPhys, Lorentzweg 1, 2628CJ Delft, The Netherlands

\* email: [c.w.hagen@tudelft.nl](mailto:c.w.hagen@tudelft.nl)

Focused electron beam induced deposition (FEED) is a technique which allows the direct fabrication of three dimensional structures at the nanoscale. This has been demonstrated recently by a number of workers [1-3]. Open structures as well as solid shapes were successfully made using simulation-guided deposition methods.

In this work the focus is on the fabrication of closed-wall structures, in particular hollow cones. The approach followed avoids the determination of deposition parameters using simulations, but rather mimics the process used in 3D-printers. That is, the structures to be deposited are built up from small building blocks, stacked on top of each other. Basically the only parameters to choose are the size of the building block, the lateral spacing between building blocks in a single layer and the lateral spacing between building blocks in adjacent layers (in the vertical direction). These parameters are kept the same throughout the deposition of the entire structure. The number of building blocks per layer is allowed to vary. Two deposition strategies are investigated: i) using small overlapping building blocks, to minimize the contribution of proximity effects, and ii) large building blocks at large spacing (gaps between building blocks), making use of the proximity effects to close the gaps between building blocks. The results and merits of both strategies will be discussed.

Observed irregularities in the top parts of hollow cones grown from the precursor MeCpPtMe<sub>3</sub>, were investigated using a dynamic FEED growth simulation (**Figure 1**), based on a Monte Carlo electron-matter interaction simulation code developed in Delft [4]. This showed that the order in which the building blocks are arranged is important. For comparison, hollow cones were also deposited using the simulation guided deposition tools [2, 3], revealing similar irregularities.

Hollow cones are of specific interest for application in a novel aperture ion source (NAIS), which is based on the electron impact ionization of gas atoms confined to a very small volume between two Si<sub>3</sub>N<sub>4</sub> membranes. A coaxial double cone structure is deposited around two holes, one in each membrane, to confine the gas volume to the apex of both cones, where an electron beam, incident through both holes, ionizes the gas atoms. This geometry allows for easier extraction of the ions, without having to apply a potential between the two membranes. An example of such a double cone structure is shown in **figure 2**. More results will be presented and discussed.

[1] L. Keller and M. Huth; *Pattern generation for direct-write three-dimensional nanoscale structures via focused electron beam induced deposition*; Beilstein Journal of Nanotechnology 9, 2581 (2018).

[2] J. D. Fowlkes, R. Winkler, Brett B. Lewis, A. Fernández-Pacheco, L. Skoric, D. Sanz-Hernández, Michael G. Stanford, Eva Mutunga, P. D. Rack, and H. Plank; *High-Fidelity 3D-Nanoprinting via Focused Electron Beams: Computer-Aided Design (3BID)*; ACS Applied Nanomaterials 1, 1028 (2018).

[3] Luca Skoric, Dédalo Sanz-Hernández, Fanfan Meng, Claire Donnelly, Sara Merino-Aceituno, and Amalio Fernández-Pacheco; *Layer-by-Layer Growth of Complex-Shaped Three-Dimensional Nanostructures with Focused Electron Beams*; Nano Letters 20, 184 (2020).

[4] L. van Kessel and C. W. Hagen; *Nebula: Monte Carlo simulator of electron-matter interaction*; SoftwareX 12, 100605 (2020).

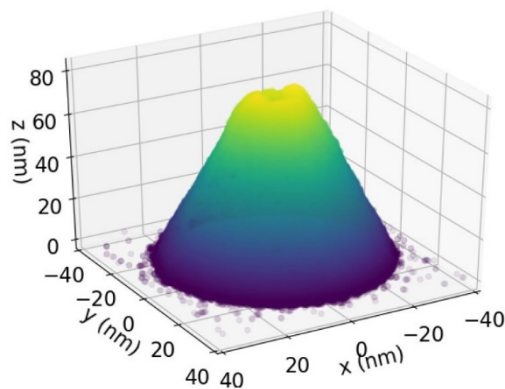


**Figure 1.** Simulated, FEED-grown, hollow cone showing an irregular apex.

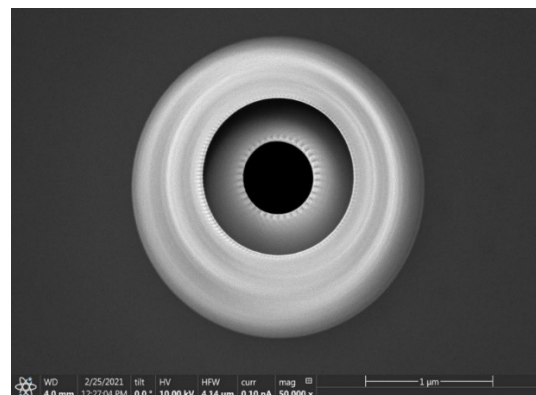


**Figure 2.** Coaxial double cone structure grown on two Si<sub>3</sub>N<sub>4</sub> membranes at a separation of 800 nm



# Advancing Design Possibilities during 3D Nanoprinting

L. M. Seewald<sup>1</sup>, R. Winkler<sup>1</sup> and H. Plank<sup>1,2,3,\*</sup>

<sup>1</sup> Christian Doppler Laboratory – DEFINE, Graz University of Technology, 8010 Graz, Austria

<sup>2</sup> Graz Centre for Electron Microscopy, 8010 Graz, Austria

<sup>3</sup> Institute of Electron Microscopy and Nanoanalysis, Graz University of Technology, 8010 Graz, Austria

\* email: [harald.plank@felmi-zfe.at](mailto:harald.plank@felmi-zfe.at)

The ongoing trend of miniaturization in science and technology is raising an increasing demand on reliable fabrication techniques able to build structures at the nanoscale. In contrast to highly developed and powerful lithography process routes particle beam induced deposition processes recently have entered the realms of true 3-dimensional printing at the nanoscale [1]. Highly localized deposition is achieved by accurately controlling the movement of the e-beam enabling the fabrication of even complex 3D structures with nanoscale features in the sub-20 nm region [2]. Though essential for particular applications (e.g. nano-plasmonics [3] and 3D-magnetic lattices [4]), such delicate structures show low mechanical rigidity and limited thermal and electrical conductivities which confines possible applications. Additionally, branch dimensions are determined for a given beam parameter setting and closely related to the desired structure's geometry, which in turn means that they cannot be chosen freely [5]. Consequently, it is highly desirable to establish a fabrication procedure which allows deliberate control over branch dimensions to remedy the former mentioned challenges. With this motivation in mind, we introduce beam blurring as an additional deposition parameter and explore its effects on fabrication of 3D structures (Fig 1a). Besides the intended diameter tunability the growth efficiency increases, caused by a shift in the working regime due to reduced current densities in beam impact regions and thus reduced precursor consumption per unit area (Fig 1b). In addition, unwanted proximal growth beneath 3D branches was strongly delayed, further increasing 3D-FEBID's reliability. On-purpose beam blurring therefore poses a viable route of crucially expanding the flexibility of this technique, enabling controlled and tunable branch dimensions for meshed objects while improving growth rates and reducing parasitic growth.

[1] Winkler et al.; *3D nanoprinting via focused electron beams*; J. Appl. Phys. 125, 210901 (2019)

[2] Frabboni et al.; *Fabrication by electron beam induced deposition and transmission electron microscopic characterization of sub-10nm freestanding Pt nanowires*; Appl. Phys. Lett. 88, 213116 (2006)

[3] Winkler et al.; *Direct-Write 3D Nanoprinting of Plasmonic Structures*; ACS Appl. Mater. Interfaces 9 8233, (2017)

[4] Keller et al.; *Direct-write of free-form building blocks for artificial magnetic 3D lattices*; Sci. Rep. 8, 6160 (2018)

[5] Winkler et al.; *Shape evolution and growth mechanisms of 3D-printed nanowires*; Addit. Manuf. 46, 102076 (2021)

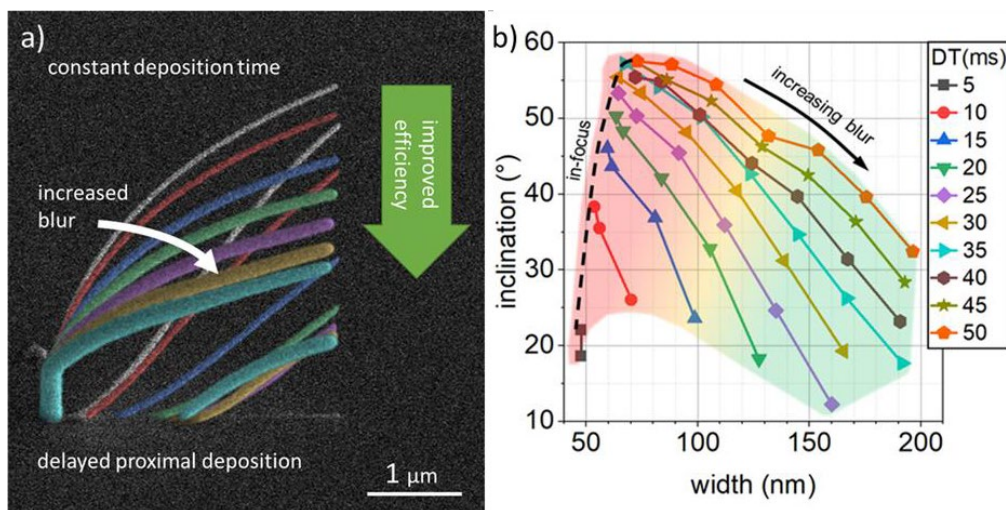


**Figure 1.** a) Collage of inclined segments illustrating the effects of a blurred electron beam in 3D-FEBID: (i) efficiency is improved at a constant deposition time while increasing beam blur, (ii) beam blur can be used to adjust either segment inclination and/or segment dimensions and (iii) highly unwanted proximal deposition underneath is strongly delayed. b) Added design flexibility: segment dimensions can be tuned over a wide range, where at in-focus conditions width and inclination can be chosen from the dashed line solely. The color shading corresponds to working regime shifts, as explained in the contribution as well.

# On the Route towards Precision - 3D-Nanoprinting of Closed Structures via FEBID

A. Weitzer<sup>1,\*</sup>, M. Huth<sup>2</sup> and H. Plank<sup>1,3,4</sup>

<sup>1</sup> Institute of Electron Microscopy and Nanoanalysis, Graz University of Technology, 8010 Graz, Austria

<sup>2</sup> Physics Institute, Goethe Universität Frankfurt, 60438 Frankfurt am Main, Germany

<sup>3</sup> Graz Centre for Electron Microscopy, Steyrergasse 17, 8010 Graz, Austria

<sup>4</sup> Christian Doppler Laboratory - DEFINE, Graz University of Technology, 8010 Graz, Austria

\* email: [anna.weitzer@felmi-zfe.at](mailto:anna.weitzer@felmi-zfe.at)

Among the few additive-manufacturing techniques capable of creating 3-dimensional objects on the nanoscale, 3D nanoprinting via Focused Electron Beam Induced Deposition (3D-FEBID) is an increasingly relevant technology for building high-fidelity nanostructures. Its capabilities of depositing feature sizes below 20 nm under optimized conditions and below 100 nm on a regular basis and its flexibility both in terms of substrate as well as precursor materials make it a unique technology with many possibilities and yet unexplored applications. While it has been used and developed further for a few years now, most fabricated structures in the past have been meshed [1], meaning a combination of differently oriented, individual nanowires, connected at specific points in 3D space according to the target application. This work leverages 3D-FEBID to the next level by expanding its capabilities from mesh-like toward closed (sheet-like) structures with a high degree of precision. The main challenge and source of most deviations from target shapes is thereby based on local beam heating and its implications on local growth rates. While well understood in meshed structures, closed objects revealed additional dependencies on the dimensions of built objects and the XY pixel position within the structures. Furthermore, electron trajectories are more complex in closed objects, introducing additional proximity effects. To address these problems, we combined finite-difference simulations with 3D-FEBID experiments and developed a Python-based compensation tool, capable of stabilizing the growth for each XY pixel point in individual patterning planes by pre-determined parameter adjustments (Fig. 1a). The gained insight allowed further expansion, now being applicable for different element-widths and -heights, as demonstrated by more advanced structures (Fig. 1b). By that, we crucially expanded FEBID-based 3D nanoprinting by opening up design possibilities for closed and consequently mixed objects for novel applications in various fields of research and development.

[1] R. Winkler et al.; 3D nanoprinting via focused electron beams; Journal of Applied Physics 125, 210901 (2019).

[2] A. Weitzer et al.; Expanding FEBID-Based 3D-Nanoprinting toward Closed High-Fidelity Nanoarchitectures; ACS Applied Electronic Materials, 4 (2), 744 (2022).

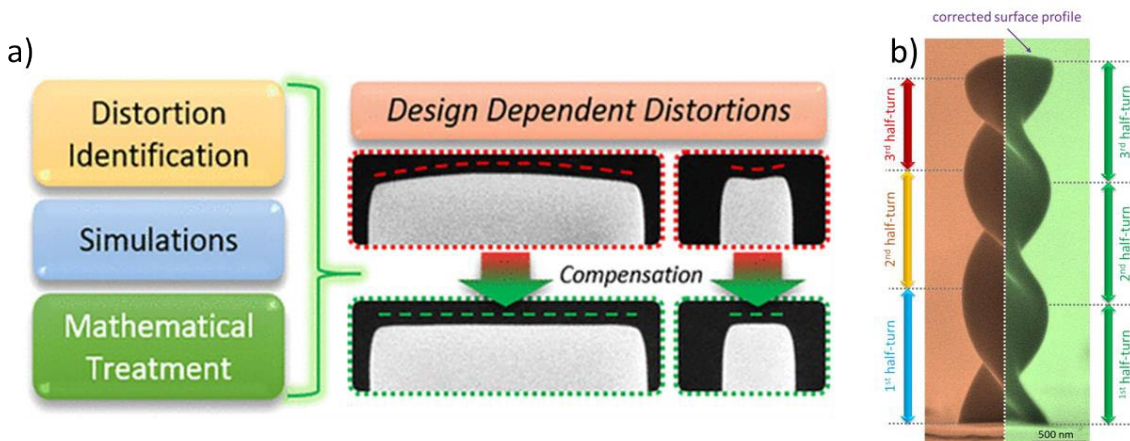


Figure 1. Improvements due to our compensation tool on the example of (a) walls and (b) a screw [2].

# Direct electron beam writing of metallic nanostructures and insight gained from surface deposition techniques

K. Höflich<sup>1,2,\*</sup>, I. Utke<sup>3</sup>, P. Swiderek<sup>4</sup>, K. Madajska<sup>5</sup>, J. Jurczyk<sup>3,6</sup>, P. Martinović<sup>4</sup>, I. B. Szymańska<sup>5</sup>

<sup>1</sup> Ferdinand-Braun-Institut gGmbH, Leibniz-Institut für Höchstfrequenztechnik, 12489 Berlin, Germany

<sup>2</sup> Helmholtz-Zentrum Berlin für Materialien und Energie, 14109 Berlin, Germany

<sup>3</sup> Empa - Swiss Federal Laboratories for Materials Science and Technology, 3602 Thun, Switzerland

<sup>4</sup> Institute for Applied and Physical Chemistry (IAPC), University of Bremen, 28359 Bremen, Germany

<sup>5</sup> Nicolaus Copernicus University in Toruń, Faculty of Chemistry, 87-100 Toruń, Poland

<sup>6</sup> AGH University of Science and Technology Kraków, 30-059 Kraków, Poland

\* email: [katja.hoeflich@fbh-berlin.de](mailto:katja.hoeflich@fbh-berlin.de)

Nanostructured materials made from group 10 (Ni, Pd, Pt) and group 11 (Cu, Ag, Au) elements have outstanding technological relevance in microelectronics, nano-optics, catalysis, and energy conversion. Processes that allow for the easy and reliable fabrication of such nanostructures are heavily sought after. Focused electron beam induced deposition (FEBID) is the only direct-write technique that can fabricate nanostructures with arbitrary shape and dimensions down to the sub-10 nm regime. However, the complex chemistry of FEBID involving electron-induced dissociation processes of metalorganic precursors molecules, surface kinetics, and thermal effects is poorly understood and far from being optimized.

Here, we review in a comparative manner the performance and the underlying chemical reactions of surface deposition processes, namely, chemical vapour deposition (CVD), atomic layer deposition (ALD), and FEBID itself [1]. The knowledge gained in CVD and ALD as related surface deposition techniques will help us to understand the spatially selective chemistry occurring in FEBID. Fundamental surface and gas-phase studies provide insight to electron-induced chemistry and desorption of precursor fragments. Specific emphasis is put on the type of the ligands and their different behaviour under thermal, surface-related, and electron-induced processes.

The comprehensive overview includes reactive environments and purification approaches as these may provide valuable information on the design of novel precursors. The evaluation of the precursor and process performance is extended to include W, Co, Fe, Ru, Rh, and Ir to represent a general guide towards future developments in FEBID. These may not only rely on the design novel compounds but also on optimized deposition strategies inspired by ALD and CVD.

Finally, a selection of directly written chiral nanostructures for nano-optical applications will be presented and their optical response discussed [2-4].

[1] I. Utke et al.; *Coordination and organometallic precursors of group 10 and 11: Focused electron beam induced deposition of metals and insight gained from chemical vapour deposition, atomic layer deposition, and fundamental surface and gas phase studies*; *Coord. Chem. Rev.*, vol. 458, 2022.

[2] P. Woźniak et al.; *Chiroptical response of a single plasmonic nanohelix*; *Opt. Express*, vol. 26, no. 15, pp. 1513–1515, 2018.

[3] P. Woźniak, I. De Leon, K. Höflich, G. Leuchs, and P. Banzer; *Interaction of light carrying orbital angular momentum with a chiral dipolar scatterer*; *Optica*, vol. 6, no. 8, pp. 961–965, 2019.

[4] K. Höflich et al.; *Resonant behavior of a single plasmonic helix*; *Optica*, vol. 6, no. 9, p. 1098, 2019.

# Nanofabrication of Metallic Palladium Deposits by a Direct Electron Beam Irradiation Process Free of Post-Treatments Steps

Alba Salvador-Porroche<sup>1,2</sup>, Lucía Herrer<sup>1,2</sup>, Soraya Sangiao<sup>1,2,3</sup>, José María de Teresa<sup>1,2,3</sup>, and Pilar Cea<sup>1,2,4,\*</sup>

<sup>1</sup> Instituto de Nanociencia y Materiales de Aragón (CSIC-Universidad de Zaragoza), Pedro Cerbuna 12, 50009, Zaragoza, Spain.

<sup>2</sup> Laboratorio de Microscopías Avanzadas (Universidad de Zaragoza), Mariano Esquillor Gomez s/n, 50018, Zaragoza, Spain.

<sup>3</sup> Departamento de Física de la Materia Condensada (Universidad de Zaragoza), Menendez Pelayo 24, 50009, Zaragoza, Spain.

<sup>4</sup> Departamento de Química Física (Universidad de Zaragoza), Menendez Pelayo 24, 50009, Zaragoza, Spain.

\* email: pilarcea@unizar.es

The ability to create metallic patterned nanostructures with excellent control of size, shape and spatial orientation is of utmost importance in the construction of next-generation electronic and optical devices as well as in other applications such as (bio)sensors, reactive surfaces for catalysis, etc. Moreover, development of simple, rapid and low-cost fabrication processes of metallic patterned nanostructures is a challenging issue for the incorporation of such devices in real market applications. In this contribution, a direct-write method that results in highly conducting palladium-based nanopatterned structures without the need of applying subsequent curing processes is presented. Spin-coated films of palladium acetate were irradiated with an electron beam to produce palladium nanodeposits (PdNDs) with controlled size, shape and height. The use of different electron doses was investigated and its influence on the PdNDs features determined, namely: (1) thickness by profilometry, (2) atomic percentage of palladium content by Energy-dispersive X-ray spectroscopy (EDS), (3) oxidation state of palladium by X-ray Photoelectron Spectroscopy (XPS), (4) morphology of the sample and grain size of the Pd nanocrystals by High-angle annular dark-field scanning transmission electron microscopy (HAADF-STEM), and (5) electrical resistivity by the four-probe technique. It has been found that the use of high electron doses, 30000  $\mu\text{C}/\text{cm}^2$  results in the lowest resistivity reported to date for PdNDs, namely 145  $\mu\Omega\text{-cm}$ , which is only one order of magnitude higher than metallic bulk palladium. This result paves the way for development of simplified lithography processes of nanostructured deposits avoiding subsequent post-treatment steps [4].

[1] T. Bhuvana, G. U. Kulkarni; *Highly conducting patterned Pd nanowires by direct-write electron beam lithograph*; ACS Nano 2, 457 (2008).

[2] M. T. Reetz, M. Winter, G. Dumpich, J. Lohau, S. Friedrichowski; *Fabrication of Metallic and Bimetallic Nanostructures by Electron Beam Induced Metallization of Surfactant Stabilized Pd and Pd/Pt Clusters*; J. Am. Chem. Soc. 119, 4539 (1997).

[3] T. J. Stark, T. M. Mayer, D. P. Griffis, P. E. Russell; *Electron beam induced metalization of palladium acetate*; J. Vac. Sci. Technol. B Microelectron. Nanom. Struct. 9, 3475 (1991).

[4] A. Salvador-Porroche, L. Herrer, S. Sangiao, J. M. De Teresa, P. Cea; *Low-resistivity Pd nanopatterns created by a direct electron beam irradiation process free of post-treatment steps*; Nanotechnology, DOI: 10.1088/1361-6528/ac47cf.

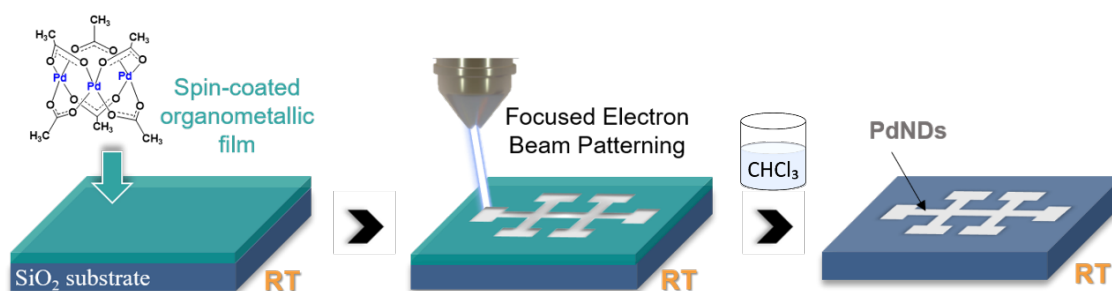


**Figure 1.** Scheme illustrating the process for the fabrication of PdNDs at room temperature.



# Direct Writing of Chiral and Nonlinear Plasmonic Devices

A. Tsarapkin<sup>1,\*</sup>, V. Deinhart<sup>1</sup>, T. Feichtner<sup>2</sup> and K. Höflich<sup>1</sup>

<sup>1</sup> Ferdinand-Braun-Institut gGmbH Leibniz-Institut für Höchstfrequenztechnik, 12489 Berlin, Germany

<sup>2</sup> Experimental Physics 5, University of Würzburg, Am Hubland, 97074 Würzburg, Germany

\* email: [aleksei.tsarapkin@fbh-berlin.de](mailto:aleksei.tsarapkin@fbh-berlin.de)

The miniaturization of electrical and optical devices over the last decades allowed many technological and economic advancements. Devices that permit control over the polarization of light are of crucial importance in telecommunication and quantum optics. Established solutions are realized as bulky optical systems, however, we aim at designing a uniquely compact plasmonic converter and detector with footprint of only a few  $\mu\text{m}$ . The device is based on a vertically oriented gold double helix coupled to a planar two-wire transmission line as it is shown in **Fig. 1 (c)**. The helix acts as a sensitive antenna for circularly polarized light [1], and the transmission line guides plasmons on-chip [2].

Using numeric modelling, we show, that antisymmetric modes can be excited in both device parts, double helix and two-wire waveguide (see **Fig. 1 b, d**). The resonances of the plasmonic helix and the transmission line dispersion strongly depend on the geometry of both structures. By adjusting their sizes one can finely match their impedances and maximize power transfer [3] to achieve best coupling efficiency between helical antenna and waveguide.

The fabrication of the separate components has been established. While the helix can be directly written with a focused electron beam using  $\text{Me}_2\text{Au}(\text{acac})$  as gold precursor, the plasmonic waveguide can be cut from single-crystalline gold flake by means of focused gallium-ion beam milling. **Figures 1 (a)** and **(e)** show scanning electron micrographs of the resulting geometries. The beam path for the double helix was created with Fib-o-Mat [4]. It resembles star-like jumping pattern (see **Fig. 1 f**) corresponds to a parallel printing approach that optimizes the growth rate and achieves highest shape fidelity.

[1] K. Höflich et al.; Resonant behavior of a single plasmonic helix; *Optica* 6, 1098 (2019).

[2] P. Geisler et al.; Multimode Plasmon Excitation and In Situ Analysis in Top-Down Fabricated Nanocircuits; *Phys. Rev. Lett.* 111, 183901 (2013).

[3] Jer-Shing Huang et al.; Impedance Matching and Emission Properties of Nanoantennas in an Optical Nanocircuit; *Nano Letters* 9, 1897 (2009).

[4] V. Deinhart et al.; The patterning toolbox FIB-o-mat: Exploiting the full potential of focused helium ions for nanofabrication; *Beilstein J. Nanotechnol.* 12, 304 (2021)

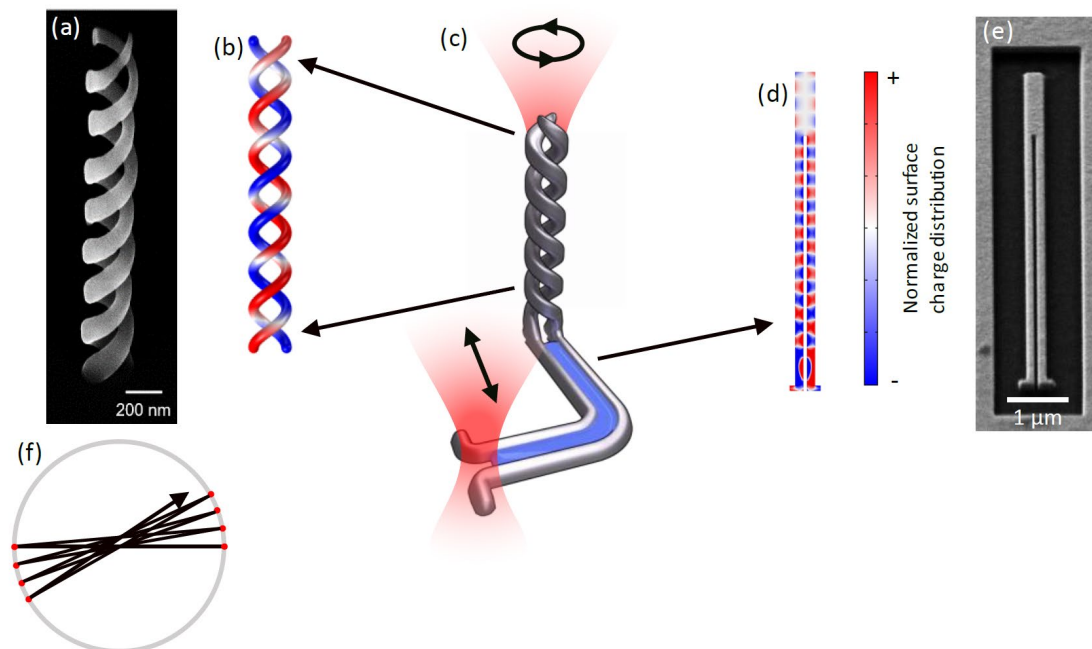


**Figure 1.** Artistic sketch of the proposed device, far-field polarizations depicted by black arrows (a); surface charge distributions of the double helix (b) and two-wire transmission line (c) show antisymmetric nature of according fundamental modes; scanning electron micrograph of the gold double helix (d) and scanning electron micrograph of the two-wire transmission line [2] (e), star-shaped beam path for double helix fabrication, created with Fib-O-Mat patterning toolbox [4] (f).

# Electron-Enhanced Atomic Layer Deposition

Steven M. George<sup>1,\*</sup>, Zachary C. Sobell<sup>1</sup> and Michael A. Collings<sup>1</sup>

<sup>1</sup> University of Colorado, Department of Chemistry, 215 UCB, Boulder, Colorado, 80309-0215, United States

\* email: [Steven.George@Colorado.edu](mailto:Steven.George@Colorado.edu)

Atomic layer deposition (ALD) is a thin film growth technique that is usually performed using sequential, self-limiting exposures to two reactants. During electron-enhanced ALD (EE-ALD), electrons can act as one of the ALD reactants. These electrons can desorb surface species by the process of electron stimulated desorption and create active sites for the adsorption of reactants. EE-ALD can obtain much lower growth temperatures than conventional thermal ALD. A variety of materials have been grown using EE-ALD including GaN, Si, BN and Co [1].

Recent work has developed a hollow cathode plasma electron source (HC-PES) for EE-ALD [2]. The HC-PES can deliver >1000 times more electron current than electron gun sources. In addition, the HC-PES is robust and can operate with chamber pressure in the mTorr range. Consequently, a background gas can be used in conjunction with EE-ALD as shown in **Figure 1**. The electrons can dissociate the background gas and the resulting radicals are able to tune the composition of the EE-ALD film.

This talk will highlight the growth of TiN EE-ALD films that were produced using sequential exposures of tetrakis(dimethylamino)titanium (TDMAT) and electrons with NH<sub>3</sub> as the background gas. TiN EE-ALD films have potential as Cu diffusion barriers for backend interconnects. Using a grid bias of 100 V, the TiN EE-ALD film grown with the NH<sub>3</sub> background gas nucleates rapidly on SiO<sub>2</sub> films as illustrated in **Figure 2**. The growth rate of the TiN EE-ALD is 0.8 Å/cycle at low temperatures of <70°C. In situ Auger electron spectroscopy indicates that these TiN EE-ALD films are pure. In addition, ellipsometry measurements reveal that the resistivity of the TiN EE-ALD films reaches ~120 μΩ-cm at thicknesses >60 Å as shown in **Figure 2**. This low resistivity is comparable to the best TiN films deposited at higher temperatures using ALD methods.

Ru EE-ALD films have also been deposited using sequential exposures of Ru(DMBD)(CO)<sub>3</sub> or Ru<sub>3</sub>(CO)<sub>12</sub> together with electrons. The Ru EE-ALD films nucleate rapidly on SiO<sub>2</sub> films. The growth rate of the Ru EE-ALD is 0.2 Å/cycle at 160°C. These Ru EE-ALD films have an excellent resistivity of 17 μΩ-cm after forming gas annealing at 450°C for 30 minutes. These Ru EE-ALD films have potential for backend interconnects.

[1] Zachary C. Sobell, Andrew S. Cavanagh and Steven M. George; *Growth of Cobalt Films at Room Temperature Using Sequential Exposures of Cobalt Tricarbonyl Nitrosyl and Low Energy Electrons*; J. Vac. Sci. Technol. A **37**, 060906 (2019).

[2] Zachary C. Sobell, Andrew S. Cavanagh, David R. Boris, Scott G. Walton, and Steven M. George; *Hollow Cathode Plasma Electron Source for Low Temperature Deposition of Cobalt Films by Electron-Enhanced Atomic Layer Deposition*; J. Vac. Sci. Technol. A. **39**, 042403 (2021).

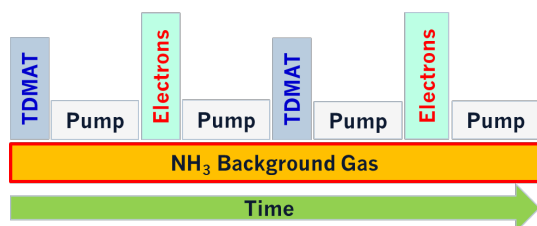


**Figure 1.** Schematic of TiN EE-ALD using TDMAT and electrons with NH<sub>3</sub> background gas.

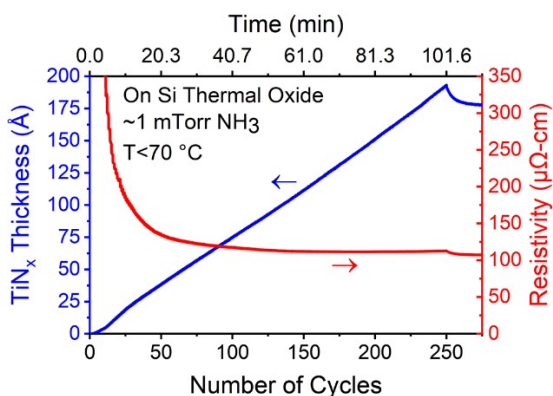


**Figure 2.** Thickness of TiN EE-ALD film and corresponding resistivity versus number of EE-ALD cycles.

# Injecting Energetic Electrons into CO<sub>2</sub> Ice

Anpan Han<sup>1,\*</sup>, Hoa Thanh Le<sup>1</sup>, Rubaiyet I. Haque<sup>1</sup>, Affan K. Waafi<sup>1</sup>

<sup>1</sup> Dept. Mechanical Eng. Technical University of Denmark, Kongens Lyngby, Denmark.

\* email: [anph@mek.dtu.dk](mailto:anph@mek.dtu.dk)

CO<sub>2</sub> gas is frozen to amorphous CO<sub>2</sub> ice thin-films inside the vacuum chamber of a scanning electron microscope. CO<sub>2</sub> gas is condensed to solid CO<sub>2</sub> at 80 K, and when heated at 10 K/min, we observed the CO<sub>2</sub> ice started to sublime at 130 K. Holding the CO<sub>2</sub> ice 80 K, energetic electrons (5 – 20 keV) are injected into it. We observed the CO<sub>2</sub> ice is locally vaporized and removed by the electron exposure. The optimal energy needed to vaporize 710-nm-thick ice is 175 J/cm<sup>2</sup>. The vaporized gas will likely consist of CO<sub>2</sub>, CO, and O<sub>2</sub>. We do not observe cross-linking of CO<sub>2</sub> ice to substances that remain solids or liquids at ambient conditions.

**Fig. 1a** illustrates the electron and CO<sub>2</sub> ice interaction. The energetic primary electron (PE) is injected into the CO<sub>2</sub> ice thin-film that is condensed onto a silicon substrate. Cascades of secondary electrons (SE) are generated. The energy of the PE is distributed into the CO<sub>2</sub> ice and the underlying substrate. The SE electrons have sufficient energy to vaporize CO<sub>2</sub> and facilitate chemical reactions (**Fig. 1b**). We reasoned that CO<sub>2</sub> ice could be both sublimated to CO<sub>2</sub> (g) and radicalized and ionized into CO\*, C\*, and O\*. The radicals and ions could recombine or cross-link into solids and liquids or acquire free electrons and become carbon monoxide and oxygen. I.e., injecting energetic electrons into CO<sub>2</sub> ice is maybe a chemical reduction reaction. We condensed between 240 and 1200-nm-thick CO<sub>2</sub> ice, and patterned the ice using 5, 12.5 and 20 keV electrons. **Figure 2a** shows an SEM image of the exposed CO<sub>2</sub> ice. CO<sub>2</sub> is locally vaporized and removed by the energetic electrons. Observing the SEM images' contrast, removing 240 nm of ice required minimal critical dose (CD) of 30 mC/cm<sup>2</sup>. The variance of CD is evaluated to  $\pm 5$  mC/cm<sup>2</sup>. Plotting the clearance dose and the ice thickness, the CD needed to remove CO<sub>2</sub> ice was independent of ice thickness. The total injected energy (TIE) is the product of the electron energy and dose. The critical TIE (CE) needed to remove 710-nm-thick ice is 150 J/cm<sup>2</sup>. For 1200-nm-thick CO<sub>2</sub> ice, we observed severe charging effects, and it was not possible to form SEM images, and we were not able to expose the dry ice. After heating the sample to room temperature, we observed deposits that remained at the area of electron exposure. The AFM images showed that the solid deposits were up to 28-nm-thick (**Fig. 2b**), and they were independent of the CO<sub>2</sub> ice thickness. These AFM images are comparable to AFM images of vacuum contamination, and the thicknesses were also comparable

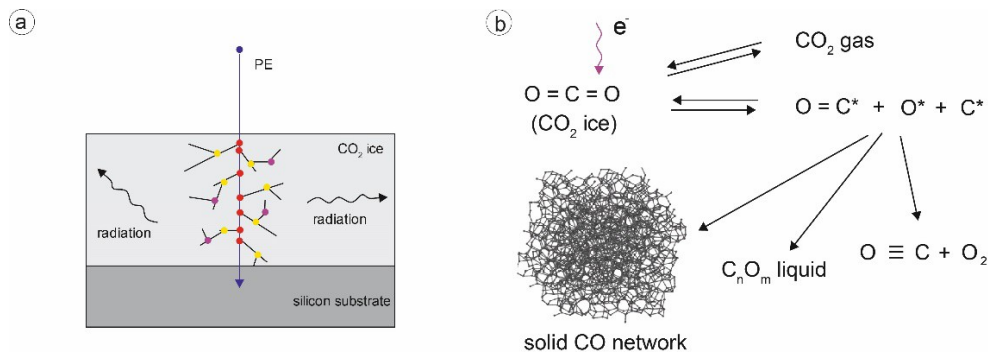


**Figure 1.** 3D Illustrations of air-core toroidal inductor chip (a), and Si fixture after removing Si core (b).

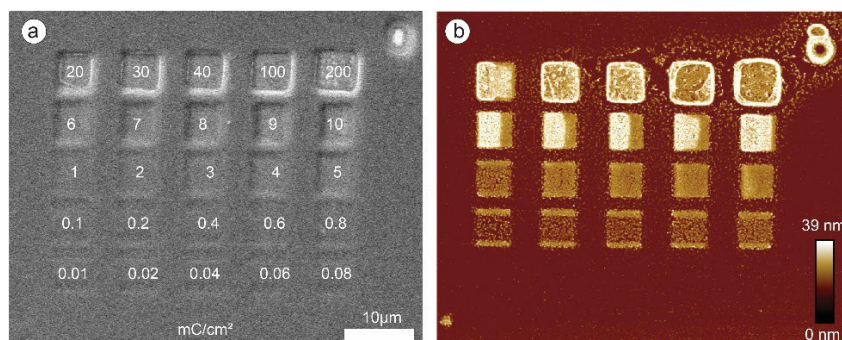


**Figure 2.** 240-nm-thick CO<sub>2</sub> ice is condensed on the gold surface of the silicon substrate, and it was exposed using 5 keV electrons with a dose ranging between 0.01 and 200 mC/cm<sup>2</sup>. (a) SEM image of patterned CO<sub>2</sub> ice just after electron exposure. The ice is held at 79 K. We observed that the minimal dose (critical dose) needed to remove all the ice is 30 mC/cm<sup>2</sup>. (b) AFM image of the same area at under ambient conditions

# Water-Assisted FEBID/FEBIE for the Deposition of High Purity Noble Metal Nanostructures

Cristiano Glessi<sup>1,\*</sup>, Kees Hagen<sup>1</sup>

<sup>1</sup> Delft University of Technology, Department of Imaging Physics, Lorentzweg 1, 2628CJ, Delft, the Netherlands

\* email: [c.glessi@tudelft.nl](mailto:c.glessi@tudelft.nl)

Focused Electron Beam-Induced Deposition (FEBID) is a nanofabrication technique that allows for the direct production of three dimensional nanostructures. One of the major backdraws of this technique is the low purity of the deposited material, often comprised of a small amount of the target metal atom and a large amount of unwanted co-deposited carbon [1]. The co-deposited carbon can originate either from contaminants of the vacuum chamber and substrate, or from carbon-based fragments originating from the organic ligands of the organometallic precursor. The removal of these unwanted fragments can be accomplished by carbon etching performed during deposition through the co-injection of an oxidant/reductant agent, such as oxygen or water [2, 3]. The simultaneous deposition (FEBID) of the metal and etching (FEBIE) of unwanted carbon poses itself as a straightforward methodology for obtaining pure deposits from already available FEBID precursors. We present FEBID/FEBIE achieved through the co-injection of gold or platinum based precursors ( $\text{Au}(\text{acac})\text{Me}_2$ ,  $\text{MeCpPtMe}_3$ ) and water. Through this fabrication procedure it was possible to reliably obtain deposits consisting of 60-70% at.% Pt, with the co-deposition of very limited amounts of carbon and oxygen. The C/Pt At.% ratio is diminished in the obtained nanostructures through the additional injection of water from 6.7 (Pt injection only) to 0.2 – 0.4 (injection of Pt and  $\text{H}_2\text{O}$ ) (Figure 1).

The deposition of highly pure Pt deposits was achieved within a pressure range compatible with a standard SEM (5e-5 mbar) and with the use of only commercially available instrumentation and precursors, offering the basis for a straightforward applicability of this method.

[1] S. Barth, M. Huth, F. Jungwirth; *Precursors for direct-write nanofabrication with electrons*; J. Mater. Chem. C 45 (8), 15884 (2020).

[2] M. Shawrav, P. Taus, H. Wanzenboeck, M. Schinnerl, M. Stöger-Pollach, S. Schwarz, A. Steiger-Thirsfeld, E. Bertagnolli; *Highly conductive and pure gold nanostructures grown by electron beam induced deposition*; Sci. Rep. 6, 34003 (2016).

[3] E. Villamor, F. Casanova, P. H. F. Trompenaars, J. J. L. Mulders; *Embedded purification for electron beam induced Pt deposition using  $\text{MeCpPtMe}_3$* ; Nanotechnology 26 (9), 095303 (2015).

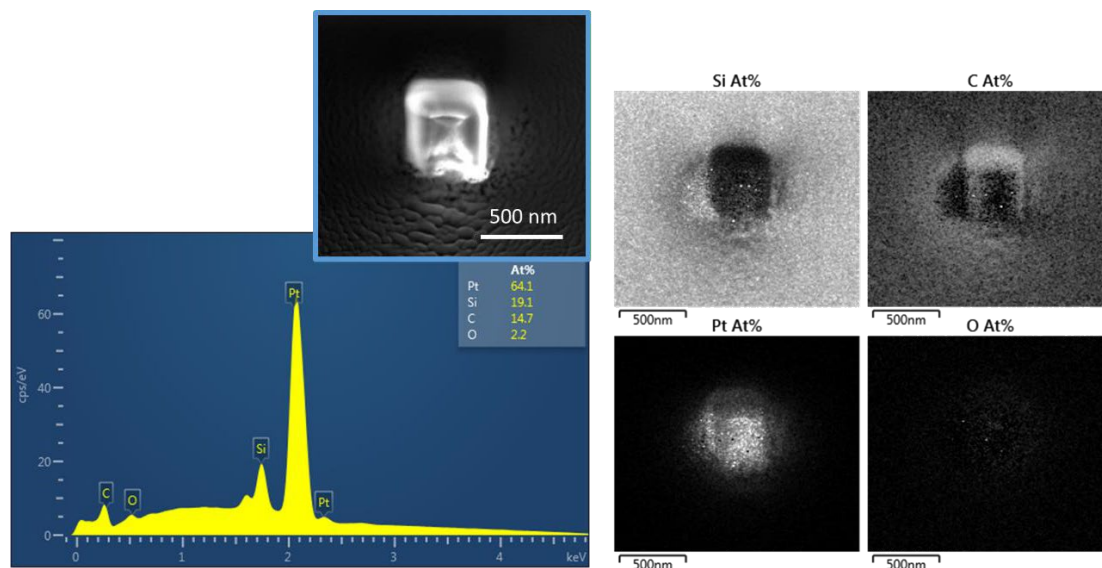


**Figure 1.** Square deposit of 400x400 nm performed at 0.54 nA, 5 kV. Point EDX and map EDX characterization of the deposit performed at 2.3 nA, 5 kV.

# Pushing the Limits of EUV Mask Repair: Addressing Sub-10 nm Defects with the Next Generation Ebeam-based Mask Repair Tool

Tilmann Heil<sup>1</sup>, Michael Waldow<sup>1</sup>, Renzo Capelli<sup>2</sup>, Horst Schneider<sup>1</sup>, Laura Ahmels<sup>1</sup>, Fan Tu<sup>1</sup>, Johannes Schöneberg<sup>1</sup>, Klaus Edinger<sup>1</sup> and Hubertus Marbach<sup>1,\*</sup>

<sup>1</sup> Carl Zeiss SMT GmbH, Industriestrasse 1, 64380, Rossdorf, Germany

<sup>2</sup> Carl Zeiss SMT GmbH, Rudolf-Eber-Strasse 2, 73447, Oberkochen

\* email: [hubertus.marbach@zeiss.com](mailto:hubertus.marbach@zeiss.com)

Mask repair is an essential step in the manufacturing process of EUV masks. Its key challenge is to continuously improve resolution and control to enable the repair of the ever-shrinking feature sizes on mask along the EUV roadmap. The state-of-the-art mask repair method is gas-assisted electron beam (e-beam) lithography also referred to as focused electron beam induced processing (FEBIP). We discuss the principles of the FEBIP repair process along with the criteria to evaluate the repairs, and identify the major contributions determining the achievable resolution. As key results, we present several high-end repairs on EUV masks including a sub-10 nm extrusion achieved with the latest generation of e-beam-based mask repair tools, the MeRiT<sup>®</sup> LE. Furthermore, we demonstrate the corresponding repair verification using at-wavelength (actinic) measurements via AIMS EUV.

[1] T. Heil, M. Waldow, R. Capelli, H. Schneider, L. Ahmels, F. Tu, J. Schöneberg and H. Marbach; *Pushing the limits of EUV mask repair: addressing sub-10 nm defects with the next generation e-beam-based mask repair tool*; Journal of Micro/Nanopatterning, Materials and Metrology, 20, 031013 (2021)

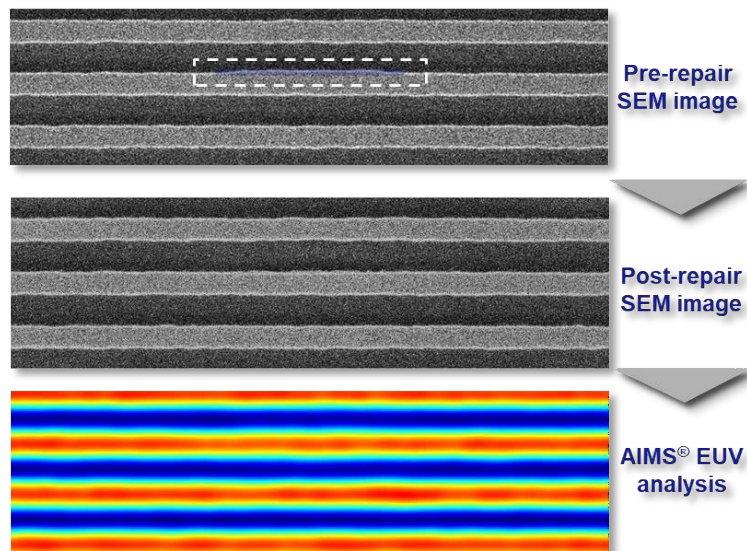


**Figure 1.** Example of successful repair of extrusion defect <10 nm with the MeRiT LE verified by SEM and AIMS as indicated.



# Hybrid superconductor/ferromagnet structures

Oleksandr V. Dobrovolskiy<sup>1</sup>

<sup>1</sup> University of Vienna, Faculty of Physics, Nanomagnetism and Magnonics, Superconductivity and Spintronics Laboratory, Währinger Strasse 17, 1090 Vienna, Austria

\* email: [oleksandr.dobrovolskiy@univie.ac.at](mailto:oleksandr.dobrovolskiy@univie.ac.at)

Ferromagnetism and superconductivity belong to the most fundamental phenomena in condensed-matter physics. Recent discoveries in these topical areas enable the exploration of new physical phenomena at their interfaces. In this regard, interactions between the fundamental quasiparticles – magnetic flux quanta (fluxons) in superconductors and quanta of spin waves (magnons) in magnetic materials – are especially fascinating. Nanoscale 2D and 3D hybrid materials offer unique platforms for experimental studies of such interactions.

In my talk, I will focus on a set of our recent experimental findings in this domain. First, the magnon-fluxon interaction in ferromagnet/superconductor heterostructures was evidenced by spin-wave spectroscopy [1]. The array of vortices in the superconductor created a periodic scattering potential for spin waves propagating in the adjacent ferromagnet and induced Bloch-like bandgaps in the spin-wave transmission spectra. It was also demonstrated, that a rather slow (0.3 km/s) motion of vortices by the applied dc current results in the Doppler shift of the bandgap frequencies. Here-with, non-reciprocity in the spin-wave dynamics can be induced by using asymmetric vortex pinning potentials [2].

It has soon become clear that increase of the vortex velocity to at least 1 km/s should open access to new types of magnon-fluxon interactions. However, such high vortex velocities had not been available because of the escape of hot (unpaired) electrons from the vortex cores – the phenomenon of flux-flow instability. The direct-write nanofabrication by FIBID and FEBID allows for the creation of both, superconductors with fast relaxation of heated electrons [3] and 3D nanomagnets with on-purpose engineered properties [4]. As a result, vortex velocities of up to 15 km/s have been achieved [5, 6] in . This has enabled the realization of the long-predicted theoretically, but so far never observed experimentally, phenomenon of Cherenkov radiation of magnons [7] and to establish superconductivity and magnetism in 3D nanoarchitectures as prospective research avenues in condensed-matter physics [8-10].

[1] O. Dobrovolskiy et. al.; Nat. Phys. 15 (2019) 477.

[2] O. Dobrovolskiy and A. Chumak; J. Magn. Magnet. Mater. 543 (2022) 168633.

[3] F. Porrati et al.; ACS Nano 13 (2019) 6287.

[4] O. Dobrovolskiy et. al.; Appl. Phys. Lett. 118 (2021) 132405.

[5] O. Dobrovolskiy et al.; Nat. Commun. 11 (2020) 3291.

[6] B. Budinska et al.; Phys. Rev. Appl. 17 (2022) 034072.

[7] O. Dobrovolskiy et al.; arXiv:2103.10156 (2021).

[8] A. Fernandez-Pacheco et al.; Materials 13 (2020) 3774.

[9] D. Makarov et al.; Adv. Mater. 2101758 (2021) 2101758.

[10] V. Fomin and O. Dobrovolskiy; Appl. Phys. Lett. 120 (2022) 090501.

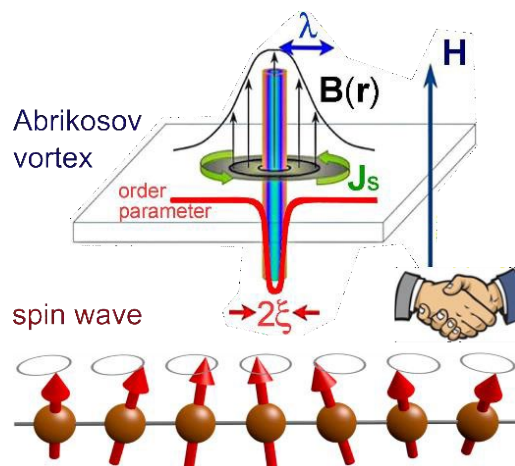


**Figure 1.** “Hand-shaking” between the fundamental quasiparticles in hybrid nanostructures – magnetic flux quanta (fluxons) in superconductors and quanta of spin waves (magnons) in magnetic materials.

# Layer by Layer FEBID 3D Printing and its Applications to Nanomagnetism

Amalio Fernández-Pacheco<sup>1,2,4,\*</sup>, Luka Skoric<sup>2</sup>, Dédalo Sanz-Hernández<sup>2</sup>, Fanfan Meng<sup>2</sup>, Claire Donnelly<sup>2</sup>, Sara Merino-Aceituno<sup>3</sup>, Aurelio Hierro-Rodríguez<sup>4</sup>

<sup>1</sup> Instituto de Nanociencia y Materiales de Aragón (INMA). CSIC-Universidad de Zaragoza, 50009 Zaragoza, Spain.

<sup>2</sup> Cavendish Laboratory, University of Cambridge, JJ Thomson Ave, Cambridge CB3 0HE, UK

<sup>3</sup> Faculty of Mathematics, University of Vienna, Oskar-Morgenstern-Platz 1, 1090, Vienna, Austria

<sup>4</sup> SUPA, School of Physics and Astronomy, University of Glasgow, Glasgow G12 8QQ, UK

\* email: [amaliopf@unizar.es](mailto:amaliopf@unizar.es)

In the last few years, the application of FEBID for 3D nano-printing has given key steps via the usage of CAD software solutions [1, 2], where meshed objects based on networks of nanowires have been successfully fabricated and investigated, for applications in fields such as scanning probe microscopy, photonics and magnetism.

In this contribution, we will show a computational framework designed for the layer-by-layer 3D printing of complex shaped surfaces and volumes by FEBID [3], going beyond the growth of meshed objects based on nanowires. Our approach follows a similar strategy as a 3D printer extruder: After the 3D object has been defined with standard CAD software, our algorithm divides it in multiple layers. Then, using a formalism based on the FEBID continuum model and a two-step calibration procedure, it calculates the necessary dwell time on each point to grow each of the layers comprising the object, including proximity effects within a layer. We will present the key features of this new algorithm, where thermal effects, beam defocusing and gas distribution anisotropies are also incorporated.

The conditions under which the algorithm is valid and its current limitations will be discussed.

We will demonstrate the power of this new approach for 3D printing of complex shaped nanostructures by presenting the successful growth of a variety of geometries using several precursors. In particular, we will focus on recent examples in the field of nanomagnetism, where the imprinting of topological spin defects [4] and stray fields [5], as well as new geometrical effects in 3D interconnectors including automotion of domain walls [6] and unconventional magnetoelectrical effects [7], have been demonstrated.

[1] J. D. Fowlkes, R. Winkler et al; *High-Fidelity 3D-Nanoprinting via Focused Electron Beams: Computer-Aided Design (3BID)*; ACS Appl. Nano Mater. 3, 1028 (2018).

[2] L. Keller, M. Huth; *Pattern generation for direct-write three-dimensional nanoscale structures via focused electron beam induced deposition*; Beilstein J. Nanotechnol. 9, 2581 (2018).

[3] L. Skoric, D. Sanz-Hernandez et al; *Layer-by-layer growth of complex-shaped three-dimensional nanostructures with focused electron beams*; Nano Letters 20, 184 (2020).

[4] D. Sanz-Hernández, A. Hierro-Rodríguez et al; *Artificial double-helix for geometrical control of magnetic chirality*; ACS nano 14, 8084 (2020).

[5] C. Donnelly, A. Hierro-Rodríguez et al; *Complex free-space magnetic field textures induced by three-dimensional magnetic nanostructures*; Nature Nanotechnology 17, 136 (2022).

[6] L. Skoric, C. Donnelly et al; *Domain wall automotion in three-dimensional magnetic helical interconnectors*; ACS Nano (2022). Preprint: arXiv:2110.04636.

[7] F. Meng, C. Donnelly et al; *Non-Planar Geometrical Effects on the Magnetoelectrical Signal in a Three-Dimensional Nanomagnetic Circuit*; ACS Nano 15, 6765 (2021).

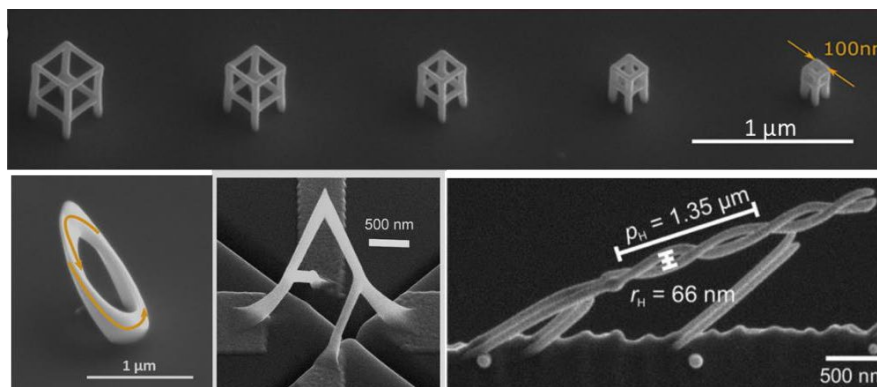


**Figure 1.** Selection of layer-by-layer 3D printed nanostructures for applications in nanomagnetism. Our algorithm is capable of growing not only meshed objects based on nanowires (nanocubes in upper row), but also complex surfaces and volumes such as Möbius strips, nano-bridge circuits and double helices (lower row)

# Plasmonic On-Demand Design via 3D Nanoprinting

David Kuhness<sup>1</sup>, Gerald Kothleitner<sup>2,3</sup> and Harald Plank<sup>1,2,3,\*</sup>

<sup>1</sup> Christian Doppler Laboratory - DEFINE, Graz University of Technology, 8010 Graz, Austria

<sup>2</sup> Institute of Electron Microscopy and Nanoanalysis, Graz University of Technology, 8010 Graz, Austria

<sup>3</sup> Graz Centre for Electron Microscopy, 8010 Graz, Austria

\* email: [harald.plank@felmi-zfe.at](mailto:harald.plank@felmi-zfe.at)

Plasmonic nanoparticles have unique optical properties due to their size and shape, and are increasingly being incorporated into commercial products and technologies, ranging from photovoltaics to biological and chemical sensors [1]. The control on shifting and tuning of the plasmonic response depend highly on the abilities to control the final shape of the nano-particles in every detail. Expansion towards the third dimension in contrast to traditionally planar plasmonic structures crucially enhances the design possibilities. 3-D nano-printing via focused electron beam induced deposition (3D-FEBID) allows flexible fabrication with nanoscale precision [2]. In addition, it has been proven to be a versatile fabrication method to achieve on-demand design of plasmonically active nanostructures [3-6].

Still, FEBID materials notoriously suffer from high carbon contents. Especially for achieving satisfying plasmonic performance, a chemical post-growth transfer into pure materials is indispensably needed, which can severely harm or even destroy FEBID-based 3D nano-architectures. We here demonstrate the abilities and limitations of 3D-FEBID towards controlled fabrication of gold nano-antennas of various dimensions. Applying flexible e-beam focus conditions through an advanced patterning approach allows for direct-write fabrication of high-fidelity shapes with nanoscale features in the sub-10 nm range. We also present a shape-stable chemical transfer into high-quality materials for plasmonically active Au nano-antennas. Its plasmonic response is demonstrated via STEM-EELS mapping measurements. The findings are complemented with corresponding modelling and plasmon simulations. The good agreement between experiment and simulation allows for on demand spectral tuning of plasmonic response via modelling and design of suitable shapes of nano-antennas via 3-D nano-printing with high precision. By that, we lay the foundation for controlled fabrication of tunable plasmonic 3D structures, ultimately driven by an upfront simulation in order to prevent exhaustive trial-and-error approaches.

[1] H. Plank et al., *Micromachines*, 11, 1 (2020).

[2] Hirt et al., *Adv. Mater.*, 29, 17 (2017).

[3] Winkler et al., *J. Appl. Phys.*, 125, 21 (2019)

[4] Höflich et al.; *Optica*, 6, 9, 1098-1105 (2019).

[5] Esposito et al.; *Advanced Optical Materials*, 2, 154-161 (2014).

[6] Kuhness et al., *ACS Appl. Mater. Interfaces*, 13, 1, 1178 (2021).

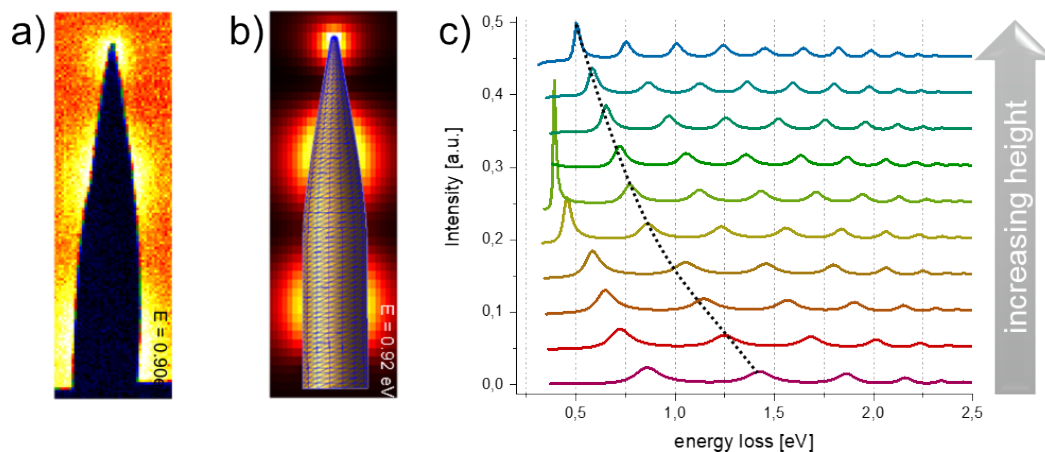


**Figure 1.** Plasmonic activity of FEBID-based Au nanoantennas. (a) scanning TEM (STEM) based electron energy loss spectroscopy (EELS) map at a plasmon loss energy of 0.90 eV, which reveals laterally resolved information about plasmonic activities. (b) EELS map simulation, based on the real morphology taken from (a), which reveals very good agreement to real data (a). (c) shows simulated STEM-EELS spectra taken from the tip region of the modelled Au nanoantennas for several shapes and sizes, revealing a spectral shift (indicated with the black dashed line) and a change of plasmon peak density as a function of height of the antennas.





**Poster** presentations



# Copper(II) complexes with pivalate and small aliphatic amines as precursors for nanomaterial fabrication

Aleksandra Butrymowicz<sup>1,\*</sup>, Katarzyna Madajska<sup>1</sup>, Wiktoria Luba<sup>1</sup>, Tadeusz Muzioł<sup>1</sup>, Iwona B. Szymańska<sup>1</sup>

<sup>1</sup> Nicolaus Copernicus University in Torun, Faculty of Chemistry, Gagarina 7, 87-100 Torun, Poland

\* email: [aleksandra.butrymowicz@doktorant.umk.pl](mailto:aleksandra.butrymowicz@doktorant.umk.pl)

Vapour deposition methods such as focused electron beam induced deposition (FEBID) needs volatile and sensitive to the electron beam compounds for nanofabrication, capable of producing 2D and free-standing 3D structures of sub-10 nm size. Until now the development of FEBID precursors has relied on thermally induced chemical vapour deposition (CVD) precursors. The choice of the volatile and sensitive to the electron or ion beam precursor is crucial for nanostructure growth success. Chemical compounds used in FEBID should: a) characterized by high thermal stability and vapor pressure at low temperatures; b) dissociate completely to a predicted material as a result of interaction with the electron beam, c) form by-products, which easily desorbed from the substrate surface. In the case of carboxylates using  $[\text{Ag}_2(\mu\text{-O}_2\text{CR})_2]$ , where R = <sup>t</sup>Bu, C(Me)<sub>2</sub>Et, CF<sub>3</sub>, and C<sub>2</sub>F<sub>5</sub> it was shown that these compounds can be dissociated through a focused electron beam to give deposits with a satisfactory metal content (57 at.%, 73 at.%, 70 at.%, and 76 at.%, respectively). However, for copper(II)  $[\text{Cu}_2(\mu\text{-O}_2\text{CC}_2\text{F}_5)_4]$  the fabricated material contains 23 at.% Cu [1, 2, 3].

Here we present the study of volatility and interaction of electrons with new, user-friendly, multinuclear copper(II) complexes with pivalate (2,2-dimethylpropanoate) and small aliphatic amines: RNH<sub>2</sub>, where R = <sup>t</sup>Bu, <sup>s</sup>Bu, <sup>i</sup>Pr, and Et and known in the literature  $[\text{Cu}_2(\text{Et}_3\text{N})_2(\mu\text{-O}_2\text{C}^t\text{Bu})_4]$  [4], which can be an alternative to previously studied carboxylates. The purpose of introducing a secondary ligand to copper(II) pivalate was to check how it would change properties such as volatility and sensitivity to the electron beam. Based on variable temperature infrared spectroscopy VT IR (10<sup>-1</sup> mbar) supported with TGA/DTA, the mechanism of thermal decomposition was determined. Bands characteristic of complexes, in the gas phase were observed in the range 160–240°C. The sublimation data provided that studied copper(II) compounds evaporate over the range 90–120°C. Thin layers were obtained by sublimation on a silicon substrate under reduced pressure (10<sup>-4</sup> mbar). The prepared samples were exposed to a beam of high-energy electrons. These studies revealed a sensitivity to high-energy electrons and confirmed that the compounds are promising as FEBID precursors. Moreover, to confirm the effective formation of metal carriers, CVD deposits were fabricated with the use of new copper(II) compounds.

[1] I. Utke, P. Swiderek, K. Höflich, K. Madajska, J. Jurczyk, P. Martinović, I. B. Szymańska; *Coord. Chem. Rev.* 458, 213851 (2022).

[2] L. Berger, K. Madajska, I. B. Szymańska, K. Höflich, M. N. Polyakov, J. Jurczyk, C. Guerra-Nuñez, I. Utke; *Beilstein J. Nanotechnol.* 9, 224 (2018).

[3] L. Berger, J. Jurczyk, K. Madajska, T. E. J. Edwards, I. B. Szymańska, P. Hoffmann, I. Utke; *ACS Appl. Electron. Mater.* 2, 1989 (2020).

[4] M. Mikuriya, H. Azuma, R. Nukada, M. Handa; *Chem. Lett.*, 57 (1999).

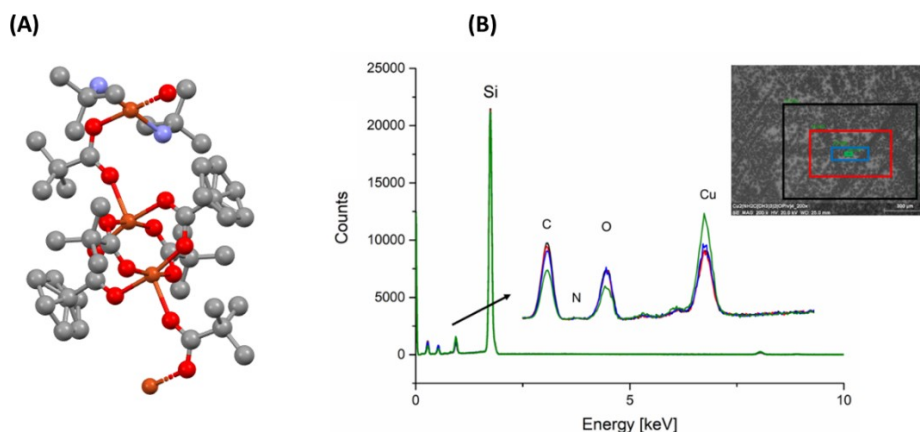


**Figure 1.**  $[\text{Cu}_3(\text{}^t\text{BuNH}_2)_2(\mu\text{-O}_2\text{C}^t\text{Bu})_6]$  (hydrogen atoms omitted): (A) – the crystal structure, (B) – a thin layer of the complex obtained in the sublimation process, deposited on a silicon wafer and exposed to a beam of high-energy electrons.

# Electron-induced fabrication of material with configurable properties for potential use as nanoscale humidity sensors

Hannah Boeckers<sup>1,\*</sup>, Petra Swiderek<sup>1</sup> and Markus Rohdenburg<sup>2</sup>

<sup>1</sup> University of Bremen, Institute of Applied and Physical Chemistry, Fachbereich 2 (Chemie/Biologie), Leobener Straße/NW2, Postfach 330440, D-28334 Bremen, Germany

<sup>2</sup> Wilhelm-Ostwald-Institut für Physikalische und Theoretische Chemie, Universität Leipzig, 04103 Leipzig, Germany

\* email: [hannah@uni-bremen.de](mailto:hannah@uni-bremen.de)

While research on focused electron beam induced deposition (FEBID) often aims at the deposition of pure metals, impure deposits also find promising applications, e.g. as nanoscale sensors. Several studies have brought forward Hall, strain or even humidity sensors produced by FEBID [1, 2, 3]. For instance, humidity sensors produced by FEBID from the precursor MeCpPtMe<sub>3</sub> were reported [2]. The deposits used as sensing materials consist of metal particles integrated into a non-conductive matrix (f. e. carbon). The adsorption of water molecules on the sensor's surface results in an enhanced charge transfer between the metal particles via tunneling, and therefore in higher currents when an external voltage is applied to the sensor [2]. Since the interaction of the analyte with the matrix is a crucial factor, the sensitivity of such humidity sensors could be improved by incorporating better binding sites into the deposit.

Motivated by studies on amorphous CN<sub>x</sub> films for which an enhanced sensitivity toward several gases was reported [4], we have investigated the incorporation of nitrogen-containing functional groups into carbenaceous deposits and its effect on the binding of H<sub>2</sub>O. To this end, deposits were produced from n-pentane, 2-methyl-2-butene (2M2B), and Bis(ethylcyclopentadienyl)ruthenium(II) ((EtCp)<sub>2</sub>Ru) and modified with cycles of electron irradiation in presence of ammonia (NH<sub>3</sub>). In each cycle, ammonia was adsorbed on the deposit and exposed to electrons followed by annealing of the sample. The incorporation of nitrogen into the carbon matrix was monitored using Auger Electron Spectroscopy (AES) and the desorption temperature of submonolayers of H<sub>2</sub>O adsorbed onto the deposit was determined as function of the number of NH<sub>3</sub> cycles via thermal desorption spectroscopy (TDS). In each case a shift of the desorption temperature was observed with best results obtained for (EtCp)<sub>2</sub>Ru (Figure 1).

[1] M. Gabureac, L. Bernau, I. Utke; Granular Co–C nano-Hall sensors by focused-beam-induced deposition; *Nanotechnology* 21, 115503 (2010).

[2] C.H. Schwalb, C. Grimm, M. Baranowski, R. Sachser, F. Porrati, H. Reith, P. Das, J. Müller, F. Völklein, A. Kaya, M. Huth; *A Tunable Strain Sensor Using Nanogranular Metals*, *Sensors* 10, 9847 (2010).

[3] F. Kolb, K. Schmoltner, M. Huth, A. Hohenau, J. Krenn, A. Klug, E. J. W. List, H. Plank; *Variable tunneling barriers in FEBID based PtC metal-matrix nanocomposites as a transducing element for humidity sensing*; *Nanotechnology* 24, 305501 (2013).

[4] L. Zambov, C. Popov, N. Abedinov, M. F. Plass, W. Kulisch, T. Gotszalk; *Gas-sensitive properties of nitrogen-rich carbon nitride films*, *Ad. Mater.* 12, 656 (2000).

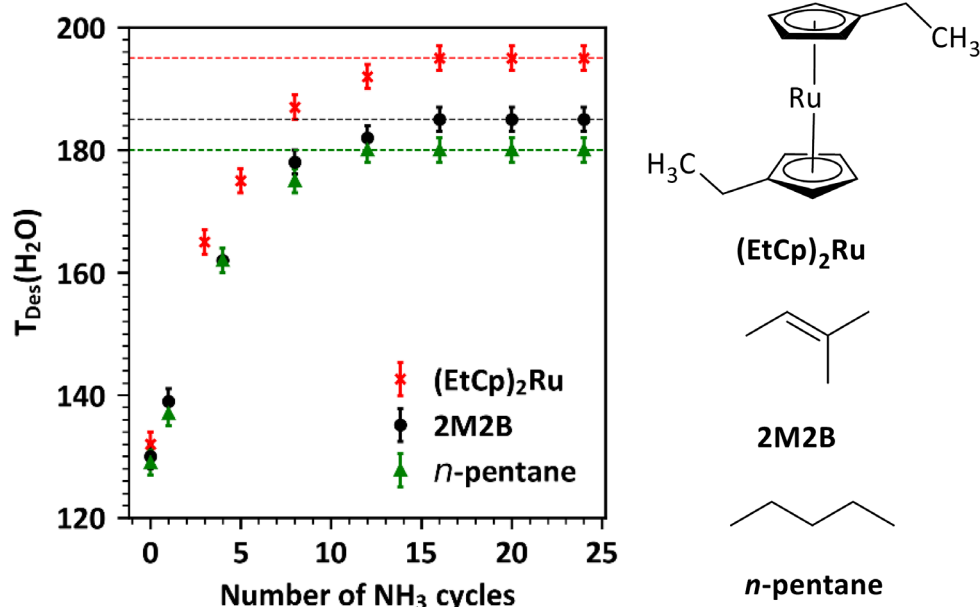


**Figure 1.** Desorption temperatures of H<sub>2</sub>O submonolayers in dependence on the number of NH<sub>3</sub> treatment cycles on deposits produced by electron irradiation from adsorbed layers of n-pentane, 2-methyl-2-butene (2M2B), and (EtCp)<sub>2</sub>Ru. The desorption temperatures refer to the center of the broad desorption peaks.

# 3D-Nanoprinting of Magnetic Force Microscopy Tips

M. Brugger-Hatzl<sup>1</sup>, R. Winkler<sup>1</sup>, L. Seewald<sup>1</sup>, S. Mietsche<sup>2</sup>, T. Radlinger<sup>3</sup>, M. Huth<sup>4</sup>, S. Barth<sup>4</sup>, and H. Plank<sup>1,2,3,\*</sup>

<sup>1</sup> Christian Doppler Laboratory - DEFINE, Graz University of Technology, Steyrergasse 17, 8010 Graz, Austria

<sup>2</sup> Institute of Electron Microscopy and Nanoanalysis, Graz University of Technology, Steyrergasse 17, 8010 Graz, Austria

<sup>3</sup> Graz Centre for Electron Microscopy, Steyrergasse 17, 8010 Graz, Austria

<sup>4</sup> Institute of Physics, Goethe University, Max-von-Laue-Strasse 1, 60438 Frankfurt am Main, Germany

\* email: [harald.plank@felmi-zfe.at](mailto:harald.plank@felmi-zfe.at)

Magnetic devices play an important role in modern electronics and data storage. To analyze magnetic nanoscale features, Magnetic Force Microscopy (MFM), an advanced mode of Atomic Force Microscopy (AFM), is an often used and very powerful characterization technology. To induce the magnetic sensitivity, commercial MFM cantilevers mostly use non-magnetic standard tips, which are covered with thin magnetic coatings. Such additional layers, however, increase the apex radii, which consequently reduce the lateral resolution capabilities in both, AFM and MFM scans. Furthermore, mechanical stress during scanning can lead to local delamination of the magnetic coating, which changes or even removes the magnetic sensitivity. To overcome those issues, a solid, fully magnetic nanoscale tip would be required, which can be a tough challenge when aiming on full cantilever chips. Following that motivation, we here demonstrate the application of Focused Electron Beam Induced Deposition (FEED) for additive, direct-write 3D-nanoprinting of magnetic tips on pre-finished AFM cantilevers [1, 2].

In this contribution we report fabrication details of magnetic nano-tips from  $\text{HCo}_3\text{Fe}(\text{CO})_{12}$  precursor [3]. We discuss the impact of process parameters such as electron energies, beam currents and patterning details revealed by SEM, EDX and TEM for consistent morphological, chemical and structural insights. Next, the basic performance of such MFM tips is demonstrated with special focus on lateral resolution, magnetic phase shift and signal-to-noise ratio. For further optimization, tip geometries were adjusted (see **Figure 1a**) and subjected to different post-processing procedures such as post-irradiation with electrons, thermal treatments and purification protocols. Finally, optimized FEED-MFM tips were then tested on various magnetic samples (magnetic multilayer system (**Figure 1b**), hard disc drives, magnetic recording tapes) and benchmarked to commercially available MFM tips (**Figure 1c-d**). Finally, we briefly show two application examples in the field of correlative-microscopy, where SEM, EBSD, TEM, AFM and MFM are used on duplex steel and CuNiFe material systems. In summary, this contribution presents an commercially relevant use case for 3D-FEED, namely the 3D-nanoprinting of MFM tips on self-sensing cantilevers, the elaboration of a suitable fabrication parameter set and the application of those special tips in (correlative) microscopy experiments on various samples.

[1] H. Plank et al.; *Focused electron beam-based 3D nanoprinting for scanning probe microscopy: A review*; *Micromachines*, vol. 11, no. 1. MDPI AG, Jan. 01, 2020. doi: 10.3390/mi11010048.

[2] J. Pablo-Navarro et al.; *Magnetic Functionalization of Scanning Probes by Focused Electron Beam Induced Deposition Technology*; *Magnetochemistry*, vol. 7, no. 10, 2021, doi: 10.3390/magnetochemistry7100140.

[3] F. Porrati et al.; *Direct writing of CoFe alloy nanostructures by focused electron beam induced deposition from a heteronuclear precursor*; *Nanotechnology*, vol. 26, no. 47, p. 475701, Nov. 2015, doi: 10.1088/0957-4484/26/47/475701.

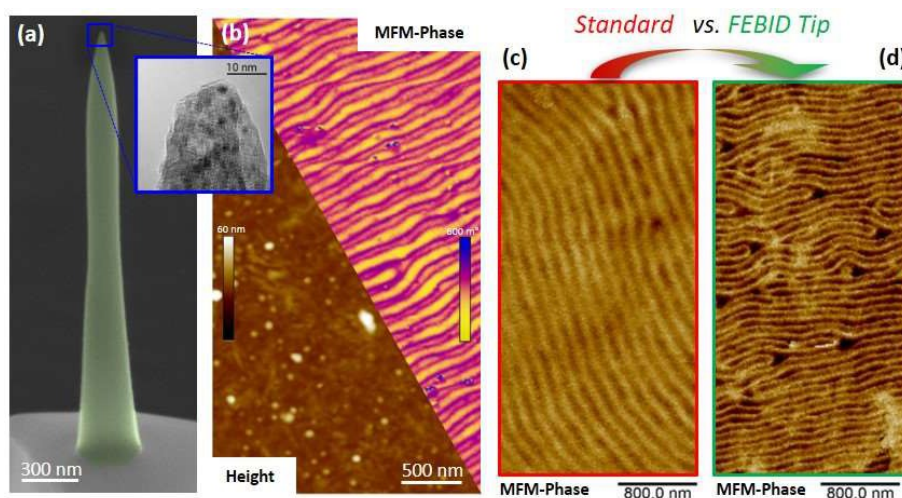


**Figure 1.** (a) specifically tailored pillar  $\text{Co}_3\text{Fe}$  nanoprobe for Magnetic Force Microscopy (MFM). The inset shows a TEM image of the tip region with a tip radius of about 10 nm. (b) height and magnetic phase of a CoPt multilayer system recorded with FEED-MFM tip. Direct comparison of magnetic maps taken with a commercial MFM tip (c) and a FEED tip (d), respectively, showing the superior performance of the FEED nanoprobe.

# FEBID 3D-Nanoprinting at Low Substrate Temperatures: Pushing the Speed While Keeping the Quality

J. Hinum-Wagner<sup>1</sup>, R. Winkler<sup>1</sup>, D. Kuhness<sup>1</sup> and H. Plank<sup>1,2,3,\*</sup>

<sup>1</sup> Christian Doppler Laboratory - DEFINE, Graz University of Technology, Steyrergasse 17, 8010 Graz, Austria

<sup>2</sup> Institute of Electron Microscopy and Nanoanalysis, Graz University of Technology, Steyrergasse 17, 8010 Graz, Austria

<sup>3</sup> Graz Centre for Electron Microscopy, Steyrergasse 17, 8010 Graz, Austria

\* email: [harald.plank@felmi-zfe.at](mailto:harald.plank@felmi-zfe.at)

Nanofabrication using Focused Electron Beam Induced Deposition (FEBID) has made great progress in the past few years on several areas, which allowed to explore new fields for applications. Recent advances have unlocked the precise fabrication of complex, freestanding 3D architectures at the nanoscale [1], elevating FIB/SEM dual beam microscopes to the status of true 3D nanoprinters. Although 3D-FIBID/FEBID is superior to other direct-write methods in many aspects [2] such as high flexibility in design, material and functionality, the low deposition speed inhibits large-scale production as needed for most industrial applications. The limiting factor for the growth rates is the local availability of precursor molecules. For flat 2D-deposits, the growth rates can be significantly enhanced by cooling the substrate temperature to cryogenic conditions (Cryo-FEBID) [3], an approach, which is not applicable for the fabrication of complex 3-dimensional geometries due to the missing precursor diffusion towards the growth front [4]. For 3D-FEBID growth, it was found that local heating by the electron beam itself can affect the precursors residence time at the growth front, which changes the effective coverage up to a point, where further growth becomes unstable [4].

Based on those insights, we here reverse the situation and lower the substrate temperature using a home-built Peltier cooling stage inside the FEBID machine to study the impact on growth stability and fabrication precision. In detail, we use a challenging 3D multi-pod designs (**Fig. 1a**) to investigate the growth dynamics (growth rates), wire dimensions, internal grain structure (transmission electron microscopy) and the influence of the support geometry in a temperature range from 5 °C to 30 °C. Results for the Pt-precursor used reveal that cooling the substrate increases the growth rates by a factor up to 5.6 (**Fig. 1b**) without loss of 3D printing quality [5], hence paving the way for more efficient fabrication of high-fidelity 3D nanoarchitectures.

[1] R. Winkler et al.; *3D nanoprinting via focused electron beams*; J. Appl. Phys. 125, 210901 (2019),.

[2] L. Hirt et al.; *Additive Manufacturing of Metal Structures at the Micrometer Scale*; Adv. Mater. 29, 1 (2017).

[3] J. M. De Teresa et al.; *Comparison between Focused Electron/Ion Beam-Induced Deposition at Room Temperature and under Cryogenic Conditions*; Micromachines 10, 799 (2019).

[4] E. Mutunga et al.; *Impact of Electron-Beam Heating during 3D Nanoprinting*; ACS Nano 13, 5198 (2019).

[5] J. Hinum-Wagner et al.; *FEBID 3D-Nanoprinting at Low Substrate Temperatures: Pushing the Speed While Keeping the Quality*; Nanomaterials 11, 1527 (2021).

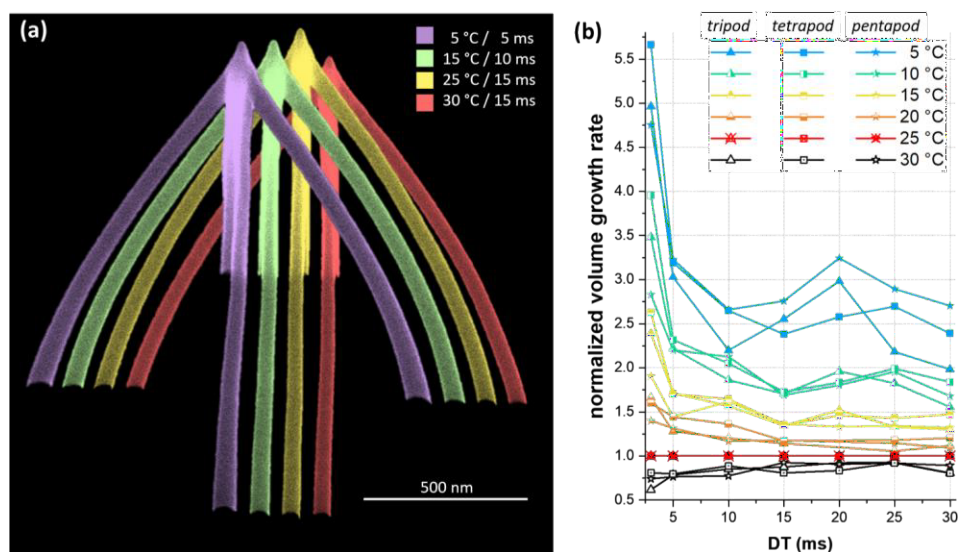


**Figure 1.** (a) The collage of FEBID-tetrapods - fabricated at substrate temperatures of 5 °C, 15 °C, 25 °C, and 30 °C and different process times - demonstrates that the shape fidelity is maintained. (b) Dwell-time dependent volume growth rates for different substrate temperatures (see legend), normalized to 25 °C for tri-, tetra-, and pentapods (see symbols), shows that the growth rates are boosted for lower substrate temperatures.

# Electron beam induced deposition of and dissociative ionization and Tetrakis(dimethylamino)silane, a potential precursor for silicon nitride deposition

Reza Tafrishi<sup>1</sup>, Maicol Cipriani<sup>1</sup>, Armin Gölzhäuser<sup>2</sup> and Oddur Ingólfsson<sup>1,\*</sup>

<sup>1</sup> Science Institute and Department of Chemistry, University of Iceland, Dunhagi 3, 107 Reykjavik, Iceland

<sup>2</sup> Faculty of Physics, Bielefeld University, 33615 Bielefeld, Germany

\* email: [odduring@hi.is](mailto:odduring@hi.is)

Here we present a study on the reactivity of tetrakis(dimethylamino)silane (TKDMAS) towards low-energy electrons in the gas phase and the composition of deposits created by Focused Electron Beam Induced Deposition (FEBID) of this precursor. This study was motivated by the use of TKDMAS to produce silicon nitride-based deposits and its potential as a precursor for FEBID.

Although there was no evidence of the formation of negative ions by dissociative electron attachment (DEA), there was clear evidence of considerable fragmentation during dissociative ionization (DI). The appearance energies of the fragments generated in DI, were determined and compared to the respective threshold energies calculated at the DFT and coupled-cluster (CC) levels of theory. This comparison reveals that hydrogen transfer processes and rearrangement reactions play a significant role in DI of TKDMAS under single collision conditions. Such reactions are generally slow and may be influenced more strongly at surfaces than direct, faster dissociation processes with less time for relaxation through energy transfer to the substrate.

In DI the average carbon and nitrogen loss per incidence was found to be about 3 and 1.5, respectively, while the C : O : Si : N composition of the deposits created with FEBID were found to be 58.6 : 23.5 : 9.4 : 8.5. This translates to an average loss of 2 carbons and 3 nitrogen per molecule. Hence, a significantly higher nitrogen loss than reflected in the gas phase DI study.

Further electron exposure in the presence of water lowered the carbon content but increased the oxygen content, resulting in a deposit C : O : Si : N composition of 40.6 : 34.5 : 13.6 : 11.3. For comparison FEBID deposits from tetraethyl orthosilicate (TEOS) were also treated with post deposition electron irradiation in the presence of water. For TEOS, however, no significant composition change was observed after the application of this purification protocol.

It is clear from this study that electron induced decomposition pathways of TKDMAS are already complex under single collision conditions and these are changed significantly in electron induced deposition at a surface. We anticipate that residual water in the HV FEBID experiments may play an important role in the deposition process as is evident in the high oxygen content in the original deposits and the effective carbon removal in post deposition purification through further electron exposure in the presence of water.



# Low-energy electron induced fragmentation of cis-PtBr<sub>2</sub>(CO)<sub>2</sub>

Maicol Cipriani<sup>1</sup>, Styrmir Svavarsson<sup>1</sup>, Filipe Ferreira da Silva<sup>2</sup>, H. Lu<sup>3</sup>, Lisa McElwee-White<sup>3</sup> and Oddur Ingólfsson<sup>1,\*</sup>

<sup>1</sup> Department of Chemistry and Science Institute, University of Iceland, Dunhagi 3, 107 Reykjavik, Iceland

<sup>2</sup> CEFITEC, Departamento de Física, Faculdade de Ciências e Tecnologia, Universidade NOVA de Lisboa, 2829-516 Caparica, Portugal

<sup>3</sup> Department of Chemistry, University of Florida, Gainesville, FL 32611-7200, USA

\* email: [odduring@hi.is](mailto:odduring@hi.is)

Platinum coordination complexes with low-carbon ligand structure are interesting to explore for their potential as precursors for platinum deposition in focused electron beam induced deposition (FEBID). Preferably such precursors fragment extensively in their electron induced dissociation and generate a high metal content deposits while ligands are fragmented from the metal and desorbed from the surface. Low-energy secondary electrons (LEE) play an important role in this process and the induced fragmentation pathways determine the deposits composition.

In the current contribution, we present a combined experimental and theoretical study on the role of low energy interactions in the fragmentation of the Pt(II) coordination compound cis-PtBr<sub>2</sub>(CO)<sub>2</sub>, and we compare our results with a previous gas phase study on low energy interaction with the analogue compound cis-PtCl<sub>2</sub>(CO)<sub>2</sub> [1], with a UHV surface science study [2] and a comparative UHV and HV FEBID study [3] on these compounds.

The main fragments produced through DEA to PtBr<sub>2</sub>(CO)<sub>2</sub> reflect the loss of one and two CO ligands, while the loss of one Br after the loss of one and two CO as well as the formation of the Br anion are minor channels with ion yields that are two orders of magnitude lower than those for carbonyl loss. Hence the CO loss dominates in DEA and we find the effective CO loss per incident to be about 1.4, while the Br loss is negligible.

In contrast to DEA, dissociative ionization also leads to appreciable Br loss and all fragmentation pathways are present in the DI spectrum. The parent cation is the most intense cation fragment as well as [PtBr]<sup>+</sup> and the formation of the bare Pt ion also are observed with considerable intensity. For DI we find the average CO loss per incident to be about 0.7, while the average Br loss per incident is found to be about 0.3.

In UHV FEBID [3] and in a UHV surface study [2] on Pt(CO)<sub>2</sub>Cl<sub>2</sub> and Pt(CO)<sub>2</sub>Br<sub>2</sub> these compounds were found to decompose by rapid CO loss leading to a PtCl deposition with the 1:2 stoichiometric ratio. This is in good agreement with the DEA results, while DI would be expected to lead to significant halogen loss from the surface. Different from UHV FEBID, HV FEBID [3] leads to deposits with high carbon content but as good as no halogen content. We expect that this significant difference in deposits content under UHV and HV may be attributed to the presence of surface water under HV conditions, that leads to hydrogen halide formation and desorption.

[1] F. Ferreira da Silva, R. M. Thorman, R. Bjornsson, H. Lu, L. McElwee-White, O. Ingólfsson; *Dissociation of the FEBID precursor cis-Pt(CO)<sub>2</sub>Cl<sub>2</sub> driven by low-energy electrons*; Phys. Chem. Chem. Phys. 2020, 22, 6100-6108

[2] J. A. Spencer, L. McElwee-White, D. H. Fairbrother; *Electron Induced Surface Reactions of cis-Pt(CO)<sub>2</sub>Cl<sub>2</sub>: A Route to Focused Electron Beam Induced Deposition of Pure Pt Nanostructures*; J. Am. Chem. Soc. 2016, 138(29), 9172–9182

[3] A. Mahgoub, H. Lu, R. M. Thorman, K. Preradovic, T. Jurca, L. McElwee-White, D. H. Fairbrother, C. W. Hagen; *Electron beam-induced deposition of platinum from Pt(CO)<sub>2</sub>Cl<sub>2</sub> and Pt(CO)<sub>2</sub>Br<sub>2</sub>*; Beilstein J. Nanotechnol. 2020, 11, 1789–1800.

# On the low energy electron induced dissociations to a potential gold precursor for FEBID technique; A gas-phase study

A. Kamali<sup>1</sup>, E. Bilgiliyoy<sup>2</sup>, A. Wolfram<sup>2</sup>, T. Gentner<sup>3</sup>, G. Ballmann<sup>3</sup>, S. Harder<sup>3</sup>, H. Marbach<sup>2</sup>, O. Ingólfsson<sup>1,\*</sup>

<sup>1</sup> Science Institute and Department of Chemistry, University of Iceland, Dunhagi 3, 107 Reykjavík, Iceland

<sup>2</sup> Physikalische Chemie II, Friedrich-Alexander Universität Erlangen-Nürnberg, 91058 Erlangen, Germany

<sup>3</sup> Inorganic and Organometallic Chemistry, Universität Erlangen-Nürnberg, 91058 Erlangen, Germany

\* email: [odduring@hi.is](mailto:odduring@hi.is)

As focused electron beam induced deposition (FEBID) of metallic structures mainly relies on organometallic precursors, its applicability for writing functional nanostructures, e.g. with well defined magnetic or conductive properties, is critically dependent on the precursors decomposition under the electron beam. Preferably such precursors have fairly high vapour pressure, are stable under ambient conditions but decompose completely under the electron beam. Gold precursors for high purity gold deposition in FEBID are precursors that have significant potential in number of applications and the potential of extending the applicability of this nanotechnology writing method [1, 2].

Here we present a study on one such precursor; Methylgold(I) trimethyl-phosphine,  $(\text{CH}_3)\text{AuP}(\text{CH}_3)_3$ , and in context to the role of low energy secondary electrons in the deposition process [3, 4], we have studied dissociative ionization of this precursor under single collision conditions in the gas phase as well as its performance in FEBID under UHV conditions. We have determined the appearance energies for individual fragmentation processes and calculated the respective thresholds at the TPSS/def2-TZVP and DLPNO-CCSD(T)/QZVPP levels of theory to aid the interpretation of the underlying fragmentation processes. Further, ion yield curves were recorded for individual fragments and used to derive the average carbon and phosphor loss per DI incident in comparison to the FEBID deposit composition. The performance of this precursor is evaluated with respect to its stability and volatility and the deposits composition is determined by means of Auger electron spectroscopy.

In a previous FEBID study on this precursor under HV conditions, by Van. Dorp et al. [5], the deposits fabricated were found to consist of 19-25 at. % Au, 54-62 at. % C, and 2-7 at. % P. We find that the gold content is increased considerably under UHV conditions and that the underlying fragmentation pathways are markedly different. In general we find Methylgold(I) trimethyl-phosphine to be a suitable precursor with respect to handling, stability and volatility and suitable for the production of fairly high gold content depositions.

[1] I. Utke, P. Hoffmann, B. Dwir, K. Leifer, E. Kapon, P. Doppelt; *Focused Electron Beam Induced Deposition of Gold*; J. Vac. Sci. Technol., B: Microelectron. Nanometer Struct.Process., Meas., Phenom., Vol. 18, 3168 (2000).

[2] I. Utke, P. Hoffmann, J. Melngailis; *Gas-Assisted Focused Electron Beam and Ion Beam Processing and Fabrication*; J. Vac. Sci. Technol., B: Microelectron. Nanometer Struct.Process., Meas., Phenom., Vol. 26, 1197 (2008).

[3] N. Silvis-Cividjian, C. W. Hagen, L. H. A. Leunissen, P. Kruit, *The role of secondary electrons in electron-beam-induced-deposition spatial resolution*; Microelectron. Eng. 2002, 61–62, 693–699.

[4] A. Botman, D. A. M. de Winter, J. J. L. Mulders; *Electron-beam-induced deposition of platinum at low landing energies*; J. Vac. Sci. Technol., B: Microelectron. Nanometer Struct. Process., Meas., Phenom. 2008, 26, 2460–2463..

[5] W. Van Dorp, X. Wu, J. Mulders, S. Harder, P. Rudolf, J. De Hosson; *Gold Complexes for Focused-Electron-Beam-Induced Deposition*; Langmuir, Vol. 30, 12097 (2014).

# Single Source Precursors in FEBID and FIBID: Similarities and Differences for CoSi<sub>x</sub> Deposition

F. Jungwirth<sup>1</sup>, F. Porrati<sup>1</sup>, D. Knez<sup>2,3</sup>, H. Plank<sup>2,3</sup>, M. Huth<sup>1</sup>, S. Barth<sup>1,\*</sup>

<sup>1</sup> Goethe University Frankfurt, Physical Institute, Max-von-Laue-Str. 1, 60438, Frankfurt, Germany

<sup>2</sup> Graz University of Technology, Institute of Electron Microscopy and Nanoanalysis, Steyrergasse 17, 8010, Graz, Austria

<sup>3</sup> Graz University of Technology, Christian Doppler Laboratory for Direct-Write Fabrication of 3D Nano-Probes (DE-FINE), Institute of Electron Microscopy, Steyrergasse 17, 8010, Graz, Austria

\* email: [barth@physik.uni-frankfurt.de](mailto:barth@physik.uni-frankfurt.de)

One of the main challenges currently encountered in focused electron (FEBID) and ion beam induced deposition (FIBID) is the availability of suitable precursor molecules for desired material compositions [1]. Besides the deposition of single metal deposits, the deposition of binary materials with defined stoichiometry is very challenging. An attractive approach to simplify the challenging task for metal silicides is the use of heterometallic precursors which already possess the desired constituent stoichiometry. This contribution compares two precursors for the FEBID/FIBID deposition of CoSi<sub>x</sub>-based materials of predefined composition, H<sub>3</sub>SiCo(CO)<sub>4</sub> and H<sub>2</sub>Si(Co(CO)<sub>4</sub>)<sub>2</sub>.

Compositional analysis via EDX shows significant differences in the FEBID and FIBID-derived materials. FEBID yields deposits with intermediate Co + Si contents of ~55-60 at% for both precursors under retention of the Co:Si ratio predefined in the precursor molecules [2]. In contrast, FIBID derived deposits show a significantly higher metal content of up to 87 at%. However, influences on compositional variations in FIBID can be observed and explained by process-related fundamentals [3].

The temperature-dependent electrical measurements indicate that the "Co<sub>2</sub>Si"-precursor derived FEBID materials are granular metals, while the FIBID material shows semi-metallic behavior. Moreover, significant differences of the electron and ion beam derived deposits can be observed in magnetotransport properties [1, 2].

Acknowledgment: S.B. acknowledges generous financial support from the Deutsche Forschungsgemeinschaft (DFG, German Research Foundation) project 413940754 and 413942347.

[1] S. Barth, M. Huth, F. Jungwirth; *Precursors for direct-write nanofabrication with electrons*; J. Mater. Chem. C 8, 15884 (2020).

[2] F. Jungwirth, F. Porrati, A. G. Schuck, M. Huth, S. Barth; *Direct Writing of Cobalt Silice Nanostructures Using Single-Source Precursors*; ACS Appl. Mater. Interf. 13, 48252 (2021).

[3] F. Jungwirth, F. Porrati, D. Knez, H. Plank, M. Huth, S. Barth; *in preparation*.

# Investigation of volatile products of electron beam interaction with solids and adsorbed phase via mass spectrometry methods

Jakub Jurczyk<sup>1,\*</sup>, Lex Pillatsch<sup>2</sup>, Luisa Berger<sup>3</sup>, Agnieszka Priebe<sup>3</sup>, Katarzyna Madajska<sup>4</sup>, Czesław Kapusta<sup>5</sup>, Iwona Barbara Szymańska<sup>4</sup>, Johann Michler<sup>3</sup> and Ivo Utke<sup>3</sup>

<sup>1</sup> Institute of Nanoscience and Materials of Aragon – CSIC, Edif. I+D, C/ Mariano Esquillor Gómez, 50018 Zaragoza, Spain

<sup>2</sup> TOFWERK AG, Schorenstrasse 39, CH-3645 Thun, Switzerland

<sup>3</sup> Empa - Swiss Federal Laboratories for Materials Science and Technology, Laboratory for Mechanics of Materials and Nanostructures, Feuerwerkerstrasse 39, CH - 3602 Thun, Switzerland

<sup>4</sup> Faculty of Chemistry, Nicolaus Copernicus University in Toruń, Gagarina 7, 87-100 Toruń, Poland

<sup>5</sup> AGH University of Science and Technology, Faculty of Physics and Applied Computer Science, Al. Mickiewicza 30, 30-059 Kraków, Poland

\* email: [jakub.jurczyk@unizar.es](mailto:jakub.jurczyk@unizar.es)

The recent advances in methods of nanomanufacturing using focused electron beam (FEB), such as focused electron beam induced deposition (FEBID) or ice lithography, induce a strong demand for developing analytical methods, which would allow the products of electron-induced fragmentation of different metalorganic and organometallic compounds to be assessed. The methods used up to now provide information about the interactions of the electrons only with gaseous or condensed phase compounds in UHV [1]. However useful, the conditions of both gas phase and condensed phase measurements are usually significantly different than conditions of FEBID measurement. Hence, the certain discrepancies between the information provided by these two methods and electron beam induced processing in HV can be observed [2, 3].

In this work, for the first time FEB is combined with time-of-flight secondary ion mass spectrometry (TOF-SIMS). This allowed us to monitor the volatile, charged products of irradiation of both solid state and physisorbed molecules. To the best of our knowledge, this has never been achieved before. The ionized fragments, formed at the focus spot of the electron beam on the surface, are electrostatically channelled from the scanning electron microscope (SEM) chamber towards a time-of-flight mass spectrometer (TOF-MS), enabling for spatial in-situ mass spectra acquisition. FEBiMS is a progression of focused ion beam secondary ion mass spectrometry (FIBSIMS) [4]. In this work, the results obtained during irradiation of various organometallic compounds, both in solid state and also gaseous molecules adsorbed on the surface, are presented.

The proposed method provides new insight in electron-induced fragmentation processes, which is important for beam lithography methods, such as FEBID, electron lithography or ice lithography.

[1] R. M. Thorman, P. A. Jensen, J.-C. Yu, S. J. Matsuda, L. McElwee-White, O. Ingólfsson, and D. H. Fairbrother, *The Journal of Physical Chemistry C* 124, 10593 (2020).

[2] J. A. Spencer, J. A. Brannaka, M. Barclay, L. McElwee-White, and D. H. Fairbrother, *The Journal of Physical Chemistry C* 119, 15349 (2015).

[3] J. Jurczyk, C. R. Brewer, O. M. Hawkins, M. N. Polyakov, C. Kapusta, L. McElwee-White, and I. Utke, *ACS Applied Materials & Interfaces* 11, 28164 (2019).

[4] L. Pillatsch, F. Östlund, and J. Michler, *Progress in Crystal Growth and Characterization of Materials* 65, 1 (2019).

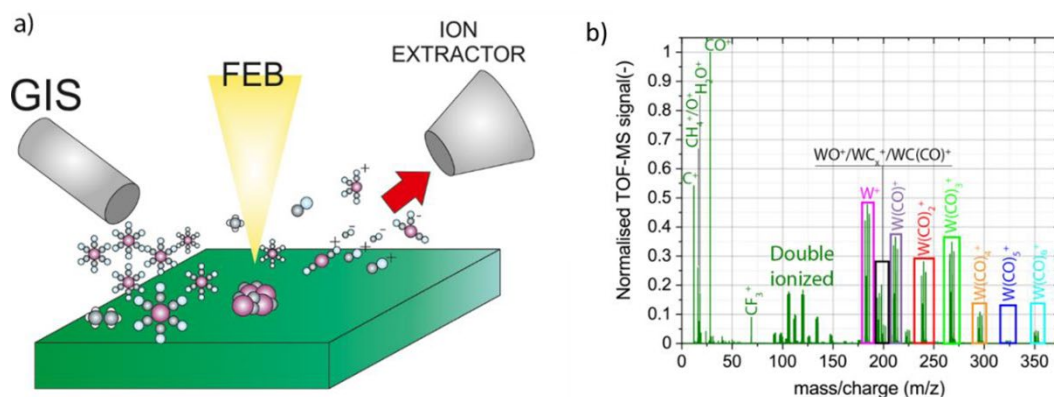


**Figure 1.** a) Schematic depiction of FEBiMS experiment: the precursor molecules are delivered via gas injection system (GIS) and dissociated with focused electron beam (FEB), while ion extractor (TOF-MS) collects the volatile charged moieties leaving the substrate. b) Positive ion mass spectrum obtained during the FEBiMS measurement using  $W(CO)_6$

# Characterisation of Direct-Write 3D Cobalt Iron Magnetic Nanostructures with Curved Geometries

S. Lamb-Camarena<sup>1,2,\*</sup>, Q. Wang<sup>1</sup>, F. Porrati<sup>3</sup>, M. Huth<sup>3</sup>, M. Urbánek<sup>4</sup>, A. Chumak<sup>1</sup>, O. Dobrovolskiy<sup>1</sup>

<sup>1</sup> University of Vienna, Nanomagnetism and Magnonics, Boltzmanngasse 5, 1090 Vienna, Austria

<sup>2</sup> University of Vienna, Vienna Doctoral School in Physics, Boltzmanngasse 5, 1090 Vienna, Austria

<sup>3</sup> Physikalisches Institut, Goethe-Universität, Max-von-Laue-Str. 1, 60438 Frankfurt am Main, Germany

<sup>4</sup> CEITEC BUT, Brno University of Technology, Brno 61200, Czech Republic

\* email: [sebastian.lamb-camarena@univie.ac.at](mailto:sebastian.lamb-camarena@univie.ac.at)

The fabrication of magnonic structures with arbitrary 3D geometry including geometric curvature on characteristic magnetic length scales has only been made possible in the past few years by advances in direct write focused electron beam induced deposition (FEBID) techniques [1, 2]. The small size of the structures that were produced by FEBID and the rich novel phenomenology induced by the structures' geometric curvature motivates the use of optical probe methods to address their magnetic characteristics and magnonic behaviour due to their significant flexibility in setup and probing configurations, this has been realised through the use of Brillouin light scattering (BLS) and magneto-optic Kerr effect (MOKE) techniques. The material properties of the FEBID magnonic structures are distinct from materials achievable through physical vapour deposition and other methods [3], the characterisation of these properties is foundational for further research into the spin wave propagation characteristics and curvature induced effects on signal propagation [4, 5]. We aim to leverage this for design of tailored structures for spin-wave signal processing.

[1] D. Makarov, O. M. Volkov, A. Kakay et al.; *New Dimension in Magnetism and Superconductivity: 3D and Curvilinear Nanoarchitectures*; *Adv. Mater.* 34, 2101758 (2022).

[2] A. Fernandez-Pacheco, L. Skoric, J. M. De Teresa et al.; *Writing 3D Nanomagnets Using Focused Electron Beams*; *Materials* 13, 3774 (2020).

[3] F. Porrati, M. Pohlitz, J. Müller et al.; *Direct writing of CoFe alloy nanostructures by focused electron beam induced deposition from a heteronuclear precursor*; *Nanotechnology* 26, 475701 (2015).

[4] O. Dobrovolskiy, R. Sachser, S. A. Bunyaev et al.; *Spin-Wave Phase Inverter upon a Single Nanodefekt*; *ACS Appl. Mater. & Inter.* 11, 17654–17662 (2019).

[5] O. Dobrovolskiy, N. Vovk, A. Bondarenko et al.; *Spin-wave eigenmodes in direct-write 3D nanovolcanoes*; *Appl. Phys. Lett.* 118, 132405 (2021).

# Study of key processes for finding new FEBID precursors

Katarzyna Madajska<sup>1</sup>, Iwona B. Szymańska<sup>1,\*</sup>

<sup>1</sup> Faculty of Chemistry, Nicolaus Copernicus University in Toruń, Gagarina 7, 87-100 Toruń, Poland

\* email: pola@umk.pl

Gas assisted focused electron beam induced deposition (FEBID) is nanostructuring technique that is employed in electron microscopes to obtain metallic nanostructures with complex shapes in a simple, one-step process. Due to the high requirements for the precursor: adequate volatility, stability and also decomposition under the influence of the electron beam, problems still persist in obtaining materials consisting only of metal. Pure structures have been fabricated for several elements, however, frequently used precursors are toxic or rapidly decompose under the influence of oxygen or moisture in the air. So far, both fluorinated and branched-chain silver carboxylates have been used in the FEBID process, obtaining structures with a purity of 59-76 at.% Ag. On the other hand, using copper(II) carboxylate [Cu<sub>2</sub>(O<sub>2</sub>CC<sub>2</sub>F<sub>5</sub>)<sub>4</sub>], a purity of 23 at.% Cu was achieved. This shows that research is still needed to understand the interaction of compounds with electrons in order to select the appropriate ligands for FEBID precursors [1–3].

Therefore, it was decided to investigate the influence of the coordination center (Cu, Ag) and O, O-, N, N-, and N, O-donor ligands (**Figure 1**) on the volatility of the potential precursors and their decomposition under the influence of low- and high-energy electrons. Heteroleptic complexes containing two secondary ligands were also tested.

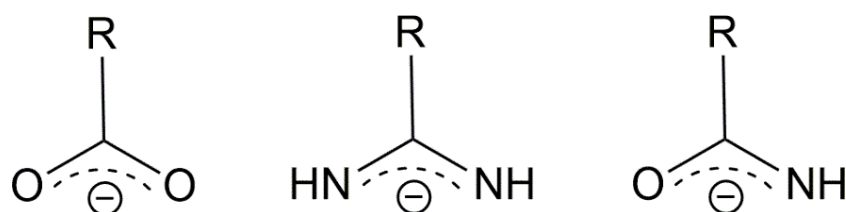


**Figure 1.** Structure of deprotonated ligands. From left to right: carboxylate, amidinate, amidate, R = perfluorinated group

Volatility studies such as electron ionization mass spectrometry, variable temperature infrared spectroscopy, thermal analysis, and sublimation experiments have shown that the new compounds can enter the gas phase without decomposition. High intensity signals of molecular ions are observed in electron impact mass spectrometry for thermally stable compounds. To initially assess the sensitivity of complexes to the high-energy electron beam, observations were made using a scanning electron microscope (SEM, 20 keV) and a transmission electron microscope (TEM, 200 keV).

The study showed that volatility and electron beam sensitivity are influenced by both the coordination center and the used ligands. Interestingly, compounds that are more thermally stable are less sensitive to low- and high-energy electrons. Among the studied compounds, the heteroleptic complex [Cu<sub>2</sub>(=NHNH<sub>2</sub>C<sub>2</sub>F<sub>5</sub>)<sub>2</sub>(μ-O<sub>2</sub>CC<sub>2</sub>F<sub>5</sub>)<sub>4</sub>] demonstrates the best parameters. The reaction between ligands induced by interaction with electrons is observed, which affects the further dissociation process.

[1] I. Utke, P. Swiderek, K. Höflich, K. Madajska, J. Jurczyk, P. Martinović, I. B. Szymańska; *Coordination and organometallic precursors of group 10 and 11: Focused electron beam induced deposition of metals and insight gained from chemical vapour deposition, atomic layer deposition, and fundamental surface and gas phase studies*; *Coordination Chemistry Reviews*, 458, 213851 (2022).

[2] S. Barth, M. Huth, F. Jungwirth; *Precursors for direct-write nanofabrication with electrons*; *J. Mater. Chem. C*, 8, 15884 (2020).

[3] I. Utke, P. Hoffmann, J. Melngailis; *Gas-assisted focused electron beam and ion beam processing and fabrication*; *J. Vac. Sci. Technol. B*, 26, 1197–1276 (2008).

# 3D Hollow Cone Nanoprobes for Electric AFM Applications

L. M. Seewald<sup>1</sup>, R. Winkler<sup>1</sup>, M. Brugger-Hatzl<sup>2</sup>, G. Kothleitner<sup>2,3</sup> and H. Plank<sup>1,2,3,\*</sup>

<sup>1</sup> Christian Doppler Laboratory – DEFINE, Graz University of Technology, 8010 Graz, Austria

<sup>2</sup> Institute of Electron Microscopy and Nanoanalysis, Graz University of Technology, 8010 Graz, Austria

<sup>3</sup> Graz Centre for Electron Microscopy, 8010 Graz, Austria

\* email: [harald.plank@felmi-zfe.at](mailto:harald.plank@felmi-zfe.at)

Since its introduction decades ago, Atomic Force Microscopy (AFM) evolved into a central characterization technology in many scientific areas. As Abbe's limit of diffraction is omitted by the use of a very sharp probe which is scanned across a sample, Scanning Probe Microscopy techniques paved the way towards new insights and innovative applications in research and development. Moreover, AFM is not restricted to probe the topography of a sample only, but enables simultaneous mapping of a variety of surface properties, such as mechanical, electrical, chemical, magnetic or thermal, in a laterally resolved manner with nanometer resolution. Those advanced operation modes, however, require functionalized probes, which are often based on standard Si tips and further coated with relevant materials to induce intended functionalities. Aside of larger apex radii, reducing resolution capabilities, such coatings are often prone to delamination effects due to mechanical stress during AFM operation, which reduce or even eliminate the targeted sensitivity. Consequently, functional nanoprobes without any coatings would be desired, while revealing tip apices in the sub-10 nm regime. A perfectly suited fabrication technique able to tackle those challenges is focused electron beam induced deposition (FEBID) [1]. It offers an unrivaled flexibility in terms of geometrical complexity and structural delicacy and poses little requirements to substrate material and surface morphology. In addition, post-growth treatments allow accurate tailoring of material's properties towards the intended application [2]. Thus, FEBID is perfectly applicable for the fabrication or modification of AFM probes on pre-structured cantilevers or pre-existing tips, respectively [3]. With this motivation in mind, we here present a Pt-based 3D hollow-cone concept for application in electrical AFM modes (CAFM, EFM, KFM). We start with fabrication on pre-structured AFM cantilevers (**Fig.1a**) and the chemical transfer into pure Pt structures (**Fig.1b**). That includes design optimization to maximize mechanical rigidity, indispensably required for AFM operation, while apices in the sub-10 nm regime are achieved on a regular basis (inset in **Fig.1b**). We then present the performance and advantages compare to commercially available standard probes, as representatively shown by resolution comparison in **Fig.1c** and **1d**. Finally, we present selected CAFM and EFM results, which further underline the advantages of such FEBID-based nanoprobes. Together with the fact, that those concepts are meanwhile patented together with our industrial partners, this contribution clearly shows the relevance of 3D-FEBID in the area of Atomic Force Microscopy.

[1] Winkler et al; *3D nanoprining via focused electron beams*; J. Appl. Phys. 125, 210901 (2019)

[2] Geier et al.; *Rapid and Highly Compact Purification*; J. Phys. Chem. C 118, 14009 (2014)

[3] Plank et al.; *Focused Electron Beam-Based 3D Nanoprining for Scanning Probe Microscopy: A Review*; Micromachines 11, 48 (2020)

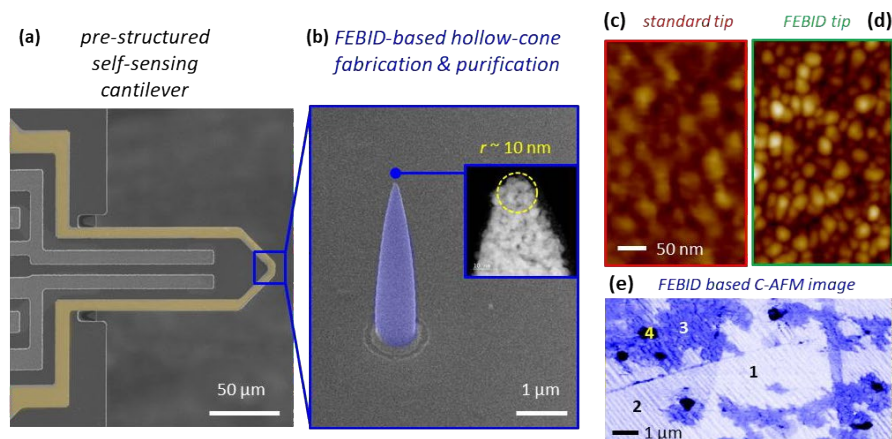


**Figure 1.** (a) shows a pre-structured AFM cantilever, which was first equipped with a PtC hollow-cone (b), further transferred into pure Pt with apex radii in the sub-10 nm regime (inset in b). (c) and (d) gives a direct AFM height comparison between commercially available C-AFM probes and the here relevant hollow-cones, respectively, which clearly shows the improved lateral resolution. (e) is a representative CAFM image, which enabled clear identification of a single-layer (1) and multi-layer graphene (2), copper oxide particles (3) and insulating Antimon particles (4) and proves CAFM applicability.



# Towards Nanoscale 3D Printing with Ice Lithography

Affan K. Waafi<sup>1,\*</sup>, Joachim Lyngholm-Kjærby<sup>1</sup>, Hoa T. Lee<sup>1</sup>, Rubaiyet I. Haque<sup>1</sup>, Giuliano Bissaco<sup>1</sup>, Anpan Han<sup>1</sup>

<sup>1</sup> Technical University of Denmark, Dept. of Civil & Mechanical Engineering, 2800 Kongens-Lyngby, Denmark

\* email: [afkawa@mek.dtu.dk](mailto:afkawa@mek.dtu.dk)

Micro and nanoscale 3D printing enabled the advancement of novel technologies, such as microfluidics, biomedical implants, nanophotonics, etc. In this project, we establish a novel approach for nanoscale 3D printing using the 3D Ice Lithography (3D IL) process [1, 2] (**Fig. 1**). In 3D IL, the structure is made by injecting precursor gas onto a cryogenically cooled substrate, which immediately freezes the precursor into a thin film of ice. Electron beam exposure is performed on the user-defined areas of the ice to trigger cross-linking, which forms robust molecular networks. A 3D structure can be built layer-by-layer by repeating this sequence, which stays stable after the remaining ice is evaporated at the end of the process [2].

To realize a 3D printing process based on 3D IL process, each process-step must be integrated and controlled based on the user input in the form of 3D structure object. This is very different from 2D lithography. We built on top of the established 3D printing process based on g-code. The 3D IL design process consists of three process steps. (i) the desired 3D object is designed and drawn using a CAD program. (ii) The CAD file is converted to a stereolithography file format (STL). (iii) Using readily available 3D printing slicer software, the 3D design is sliced into its respective layer based on the user specification. Within each layer, the structure is broken down into coordinates, then grouped into g-code commands containing starting and endpoints of exposure paths. The layer thickness is encoded in the g-code coordinates. The exposure paths in the g-code are reconstructed into an exposure map by filling in the pixels between the starting and endpoints. The exposure within a pixel is controlled by defining the exposure dose as,  $Q_A = \frac{I_b * t}{A}$ . Here,  $Q_A$  is the area dose (mC/cm<sup>2</sup>),  $I_b$  is the beam current (mA), and  $t$  and  $A$  are the dwell time (s) and the area (cm<sup>2</sup>) of each pixel, respectively.

The process and control electronics are implemented using NI components and Labview. Given G-code as input, the software takes control of the SEM scan coils, SEM focus, and the automatic GIS and carries out 3D IL. **Figure 1** shows the process of manufacturing a 3-layer half-ring structure. Starting with drawing the object with a 1000:1 scale to comply with the slicing program resolution, e.g., a 1 μm feature is drawn as 1 mm. The g-code file is uploaded to our homebrewed 3D printing control program, which rescales the structure back to its correct size and constructs exposure maps with 50 x 50 nm<sup>2</sup> pixel size. We printed the final 3D structure out of W(CO)<sub>6</sub> precursor utilizing our 3D IL system [3], with 5 KeV beam acceleration voltage and exposure dose of 10 mC/cm<sup>2</sup>, resulting in 100 nm layer thickness.

[1] A. Han et al.; *Ice lithography for nanodevices*; Nano Letter vol. 10, (2010). doi: 10.1021/nl1032815.

[2] W. Tiddi et al.; *Organic Ice Resists*; Nano Letter vol. 17, (2017). doi: 10.1021/acs.nanolett.7b04190.

[3] R. I. Haque et al.; *80 K cryogenic stage for ice lithography*; Micro Nano Engineering vol. 14, p. 100101 (2022). doi: 10.1016/j.mne.2021.100101.

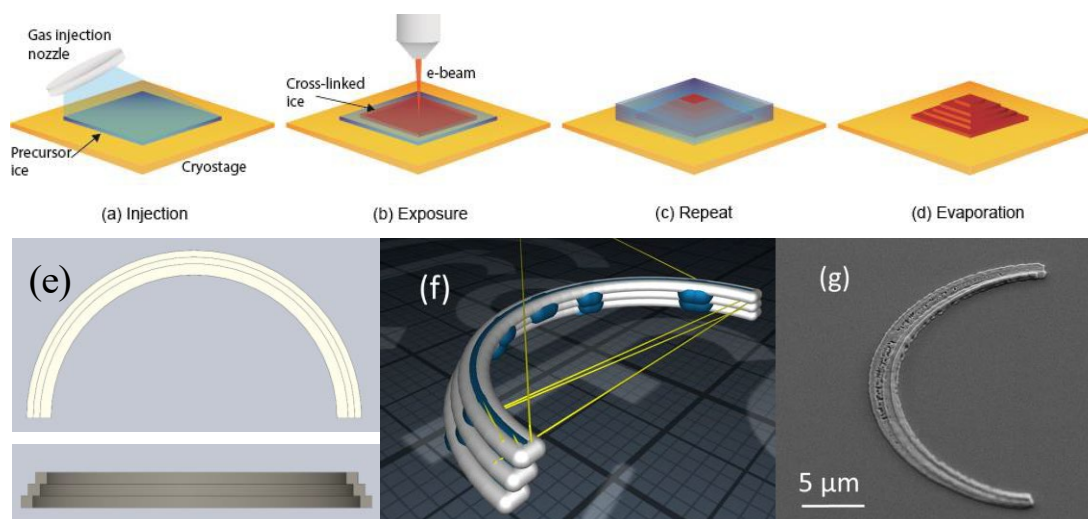


**Figure 1.** 3D IL process; The precursor gas is injected onto a pre-cooled substrate to deposit an ice layer (a). E-beam exposure on certain area crosslinks the precursor into solid pattern (b). Repetition of injection and exposure to build more layers (c). Finally, cryostage is heated up to remove the residual ice (d). Step-by-step of nanoscale 3D printing process utilizing 3DIL technique, starting with drawing the print object (e), slicing the 3D object into exposure path in g-code format (f), and the final product of nanoscale 3D printing using 3D IL (g).

# Controlled Bending of 3D-Nanoprinted Structures via Electron Beam Curing

A. Weitzer<sup>1,\*</sup>, L. Seewald<sup>2</sup>, D. Kuhness<sup>2</sup> and H. Plank<sup>1,2,3</sup>

<sup>1</sup> Institute of Electron Microscopy and Nanoanalysis, Graz University of Technology, 8010 Graz, Austria

<sup>2</sup> Christian Doppler Laboratory - DEFINE, Graz University of Technology, 8010 Graz, Austria

<sup>3</sup> Graz Centre for Electron Microscopy, Steyrergasse 17, 8010 Graz, Austria

\* email: [anna.weitzer@felmi-zfe.at](mailto:anna.weitzer@felmi-zfe.at)

Additive manufacturing via Focused Electron Beam Induced Deposition (FEBID) is an increasingly relevant technique for depositing high-fidelity architectures on the nanoscale. While most such structures in the past were of a meshed nature [1], recent developments towards building closed (sheet-like) elements have opened up the field for a whole new range of possibilities [2]. In a next step we now explored post-growth electron beam curing (EBC) [3], where the structures are locally irradiated without precursor gas present. This process impacts the inner structure and the overall volume of exposed elements and, if only applied partially, enables controlled deformation. We therefore performed experimental series, analyzed via SEM and TEM and complemented by Monte Carlo Simulations to explore and identify ideal parameters for smooth, stable and reproducible morphological bending. **Figures 1a** and **1b** show a vertical wall with a width of 1  $\mu\text{m}$  and a height of 2  $\mu\text{m}$  that was bent via electron beam irradiation within a defined area across the structure. **Figure 1c** shows a more complex (originally straight) screw element where two areas have been exposed to EBC, clearly illustrating the bending effect towards the incidence direction. We attribute this “forward” bending to smaller interaction volumes of the incoming electrons compared to the wall thickness mainly influencing the front part of the elements in comparison with the back side. We evaluated the impact for a variety of parameters, such as voltage, point pitch, dwell time, overall dose and bending angle to achieve controlled and reproducible results. The expansion to more complex EBC pattern leads furthermore to more complex bending as will be presented as well. We thereby extended the post-growth treatment possibilities of FEBID, showing the flexibility of EBC for various applications in research and development, some of which clearly go beyond the capabilities of sole 3D FEBID (e.g. spatially tuned mechanics).

[1] R. Winkler et al.; *3D nanoprinting via focused electron beams*; Journal of Applied Physics 125, 210901 (2019).

[2] A. Weitzer et al.; *Expanding FEBID-Based 3D-Nanoprinting toward Closed High-Fidelity Nanoarchitectures*; ACS Applied Electronic Materials, 4 (2), 744 (2022).

[3] F. Porrati et al.; *Tuning the electrical conductivity of Pt-containing granular metals by postgrowth electron irradiation*; Journal of Applied Physics 109, 063715 (2011).

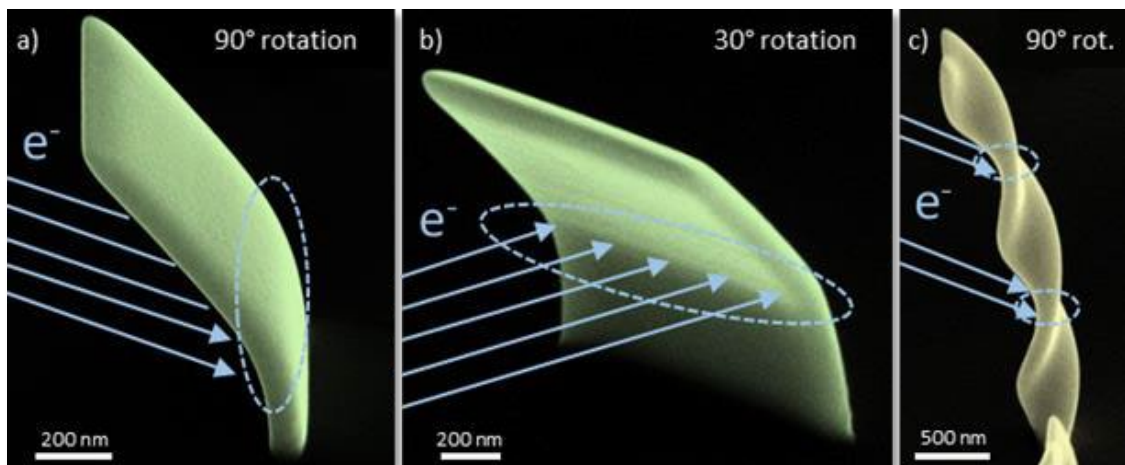


**Figure 1.** Bending of sheet-like 3D FEBID elements. Bent wall from a side angle (a) and from a 30° rotated point of view (b) and twofold bent screw structure (c)